University of Iowa

Iowa Research Online

Theses and Dissertations

Spring 2019

Continuous watershed-scale hydrologic modeling of conservation practices for peak flow reduction

Michael Krasowski
University of Iowa

Recommended Citation
Krasowski, Michael. "Continuous watershed-scale hydrologic modeling of conservation practices for peak flow reduction." MS (Master of Science) thesis, University of Iowa, 2019.
https://doi.org/10.17077/etd.o6o3-2924

CONTINUOUS WATERSHED-SCALE HYDROLOGIC MODELING OF
CONSERVATION PRACTICES FOR PEAK FLOW REDUCTION

by

Michael Krasowski

A thesis submitted in partial fulfillment
of the requirements for the Master of Science
degree in Civil and Environmental Engineering in the
Graduate College of
The University of Iowa

May 2019

Thesis Supervisors: Professor Larry Weber
Assistant Research Engineer Antonio Arenas Amado

Graduate College
The University of Iowa
Iowa City, Iowa

CERTIFICATE OF APPROVAL

_____

MASTER'S THESIS

_____

This is to certify that the Master's thesis of

Michael Krasowski

has been approved by the Examining Committee
for the thesis requirement for the Master of Science
degree in Civil and Environmental Engineering at the May 2019 graduation.

Thesis Committee: _____
                          Larry Weber, Thesis Supervisor

                  _____
                          Antonio Arenas Amado, Thesis Supervisor

                  _____
                          A. Allen Bradley

                  _____
                          David Cwiertny

ACKNOWLEDGEMENTS

Thank you to my advisors for their advice and guidance throughout this project. Thank you to Larry Weber for scheduling a visit with field researcher and ex-hazardous waste transportation jockey with a degree in geology and seeing the potential for a thoughtful graduate student. Thank you to Antonio Arenas Amado for helping teach me the intricacies of hydrologic modeling and for putting in the hours to work with me to produce my best work.

Thank you to my committee members for their willingness to lend their expertise and perspectives to this thesis. Thank you to Allen Bradley for your steady instruction both in the classroom and in our work on the India project. Thank you to Dave Cwiertny for seeing the value behind well rounded water resource engineers and enabling me to be a part of the Sustainable Water Development program.

Thank you to Chad Drake, Maral Razmand, Iris Brenner, Matthew Meulemans, and Anthony Emigh for always being willing to help me talk through research and coursework. Your collective efforts and your friendship have made my time at the Stanley Hydraulics Lab something I cherish.

Thank you to Mackenzie Marti for supporting me throughout my turn through graduate school and for the insights she brought to both the graduate school and writing processes.

Thank you to my parents Ken and Karen Krasowski for supporting the academic spirit.

ABSTRACT

Iowa first started seeing largescale changes to its landscape with the arrival of Europeans and ensuing conversion of forest and prairie to row crops and pasture and would see its landscape altered again in the early 1900s through the conversion of wetlands to row crops. Watersheds in Iowa, and the Midwest at large, have been drastically altered hydrologically—through land use change, tile drainage, digging of drainage ditches, and channelizing of meandering streams. Though drainage practices maximize arable land, they also induce higher flood peaks. Along with these practices, climate change also has the potential to increase flood peaks. Conservation practices —typically employed to reduce erosion and agricultural pollution—have been proposed to be used to reduce flood peaks, but little analysis has been done on their ability to do so at the watershed-scale.

To quantify the impact implementing conservation practices at the watershed-scale has on flood peaks, a novel hydrologic model is run to simulate five conservation scenarios under both historic and increased precipitation continuously for seventeen years. The Generic Hydrologic Overland-Subsurface Toolkit (GHOST) is used to model the Boone River, an agriculturally dominated watershed in Iowa. The Boone River model is calibrated against the United States Geological Survey gaging station near the outlet of the watershed and achieves notable success. For the seventeen year study period from 2002 to 2018, calibration achieved a Nash Sutcliffe efficiency of 0.79, percent bias of -6.0 percent, and R^2 of 0.80.

To simulate the change from the baseline to a conservation practice, changes were made to the parameters of the baseline, calibrated model to reflect the effects of conservation practices. Scenarios run were the return of row crop acres to native vegetation, improved soil health via cover crops and no-till farming, distributed wetlands, conversion of river-adjacent row crop elements to native vegetation, and conversion of stream order one river-adjacent row crop elements to native vegetation. Results for the seventeen year study period show the average peak flow reductions simulated for the conservation scenarios are 82, 39, 9, 13, and 9 percent

respectively for annual maximums and 75, 29, 10, 11, and 7.5 percent respectively for the peaks over the 2-year flood threshold. Of the five scenarios modeled, only native vegetation and cover crops were able to offset the increased precipitation anticipated from climate change.

PUBLIC ABSTRACT

Watersheds in the Midwestern United States have been drastically altered hydrologically through land use change, tile drainage, drainage ditches, and stream channelization. Though these practices maximize arable land, they also induce higher flood peaks. Furthermore, climate change has the potential to increase flood peaks through increased precipitation. Conservation practices —typically employed to reduce erosion and agricultural pollution—have been proposed to be used to reduce flood peaks, but little has been done to study their ability to do so at the watershed scale. To quantify the impact implementing conservation practices at the watershed scale has on flood peaks, a novel hydrologic model is run to simulate five conservation scenarios. The Generic Hydrologic Overland-Subsurface Toolkit (GHOST) is used to model the Boone River—an agriculturally dominated watershed in central Iowa. The Boone River model is calibrated against the United States Geological Survey at Webster City for the seventeen year study period and achieves notable success. The calibrated model is then modified to simulate ten scenarios: one each of the return of row crop acres to native vegetation, improved soil health via cover crops and no-till farming, distributed wetlands, conversion of river-adjacent row crop elements to native vegetation, a similar scenario for stream order one elements, and a duplicate of each with increased precipitation. The seventeen year average annual peak flow reductions for the scenarios are 82, 39, 9, 13, and 9 percent respectively and of the five scenarios modeled, only native vegetation and cover crops were able to offset increased precipitation.

TABLE OF CONTENTS

LIST OF TABLES

LIST OF FIGURES

x

xi

xii

xiii

CHAPTER 1: INTRODUCTION

The state of Iowa has a rich natural history in which water and agriculture have played major roles. This is perhaps most evident in what is known as the Des Moines Lobe (the Lobe)—one of Iowa's six major landform regions which covers approximately one fifth of the state. The Lobe was formed as the result of glacial activity starting approximately 15,000 years ago and ending approximately 12,000 years ago (Prior, 1991). The present landscape was revealed following the retreat of the glaciers, with remarkably flat areas known as glacial advances covering a large portion of the Lobe's surface and raised linear features known as moraines which mark pauses in the glacier's retreat (Prior, 1991). The glaciers left behind varying glacial deposits characterized by their poor ability to drain water, which led to the formation of what are known as prairie potholes—the common name for the small, poorly connected wetland networks formed on the Lobe with the end of glaciation (Prior, 1991).

With the spread of modern agricultural practices and the implementation of policies to provide government assistance in the drainage of wetlands, these prairie potholes have largely been eliminated from the landscape (McCorvie & Lant, 1993; Miller, Crumpton, & Valk, 2009; Miller, Crumpton, & van der Valk, 2012). In the state of Iowa between the years of 1870 and 1959, 6.2 million acres (or roughly one sixth of the total land area of the state) were newly incorporated into drainage districts (McCorvie 1993). This large-scale conversion of land cover, from both wetland and prairie to row cropped fields has had the effect of increasing streamflows in Iowa (Villarini 2014, Schilling 2010, Kelly 2017). In addition to large scale changes to the landscape, climate change has also begun to influence the hydrology of the Midwest. Increasing trends in extreme precipitation events in Iowa and across the Midwest have been documented (Villarini et al., 2011; Villarini, Smith, & Vecchi, 2013), as have, unsurprisingly, increases in flood frequency (Mallakpour & Villarini, 2015).

These changes in hydrology due to agricultural practices and climate change are being felt in the City of Des Moines. The river passing through the heart of Des Moines is the Des

Moines River whose watershed rests solely on the Des Moines Lobe. Before the settlement of Europeans, parts of the Des Moines Lobe were made up of as much as 54 percent wetland by area (Miller et al., 2009). Today, only 3-4 percent of those original wetlands remain (Miller et al., 2012). These changes within the city of Des Moines' watershed have undoubtedly impacted the hydrology of the Des Moines River. Of the 82 historic crests recognized above the National Weather Service's action stage on the Des Moines River at 6th Street (downstream of the confluence of the Des Moines and Raccoon Rivers) from 1903 to 2018, 30 have occurred since 1990 including six of the top ten all-time highs (National Weather Service, 2018). To combat this, the City of Des Moines has spent nearly 500 million dollars on infrastructure since 1993 with plans to spend more by 2035 (City of Des Moines, 2015). Much of this spending has been on traditional engineering projects such as raising and extending levees, elevating bridges, and expanding storm water pumping capacity (City of Des Moines, 2015). As they approach the limit of what can be done in the City, they are now turning upstream to the Des Moines River watershed.

There is precedent for combating flooding by turning to the watershed. Efforts exist at the state and local levels in Iowa to help mitigate the impacts of flooding at the watershed scale (Enloe, Schulte, & Tyndall, 2014; Weber et al., 2018). These projects aim to implement conservation practices to increase the retention and processing of water on the landscape instead of the traditional infrastructure-based approach of sending water downstream as quickly as possible. Two strategies exist for increasing retention; first, structural conservation practices like wetlands detain water and attenuate peak flows (Zedler, 2003). Second, in-field management practices such as no-till and cover crops can increase the retention and processing of water by cultivating healthy soils (Basche, 2017). In-field management conservation practices increase the processing of water on a landscape by introducing more perennial species with longer growing periods (VanLoocke, Twine, Zeri, & Bernacchi, 2012) and introducing winter cover crops to traditional crop rotations to increase annual evapotranspiration (Basche, 2017). These practices can decrease soil saturation during the crucial period leading up to spring and early summer

2

flooding (National Weather Service, 2019). Identifying where conservation practices should be implemented is an important factor in their ability to reduce flooding. Geographic information systems (GIS) can be used to identify where conservation practices are both feasible and advantageous (Tomer, Porter, et al., 2013).

Studies investigating landscape changes to mitigate flooding have focused on land use and flood storage changes using tools which are limited in refinement and scope. One such study analyzed the effects of land use changes on flood peaks using a lumped hydrologic model (Schilling, Chan, Liu, & Zhang, 2010; Schilling et al., 2014). Other studies have evaluated the effects of restoring the connectivity of a river and its floodplain to reduce flooding by expanding flood storage in the river corridor using small scale, event-based simulations (Guida, Remo, & Secchi, 2016; Jobe, Kalra, & Ibendahl, 2018). While these methods have merit, a combination of studying land use changes alongside structural practices comes with the ability to make comparisons which would be useful in directing the often limited resources necessary to make changes. A novel hydrologic model, the Generic Overland-Subsurface Toolkit (GHOST), meets these needs (Politano, 2018). GHOST is a continuous, physically-based, distributed hydrologic model developed by Politano at the University of Iowa, IIHR Hydrosciences and Engineering.

1.1 Goals and Objectives

The goals of this thesis are three fold:

1) To quantify the reductions expected by the adoption of different conservation practice scenarios

2) To quantify the impacts of increased precipitation in the context of both the baseline and conservation practices

3) To assess the comparative effects of changes made exclusively to the riparian corridor.

To determine the ability of different conservation practices to reduce flood peaks in an agricultural watershed in the present and in the future with a changing climate, the Boone River

watershed is modeled under ten scenarios. Two each of native vegetation, cover crops, wetlands, and two riparian corridor scenarios; the first with observed rainfall and the second with amplified extreme events. The baseline condition is calibrated to the period from 2002 to 2018 against discharge data at the U.S. Geological Survey (USGS) gaging station at Webster City, Iowa (05481000). The native vegetation scenario represents idealized conditions where in-field conservation practices are maximized. The second scenario models in-field practices by simulating complete adoption of cover crops and no-till practices on all row crop acres of the watershed for the purpose of improving soil health (Basche, 2017; Edwards, Norton, & Redmond, 1988; Radke & Berry, 1993) The third scenario simulate the construction of wetlands distributed across the watershed in a fashion that is consistent with nutrient removal wetlands as sited by the Agricultural Conservation Planning Framework (Porter, Tomer, James, & Boomer, 2016). The fourth scenario tries to answer whether or not the riparian corridor plays an outsized role in the reductions seen from the native vegetation scenario by modeling native vegetation implementation only in areas adjacent to the river network. The fifth scenarios assesses the potential for native vegetation implemented along steam order one streams to produce disproportionately large reductions.

1.2 Summary

To better understand the potential for conservation practices to mitigate flooding in the city of Des Moines, this thesis is focused on the hydrologic assessment and modeling of the Boone River watershed as a first step for assessing the entire Des Moines River watershed. The Boone River watershed is simulated with GHOST and is calibrated against observations in the watershed with an emphasis on accurately replicating peak flows. Once the model is calibrated, changes are made to represent each of the four scenarios described and the model is re-run with these changes. Each scenario will then be compared against the baseline calibrated model to quantify the reductions in flood peaks.

The challenges brought upon Iowa and the greater Midwest by the hydrologic consequences of both land use and climate change have to be met with action. The first step in addressing these challenges is gaining an understanding of the natural systems in which they manifest to better understand the impacts of the changes made to them. Hydrologic modeling demonstrates a high level of understanding of the system and the effects of implementing BMPs and informs decision making and resource allocation for effective flood mitigation. This thesis aims to provide for the City of Des Moines an assessment of the viability of different conservation practices from a hydrologic perspective.

CHAPTER 2: LITERATURE REVIEW

2.1 Introduction

The study of watershed scale, sustainable water resources management is an area of ongoing research with a high degree of interconnectivity with the systems surrounding it. The topics discussed here include: the history of the study area, the impacts of climate change, the history of conservation in Iowa, benefits of conservation practices, the history of hydrologic modeling, a brief recap of modern applications of hydrologic modeling, the merits of the modeling approach used (a comparison of modeling approaches), hydrologic modeling of conservation practices, and conservation siting tools. It is through these lenses both the merit and the quality of the work presented can best be viewed.

2.2 Hydrologic History of the Des Moines Lobe

The Midwestern landscape saw dramatic alterations with the passage of the Swamp Land Acts in the late 1800s and the move to expand agricultural output in the early 1900s (McCorvie & Lant, 1993; Thompson, 2002; U.S. Geological Survey, 1996). Some of those changes came directly from actions taken to make lands which were previously too wet arable; specifically, the installation of tile drainage, drainage ditches, and the channelization of existing rivers. With these practices in place to dry (and keep dry) some of the wettest parts of the natural landscape, water is artificially swept off faster and more thoroughly than by natural processes (Hartmann, 2002; Kelly, Takbiri, Belmont, & Foufoula-Georgiou, 2017; Thompson, 2002). Subsurface tile drainage, specifically, has been found in a study done in a small, agricultural watershed with well-developed drainage to induce baseflow increases anywhere from 0 to 54 percent (Schilling, Jindal, Basu, & Helmers, 2012). Through these built practices, the Lobe has been left with 3 to 4 percent of its original wetland area (Miller et al., 2012), which was approximately 44 percent of the total land area of the Des Moines Lobe and 54 percent of the Boone River watershed pre-development (Miller et al., 2009).

6

Other changes—like the switch from the existing land covers of prairie, forest, and floodplain—were incidental and implicit in the expansion of agricultural land. Work done on the Upper Mississippi River Basin upstream of the USGS gaging station at Keokuk Iowa has demonstrated about 30 percent of the increase in discharge observed at Keokuk can be attributed to land use and land cover change (Schilling et al., 2010). A study done on four large river basins in the Midwest that span seven states from 1915 to 2015 found watersheds which saw greater increases in agricultural activity saw low flows increase 2 to 4 times and high and extreme flows increase 1.5 to 3 times (Kelly et al., 2017). Another study, done on the Raccoon River watershed, separately attributed observed changes in hydrology to agricultural practices and climate change finding rainfall variability responsible for the majority of changes in hydrology and land use changes responsible for increasing severity of both flooding and droughts (Villarini & Strong, 2014).

2.3 Impact of Climate Change on Hydrology

Knowledge about the historical behavior of a watershed plays an important role in our ability to characterize the flood hydrology now and into the future. This extension of past behavior into the future rests upon an assumption of stationarity—that the system being studied is not changing and is therefore stationary. Studies have shown this assumption to be flawed in the modern context (Villarini et al., 2011) and it is certainly not suitable in the years to come due to anthropogenic climate change (Hoegh-Guldberg et al., 2018; Milly et al., 2008). As a result, there is uncertainty about what a changing climate means for the hydrology of a watershed; the future can no longer be sufficiently informed by the past alone. In the modern setting an assessment of the functioning of a climate influenced system (of which a watershed qualifies) would not be complete without a discussion on the impacts anthropogenic climate change will have in the coming years.

Before focusing our attention ahead to the future, changes in the climatology of the Midwest and the state of Iowa are becoming apparent in the present. Analyzing rain gages in the

7

Midwestern United States with daily rainfall data and a period of record of 75 years or greater, Villarini et al. (2011) found a slight increase in annual maximum daily rainfall. These changes in precipitation have been linked to changes in the current hydrology of the central United States and have also been observed at the basin scale. Focusing on the central United States, Mallakpour and Villarini (2015) found limited change in the magnitudes of flood peaks, but strong evidence of an increase in the frequency of flooding. A study done at the basin scale in the state of Iowa analyzed an agricultural watershed to elucidate the relative influences of climate and agricultural land use found climate variability to be responsible for the majority of discharge behavior with agricultural land use being positively correlated with decreased low flows and increased high flows (Villarini and Strong 2014).

Going forward, the impacts of climate change will vary greatly depending on the region of the globe being assessed. Chapter 3 of the Intergovernmental Panel on Climate Change's *Special Report: Global Warming of 1.5 ºC* titled *Impacts of 1.5°C of Global Warming on Natural and Human Systems* reports on the most current consensus on the impacts of climate change (Hoegh-Guldberg et al., 2018). These impacts come in many forms, including changes in temperature, precipitation, and basin scale runoff. The IPCC divides the world's continents into 26 regions, with Iowa in the Central North American region (CNA, also noted as region 4). The changes in precipitation reported by the IPCC are quantified by region in a number of metrics. For the CNA region, these metrics show significant increases in the proportion of rain falling as 95th percentile or higher, the proportion of rain falling as 99th percentile or higher, intensity of maximum yearly 1-day precipitation and intensity of maximum yearly 5-day precipitation. Metrics showing increases rather than significant increases are mean precipitation, the number of consecutive wet days, the number of days with precipitation >10 mm, and the number of days with precipitation >20 mm. The only metric showing a decrease for the CNA region is the number of days with precipitation >1 mm (IPCC 2018). These metrics combine to form a narrative of a wetter CNA region with much of the increased precipitation coming in extreme, prolonged events. A recent study done in the Raccoon River watershed agrees with the findings

of the IPCC and found increases in precipitation drove discharge increases and did so most significantly for 60th percentile flow and up (Villarini et al. 2015). While there is some agreement on the impacts anthropogenic climate change is anticipated to have on the hydrology of the Midwest and Iowa in particular, there is also ongoing discussion on the uncertainties associated with these impacts (Giuntoli et al. 2018).

Climate change must be a part of the discussion where the sustainable management of water resources is concerned. There is strong evidence of the Midwest getting more frequent extreme precipitation events and as a result more frequent flooding. The IPCC's 2018 *Special Report: Global Warming of 1.5 ºC* paints a grim picture for the future of flooding in the Midwest. Meeting this challenge will to require new approaches to the ways problems have traditionally been solved. Already there are calls for the standards used in engineering design to be adjusted to take into account the future realities of climate change (Villarini et al. 2015, Quintero et al. 2018). Watershed management strategies which rely on practices both built and managed should reflect the calls for design with climate change in mind.

2.4 History of Conservation in Iowa

The history of conservation in Iowa started with the Swamp Land Acts of the mid to late 1800s which, at the time, were billed as conservation efforts. In modern terms, conservation means something different and is nearly antithetical in practice. The modern conservation movement started in response to the Dust Bowl with the creation of the Soil Conservation Service (now the NRCS) (Cain & Lovejoy, 2004). The SCS kicked off demonstration projects like the Soil Conservation Experiment Station in Clarinda, Iowa, programs with lasting impacts like fence row tree lines and ambitious projects like the Great Plains Shelterbelt—the 100 mile wide forested zone planned in response to the Dust Bowl (Cain & Lovejoy, 2004). In Iowa, conservation ethos can be tracked back further to the turn of the twentieth century and individuals such as Ada Hayden, John F. Lacey, Bohumil Shimek, Louis Pammel, Ding Darling, Aldo Leopold, and Henry Wallace (Iowa Association of Naturalists, 1995).

2.5 Benefits of Conservation Practices

To restore some of the natural hydrologic character to heavily altered watersheds, it has been proposed to construct and implement conservation best management practices (BMPs). These conservation BMPs come in a variety of forms including contour buffer strips (CBS), riparian practices (RP), grassed waterways (GWW), water and sediment control basins (WASCOB), drainage water management (DWM), nutrient removal wetlands (NRW), cover crops (CC) and no-till (NT). These BMPs are sited by a geographic information system (GIS) tool known as the Agricultural Conservation Planning Framework (ACPF)(Porter et al., 2016). The ACPF was developed by the United States Department of Agriculture's Agricultural Research Service National Laboratory for Agriculture and the Environment with the intent of identifying locations where practices would be most effective, based upon existing topography, soils, and land cover properties (Tomer, Porter, et al., 2013). Using the ACPF, BMPs can be sited in a watershed appropriately and subsequently in a hydrologic model to see what their effects may be on streamflow down-watershed.

Alongside these hydrologic benefits, conservation practices can also be beneficial to water quality. The main benefits to water quality for many of these BMPs are the increases in sediment trapping and processing of agricultural pollutants through phytoremediation (Dietz & Schnoor, 2001; Schnoor, Licht, McCutcheon, Wolfe, & Carreira, 1995; Tomer, Porter, et al., 2013).

2.5.1 Contour Buffer Strips, Riparian Practices, and Grassed Waterways

The primary hydrologic benefit of a number of BMPs is the increase in the infiltration of rainfall and runoff they can provide (Chiang, Chaubey, Hong, Lin, & Huang, 2012). Infiltration has the potential to play a key role in the benefits of GWWs, CBSs, and RPs, largely due to the changes from bare soil and row crops to densely planted grasses (Deletic, 2001). The effectiveness of any particular grassed area in promoting infiltration is a function of the land cover type (grassed vs bare), slope (flat vs steep), and flow path length through the grassed area

10

(long vs short). Grassed waterways are targeted plantings of grasses along concentrated flow paths. In one study GWWs were found to increase infiltration on the order of 0 to 5.82 percent over a stretch of just 39.4 feet (Mishra, Neelkanth, Babu, & Kumathe, 2006). In another study, researchers tested two different approaches to implementing GWWs, and found runoff volumes reduced by 90 and 49 percent depending on the approach (Fiener & Auerswald, 2005). Another study found a relationship between rainfall and infiltration showing infiltration can range between 100 and 22 percent depending on the rainfall rate (Deletic, 2001).

Much attention has been paid to targeting management efforts on the riparian zone. Riparian practices go by different names such as grass strips, prairie strips, vegetative buffers, or riparian buffers, but all include some sort of permanent vegetation interceding between agricultural lands and the river system. Many studies have evaluated the water quality and quantity benefits of riparian and similar perennial vegetation based practices (Asbjornsen et al., 2014; Michael G. Dosskey et al., 2010; Hladik et al., 2017; Schulte et al., 2017). Though the ability of these and similar practices to reduce runoff is well characterized, little research has been done evaluating the comparative effects of practices done upslope in a field versus in the riparian zone. Studies such as one done by Hernandez-Santana et al. (2013) looked at the effectiveness of prairie strips placed at different points on hillslopes and found a relationship between placement and runoff reduction potential. This indicates a dependency on relative placement in the landscape of these types of practices which needs to be further explored.

2.5.2 Water and Sediment Control Basins

Infiltration is also a key process for WASCOBs and their potential to help reduce runoff, but rather than solely relying on grasses to aide in infiltration, WASCOBS detain waters and pool them behind a low impoundment to spur infiltration (Her, Chaubey, Frankenberger, & Jeong, 2017). WASCOBs have an outflow pipe to prevent extended inundation or overtopping of the impoundment. Existing literature on the explicit benefits of WASCOBs to streamflow is lacking, but one research report done for the Ausable Bayfield Conservation Authority Ontario

11

Ministry of Agriculture and Food found maximum flow volume reductions of approximately 10 percent with the average flow reduction of 32 WASCOBs at approximately 4 percent (Yang, Liu, Simmons, Oginskyy, & McKague, 2013).

2.5.3 Drainage Water Management

Drainage water management is the control of outflow from tile drainage lines to keep more water in the subsurface. Several studies indicate DWM has the potential to reduce runoff, but one study suggests a greater caution with the implementation and application of DWM. A collection of studies conducted in different parts of Iowa have found DWM to produce anywhere from 21 to 60 percent flow reductions (Helmers, Christianson, Brenneman, Lockett, & Pederson, 2012; Jaynes, 2012; Schott et al., 2017). A review paper examining 13 other studies found reported reductions in flow from 16 to 89 percent (Skaggs 2012). Concern was raised by a study done in east-central Illinois which focused on the fate of retained flows and cautioned implementation without consideration of adjacent fields and the possibility of lateral subsurface flows (Lavaire, Gentry, David, & Cooke, 2017). Tangentially, recent studies have found potential for crop yields to be boosted by actively managing groundwater levels in cropped fields which highlight an opportunity to see both flow and crop yield benefits from DWM (Archontoulis, Licht, Castellano, Ordonez, & Iqbal, 2017; Jaynes, 2012).

2.5.4 Nutrient Removal Wetlands – Water Quantity

One conservation practice with high potential for runoff reduction is wetlands. Studies indicate as the proportion of wetland area to total watershed area decreases, the likelihood of flooding increases. An evaluation of the Midwest as a whole found watersheds containing 5 to 10 percent wetlands by area (as compared to those containing none) saw peak flood reductions of 50 percent (De Laney, 1995). Similar studies have found when less than 10 to 20 percent of a watershed area is wetlands, the risk of flooding increases disproportionately (Cedfeldt, Watzin, & Richardson, 2000; Johnston, Detenbeck, & Niemi, 1990). Currently, the Des Moines Lobe

12

only has 3 to 4 percent of its original wetland area (Miller et al., 2012), which was approximately 44 percent of the total land area of the Des Moines Lobe pre-development (Miller et al., 2009).

Several studies have examined wetlands and their capacity to reduce and attenuate flows and generally agree on the potential for reductions (Kadlec & Wallace, 2009; Zedler & Kercher, 2005). One such study done in central Indiana found wetlands can reduce the peak flow produced from a rainfall event from 20 to 41 percent, flood areas by up to 55 percent, and maximum stream velocities by 15 percent (Javaheri & Babbar-Sebens, 2014). Another study carried out in in Manitoba, Canada, in an area which is also dominated by the prairie pothole landscape, found wetland restoration can reduce peak discharges by as much as 23.4 percent (Yang et al., 2009). A similar study done in west-central Minnesota, an area which has retained its wetlands, found the loss of the first 10 percent of the existing wetlands would result in a 40 percent increase in peak streamflows (Wang et al., 2010).

2.5.5 Nutrient Removal Wetlands – Water Quality

Along with the potential for conservation practices to reduce flooding, they have also been shown to have positive impacts on water quality. This is perhaps most apparent and most widely studied in the case of wetlands. Wetlands are capable of removing a variety of pollutants associated with agricultural runoff, including sediments, nutrients, organic chemicals, and pathogens (De Laney, 1995; Kadlec & Wallace, 2009; Zedler, 2003). One study showed intercepting just 30 percent of the tile flow from a watershed could reduce nitrate loads by an average of 11-13 percent (Tomer, Crumpton, Bingner, Kostel, & James, 2013). A study done in the Minnesota River Basin, an area which has retained a high proportion of its original wetlands, found wetlands to be five times more efficient per unit area at removing nitrate when compared to other land-based strategies including cover crops and land retirement (Hansen, Dolph, Foufoula-Georgiou, & Finlay, 2018). A study done near the confluence of the Minnesota and Mississippi rivers found wetlands could reduce levels of sediment, specific conductivity, fecal

13

coliform, phosphorous, nitrate, total suspended inorganic solids, and ammonium (Johnston et al., 1990).

2.5.6 Cover Crops

Cover crops are a widely studied management practice and have been shown to have benefits in terms of both water quality and quantity. Some popular cover crops include cereal rye, oats, common vetch, hairy vetch, turnip, radish, millet, and winter pea. Cover crops come with diverse characteristics and may be selected for a multitude of reason such as commercial value, cost to plant, nitrate leaching reduction potential, inter-cropping ability, erosion control, pest suppression, soil fertility and health and boosting cash crop yields (Snapp et al., 2005). Cover crops have recently gained interest for another surprising ability: their potential to help with flooding. In a report for the Union of Concerned Scientists Andre Basche identified 81 studies indicating cover crops had a positive effect on infiltration rates with as high as 50 percent increases (Basche, 2017). Cover crops also have the ability to regulate water fluxes in farm fields at once reducing runoff and boosting soil water availability (Basche, 2017). Cover crops have been shown to be effective in the management of nutrient losses and pest weeds and insects, thereby reducing the need for herbicides and insecticides (Sustainable Agriculture Research and Education, 2012).

2.5.7 No-Till

In modern agriculture the current practice is to till as much as the top 6 inches of row crop fields to prepare them for seeding. A rising movement is the practice of no-till farming; in which seeds are either planted directly into the ground, commonly by a drill planter, or broadcast seeded (United States Department of Agriculture, 2015). The goal of no-tilling is to improve soil health by not disrupting the soil, allowing soil macro- and micro-fauna to flourish and create macro-pores (Edwards et al., 1988). These changes in the soil structure help to increase the porosity and infiltration rates of soils which help to reduce the generation of runoff (Basche, 2017; Edwards et al., 1988; Lee, 1985). No-till practices also affect the soil surface by

14

effectively increasing roughness which can slow runoff and increase infiltration (Mohamoud, 1992).

2.5.8 Biodiversity

On the eve of what has been popularly termed the Sixth Extinction, (Kolbert, 2015) and with recent headlines about the collapse of insect populations (Lister & Garcia, 2018; Sánchez-Bayo & Wyckhuys, 2019) BMPs which encourage the flourishing of wildlife could be a crucial part of maintaining biodiversity in agricultural landscapes. Wetlands and native prairie in particular have the potential to support a wide variety of species (Kadlec & Wallace, 2009; Schulte et al., 2017; Zedler & Kercher, 2005). In a report by the Iowa Cooperative Fish and Wildlife Research Unit, 27 constructed wetlands occupying 930 acres could provide habitat for 192 wildlife species (Otis et al., 2010). One study examined wastewater treatment wetlands for their impact on biodiversity and found increases in numbers of species and a correlation between wetland size and number of species (Hsu et al., 2011). In a review paper by Knight (1997) wetlands in the U.S. were found to support over 600 species of plants which in turn support myriad animal species.

2.6 History of Hydrologic Modeling

Hydrologic modeling can trace its roots back to the nineteenth century as cities continued to grow and improved approaches to designing elements of urban infrastructure such as canals, sewers, and water supply systems were needed (Singh and Woolhiser 2002). Early on, hydrologic modeling was largely limited to what are now called component models, which, rather than capturing an entire watershed, focus on singular components and mechanisms of hydrologic systems such as runoff generation (Sherman 1932), overland flow (Horton 1939), and evaporation (Richardson 1931). Watershed modeling in the holistic sense would first be achieved with the creation of the Stanford Water Model (SWM) in 1966 (Crawford and Linsley 1966). The field would continue to grow with the digital revolution and the spread of computers (Singh and Woolhiser 2002) with many watershed scale models being developed such as the Penn State

15

Integrative Hydrologic Model (PIHM), the Hydrological Simulation Program – FORTRAN (HSPF), the Soil and Water Assessment Tool (SWAT), the Hydrologic Engineering Center's Hydrologic Modeling System (HEC-HMS), the National Weather Service model (NWS), HydroGeoSphere (HGS), Systeme Hydrologique Europeen (SHE), and Vflo among many others.

Today, hydrologic modeling is a powerful tool in helping to understand processes operating at watershed scales to better inform decision making for land use, conservation, and sustainability efforts. Models like HSPF, SWAT, HEC-HMS, SHE, their variants, and many others are still in use today and each have their specialties in application. For example, HSPF can specialize in pollutant loadings, erosion, and fate and transport and operates on daily timescale; MIKE-SHE specializes in subsurface flows and groundwater quality and operates on seconds to daily timescales; and SWAT focuses on plant growth, and sediment, nutrient, and pesticide transport and operates on a daily timescale (Moriasi, Wilson, Arnold, & Gowda, 2012). Each of these models is different in temporal and spatial resolutions, modeling approach, complexity, and ability which can make them more or less advantageous for different applications.

2.7 Modern Uses of Hydrologic Modeling to Study Flooding

The use of hydrologic models to study flooding is an active area of research. There are a few regularly studied themes: floodplain connectivity restoration, land use change, climate change, and flood-related contaminant fates. Floodplain connectivity studies typically center around the built environment and the controls put in place to restrain natural, riverine systems. Three recent studies from 2012, 2016, and 2018 each addressing a different study area and each bringing their own approach have studied flood reductions through floodplain-river reconnection (Dierauer, Pinter, & Remo, 2012; Guida et al., 2016; Jobe et al., 2018). As the built and human environments have expanded, so too has the study of land use change impacts on flooding. The impacts of land use change on watershed hydrology were investigated with hydrologic modeling in three papers from 2014 and 2016 (Ahiablame & Shakya, 2016; El Alfy, 2016; Schilling et al., 2014). As hydrologic modeling helps us to understand the flooding implications of changes in

16

land use, so too can it help us understand the implications of climate change. In 2012 and 2016 three papers with work done in climatically diverse study areas investigated mitigation strategies and impacts of climate change using hydrologic modeling (Dudula & Randhir, 2016; Karamouz, Fallahi, & Nazif, 2012; Karim et al., 2016). The transport of chemicals is also a dynamic problem to which hydrologic modeling can provide insight. Three recent papers from 2016, 2018, and 2019 have looked at the spatial and temporal patterns of the transport of polychlorinated biphenyls, metals, and nutrients during flooding (Alam & Dutta, 2016; Beck et al., 2019; Lu et al., 2016; Mansoor, Louie, Lima, Van Cappellen, & MacVicar, 2018). The use of hydrologic modeling to understand behavior and response to changes in hydrologic systems is an ongoing area of research with many different approaches and questions being answered.

2.8 Comparison of Modeling Approaches

The watershed scale hydrologic models developed since the late 1960s and those in use today vary in their formulation. Many authors have proposed their preferred schemes for grouping hydrologic models (Daniel et al., 2011; Devia, Ganasri, & Dwarakish, 2015; Jajarmizadeh, Harun, & Salarpour, 2012; Xu, 2002). One of the most nuanced comes from Jarjamizadeh et al. 2012 in which the authors assert the main ways in which hydrological models differ are in the laws and approximations used (empirical, conceptual, or physical), the types of equations used (deterministic or statistical), the subunits parameterized (lumped, semi-distributed, or distributed), the time frames they capture (event-based or continuous), and the computations performed (analytical or numerical) (after Bradley (2018) adapted from Jajarmizadeh (2012)).

There are three possible categories for a model to be in when it comes to the laws and approximations, an empirical model, a conceptual model, or a physical model. Often, models employ a mix of these approaches to accomplish their means. Empirical models—also called "black box" models—are mathematical equations which derive outputs from data-driven inputs. Conceptual models—also called "grey box" models—rely on parameters derived from both field

17

data and calibration to describe the interactions between different reservoirs internal to the model. Physically-based models—also called "white box" models—rely on measurable parameterized equations based in physics and incorporate some level of the morphology of a watershed (Devia et al., 2015). A model may be called either deterministic or statistical based upon the equations used (Jajarmizadeh et al., 2012). If a model produces singular values as its output for a simulation or forecast, that model is said to be deterministic, whereas if a model produces a range of possibilities or likelihoods as an output, that model is statistical or stochastic (Daniel et al., 2011). A model is lumped if a its base unit is an entire watershed and uses parameters representing the averages of the spatially heterogeneous watershed, semi-distributed if it breaks down a watershed into smaller sub-basins characterized by being spatially and parametrically distinct from one another, or distributed if it uses subdivisions set at a high resolution determined by the modeler to allow adequate levels of capturing spatial heterogeneity (Daniel et al., 2011). Hydrological models can be grouped into two categories based upon the timeframes over which they are meant to operate: event-based or continuous. Event based models capture singular phenomena such as a storm or a one year drought and are aimed at understanding a system's response to a singular condition. Continuous models run for long periods of time and are often aimed at understanding a systems behavior over a broad range of conditions. The computations performed by a model can be grouped as either analytical or numerical—directly calculated or solved via partial differential equations.

Literature shows there are clear advantages associated with some modeling methods for modeling performance and accuracy and selecting a model for a specific application should reflect this (Xu, 2002). For instance, when comparing distributed vs lumped models, distributed models are able to more accurately capture spatial heterogeneities which may be important for the hydrologic processes operating within a watershed (Beven & O'Connell, 1982; Daniel et al., 2011). Distributed hydrologic models can use different types of elements to compose their meshes; the most common are orthogonal grids and triangular irregular networks (TINs). These different discretization methods have advantages. Orthogonal grids are often employed for their

18

ease of use and TINs are used when capturing terrain or surface geometry is important (Bates, Marks, & Horritt, 2003; Casas, Benito, Thorndycraft, & Rico, 2006). Whereas conceptual models can have little relation to the natural world, physically-based hydrologic models use a variety of different methods for directly representing the physical processes and parameters they approximate. Five of the main processes are interception; evapotranspiration; snowmelt; soil moisture, infiltration, and subsurface flow; and surface flow and routing (Islam, 2011). In a physically-based model, these processes are represented with equations derived from the principles of the conservation of mass, momentum, and energy and therefore can be expected to adhere to behaviors consistent with natural systems (Islam, 2011). One of the drawbacks to physically-based, fully distributed watershed modeling is the large amounts of spatially expansive data it requires to be advantageous; in the absence of data gaps, these models have been shown to outperform conceptual and lumped models (Devia et al., 2015)

2.9 Conservation Siting Tools

To be judicious in the pursuit of conservation practices and implement them where the potential impact is greatest, a number of conservation siting tools have been developed. Tools developed to assist in this endeavor include the Conservation Reserve Program-Decision Support System (CRP-DSS), which was developed to assist in the prioritization of CRP enrollments, a GIS based tool to advantageously site wetlands (Babbar-Sebens, Barr, Tedesco, & Anderson, 2013), and the GIS-based AgBufferBuilder which was designed to custom prescribe riparian buffer strip widths based on terrain and conservation needs (M. G. Dosskey et al., 2015).

Of particular interest is a tool developed at the National Laboratory for Agriculture and the Environment (NLAE), called the Agricultural Conservation Planning Framework (ACPF) (Porter et al., 2016). The ACPF uses light detection and ranging (LiDAR) based 2-meter resolution digital elevation models (DEMs), soils from National Resources Conservation Service's (NRCS) gSSURGO product, land use from the National Agricultural Statistics Service (NASS) crop data layer (CDL), and farm field extents to identify optimal placement of a wide

19

variety of conservation practices (Tomer, Porter, et al., 2013). The ACPF is intended to operate at the hydrologic unit code 12 (HUC 12) scale and the NLAE makes available online all of the resources necessary to use it (Porter et al., 2016).

2.10 Summary

Finding sustainable solutions to water resources challenges necessitates understanding systems in context. Changes in land use and climate have impacted the hydrology of the Des Moines River watershed, Iowa, and the greater Midwest and will continue to induce flooding going forward. There is a large body of existing literature on the study of flooding, hydrologic modeling, the use of BMPs to mitigate both flooding and agricultural pollutant runoff, and the impacts of climate change. Together, they show the potential benefits of these BMPs for peak flow reduction and water quality are provocative and merit further investigation with hydrologic modeling for specific applications.

20

CHAPTER 3: DESCRIPTION OF THE WATERSHED

3.1 Introduction

     The Boone River watershed occupies 15 percent of the Des Moines River watershed north of the City of Des Moines and lies entirely on the Des Moines Lobe; one of Iowa's six major landforms. The watershed is 908 square miles and spans six counties—Hamilton, Hancock, Humboldt, Kossuth, Webster and Wright. Webster City is the major population center of the Boone River watershed (Figure 3-1)(Iowa Geodata, n.d.). In order to understand the effects of the conservation scenarios, an understanding of both the physical and hydrological characteristics of the Boone River watershed is needed.

21
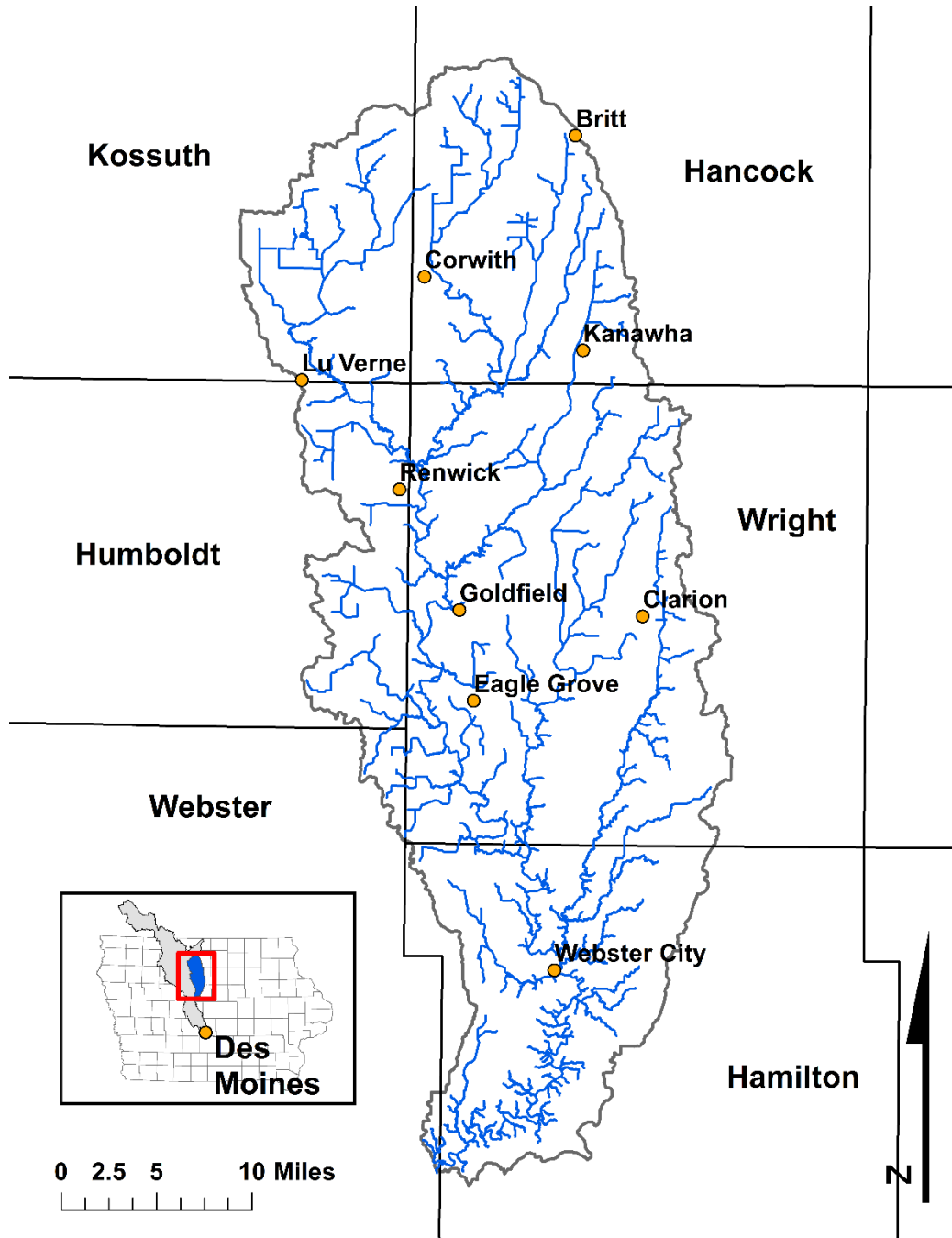
Figure 3-1: The Boone River watershed in relation to the counties of Iowa and the watershed for the Des Moines River north of the City of Des Moines.

3.2 History of the Des Moines Lobe

The Lobe was formed as a result of the last gasp of the Wisconsinan Glaciation 12-14,000 years ago and is the youngest of Iowa's six major landforms (Prior, 1991). As such, the Lobe has had relatively little time to develop hydrologically from the remarkably flat, pristine glacial till left in the wake of the glacier's retreat (Miller et al., 2009; Pidwirny, 2006; Prior, 1991). The landscape which would form in the time between the end of glaciation and the arrival of Europeans is known as the Prairie Pothole Region – a landform and eco-region marked by an extended, loosely hydrologically connected network of lakes and wetlands formed in small depressions known as prairie potholes (also known as kettles) (Prior, 1991; Vanderhoof, Christensen, & Alexander, 2017). The Des Moines Lobe would remain near this condition until the late 1800s and early 1900s when the legal framework was established at both the state and national levels to begin to alter it with the passage of the Swamp Land Acts and the creation of Drainage Districts (Andersen, 2000; McCorvie & Lant, 1993; Thompson, 2002). The goal of this push was to eliminate the prairie pothole landscape to create newly arable land (and, among other things, because wetlands were thought to cause miasmas through the exuding of gases) (Carlson, 2010).

3.3 Land Use/Land Cover

The Boone River watershed is dominated by row crop agriculture with over 84 percent of the watershed's land area in use for the production of either corn or soybeans (National Agricultural Statistics Service, 2016). The next highest land use is for developed areas at 6.6 percent, pasture/hay at 5.2 percent, and forest at 4.0 percent (Figure 3-2). The spatial distribution of row crop agriculture is nearly uniform, with exceptions carved out for urban, developed centers and the forested areas tightly following the river corridor.

Land Cover

- Row Crop
- Pasture/Hay
- Forest
- Developed

0   2.5   5   10 Miles

N
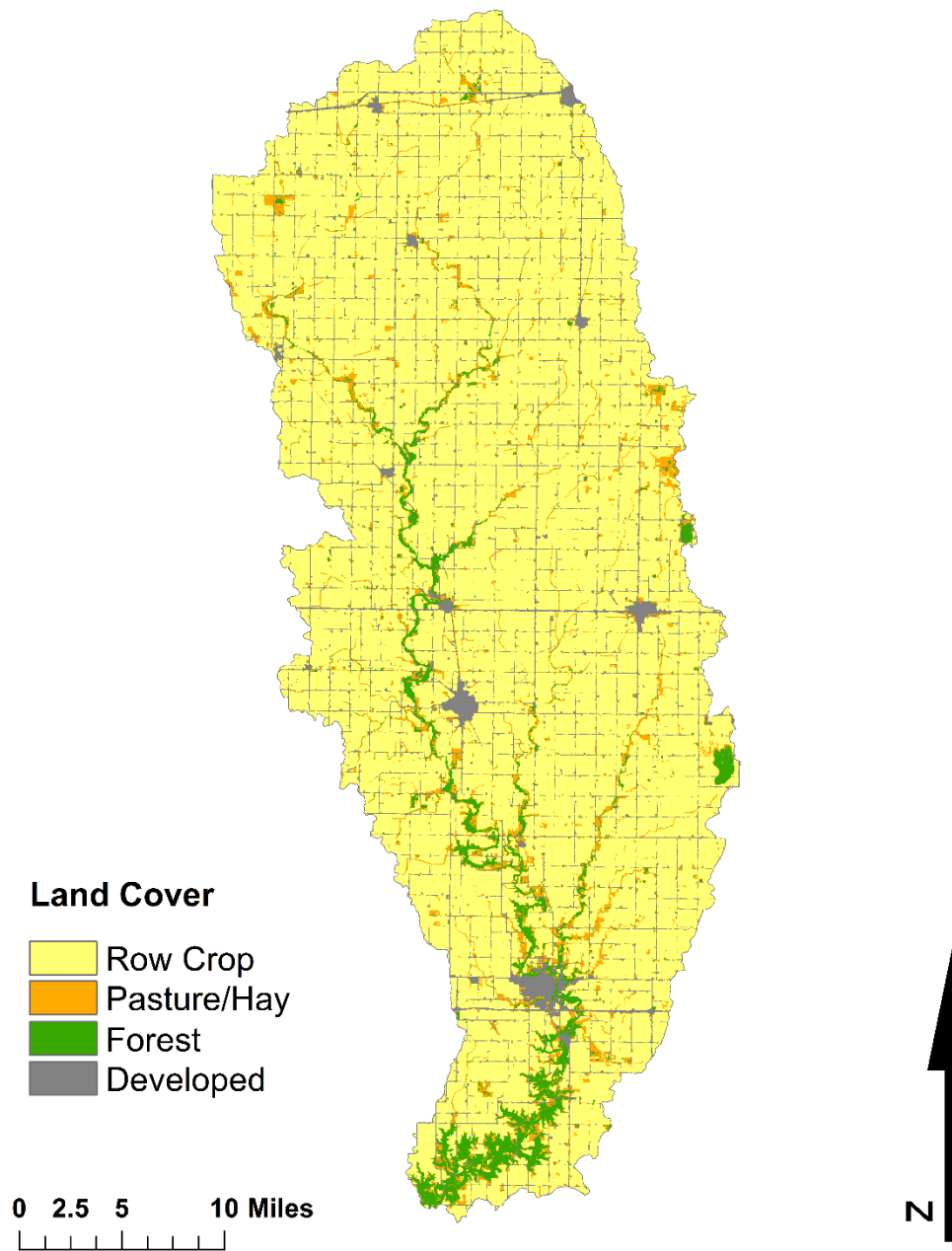
Figure 3-2: Land cover for the Boone River watershed grouped into four types.

3.4 Topography

The Boone River watershed topography starts high in the north and east and gradually falls off to the south and southwest. Mean, maximum, and minimum elevation of the Boone River watershed are 1150 ft (350 m), 1320 ft (402 m), and 910 ft (277 m) respectively (Figure 3-3). The majority of the watershed is close to the mean with exceptions for the down-cutting river network in the south and the northern- and eastern-most extents of the watershed due to the Algona Advance and Moraine and the Altamont II Moraine (Figure 3-4) (Iowa State University: Geographic Information Systems Facility, n.d.).

25
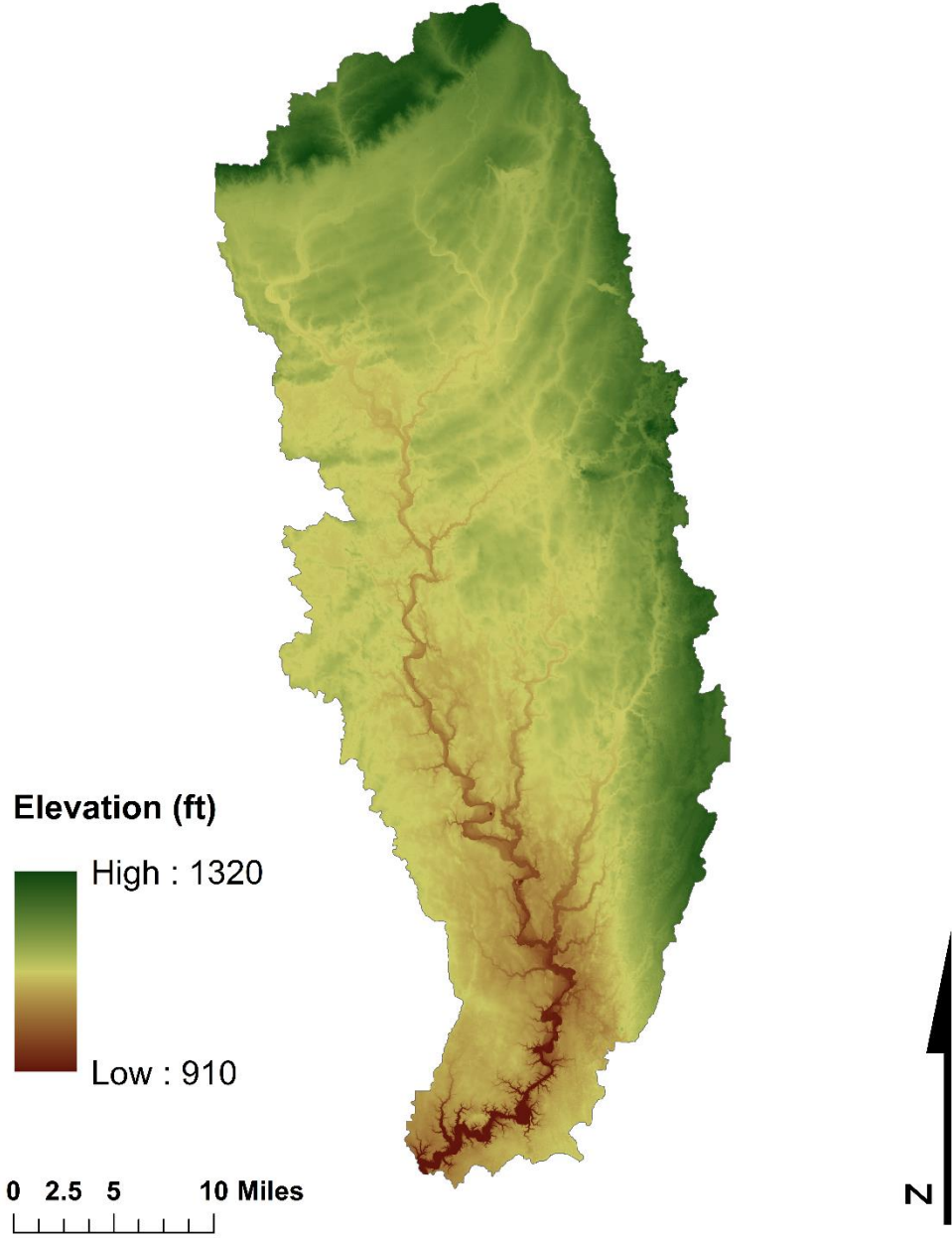
Figure 3-3: Digital Elevation Model derived topography.

3.5 Geology

Surficial geology of the Lobe can be broken up further into the features left behind by the Des Moines Lobe glaciers. The Boone River watershed is dominated by the Altamont Advance at 90 percent of surface geology followed by the Algona Advance, the Altamont II Moraine, the Algona Moraine, the Renwick Moraine, and the West Bend Moraine at 3, 3, 2, 1, and 1 percent respectively (unmapped is the Altamont lake zone which sits in the far southeastern and southern portions of the watershed overlaying the Altamont Advance (Miller et al., 2009)) (Figure 3-4) (Iowa Geodata, n.d.).
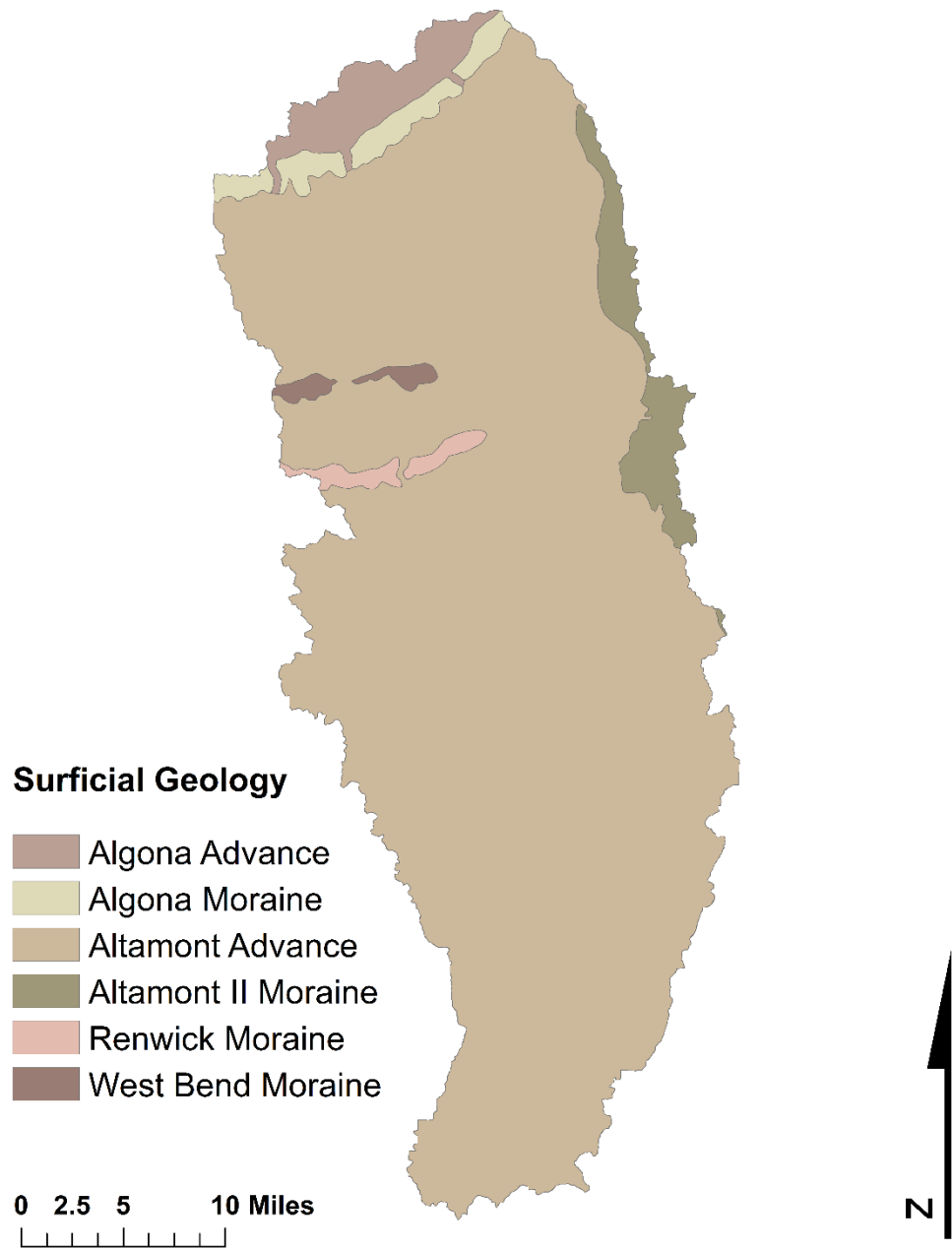
Figure 3-4: Simple surficial geology of the Des Moines Lobe in the Boone River watershed.

3.6 Soils

Soils from the Boone River watershed are dominated by clay loams at 54 percent followed by sand dominated; silt dominated; clay dominated; and sand dominated, very gravely soils at 21, 16, 6, and 2 percent respectively (Figure 3-5)(Soil Survey Staff, 2015). Drainage Class rankings are led by poorly drained at 54 percent followed by somewhat poorly, well, moderately well, very poorly, somewhat excessively, and excessively at 21, 11, 7, 5, and 0 percent with 7 percent unclassified (Figure 3-6) (Soil Survey Staff, 2015). Hydrologic soil group classifications are dominated by group C/D at 77 percent followed by C, B, B/D, A, A/D, and D at 12, 5, 3, 1, and 0 percent with 1 percent unclassified (Figure 3-7) (Soil Survey Staff, 2015). The prevalence of clay loams indicate a clay-weighted balance of constitutional particles (Soil Science Division Staff, 2017). The prevalence of poorly drained soils indicate soils which stay wet for long periods and are occasionally too wet for crop growth (requiring artificial drainage) (Soil Science Division Staff, 2017). The prevalence of hydrologic soil group C/D indicates soils with moderately high runoff potential, low saturated hydraulic conductivity, and a water table within 60 cm of the surface (Natural Resources Conservation Service, 2007).

29

Soil Texture

- Clay Dominated
- Clay Loam
- Sand Dominated
- Silt Dominated
- Sand Dominated, Very Gravelly

0   2.5   5   10 Miles

N
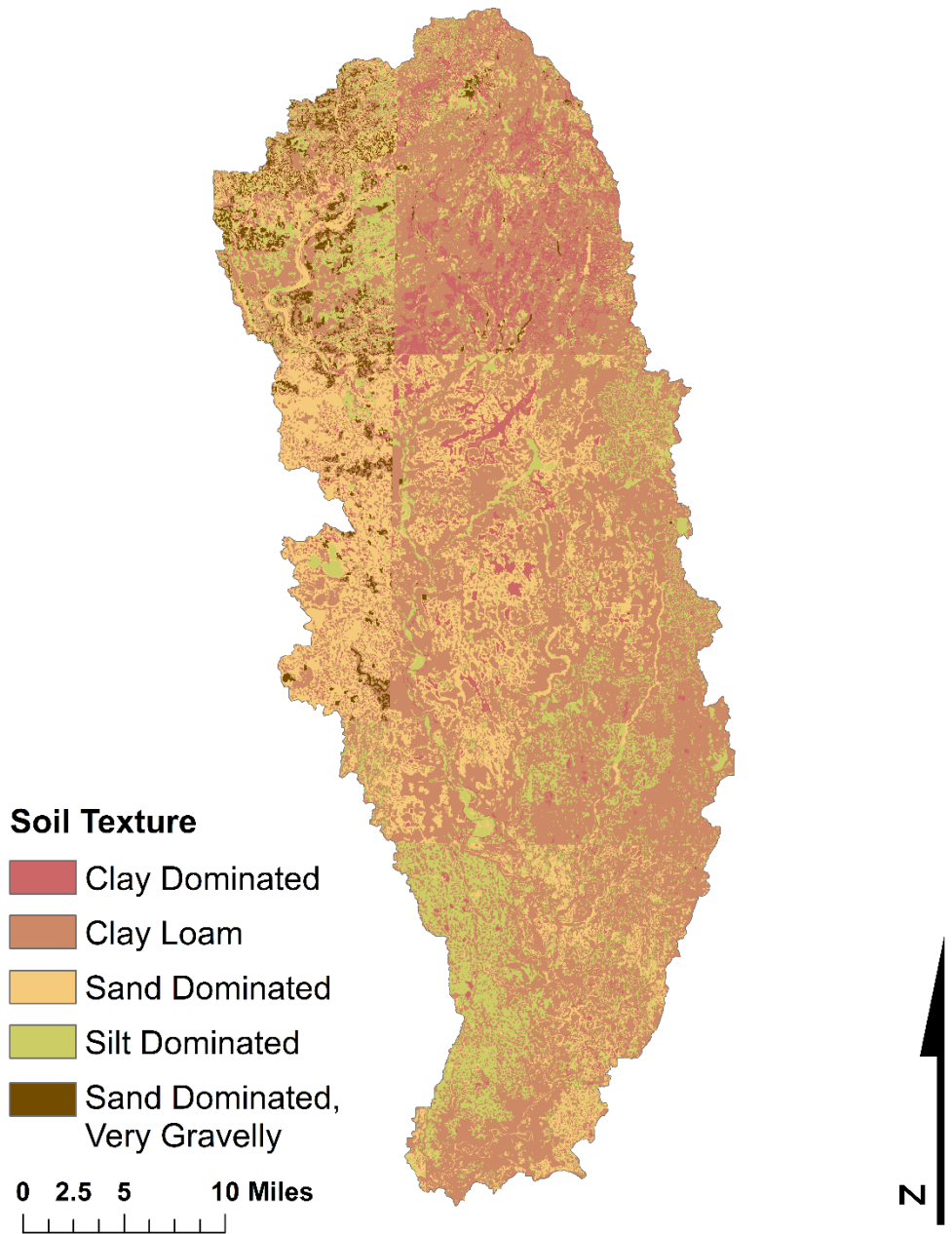
Figure 3-5: Soils data from gSSURGO. Clay Dominated includes gSSURGO classifications clay, muck and silty clay. Clay Loam includes clay loam, gravelly clay loam, and loam. Sand Dominated includes coarse sand, fine sandy loam, gravelly coarse sand, gravelly loamy coarse sand, gravelly loamy sand, gravelly sand, loamy coarse sand, loamy fine sand, sand, sandy clay loam, and sandy loam. Silt dominated includes mucky silty clay loam, silt loam, and silty clay loam. Sand Dominated, Very Gravely includes stratified very gravelly coarse sand to sand, very gravelly coarse sand, very gravelly loamy coarse sand, very gravelly loamy sand, and very gravelly sand.
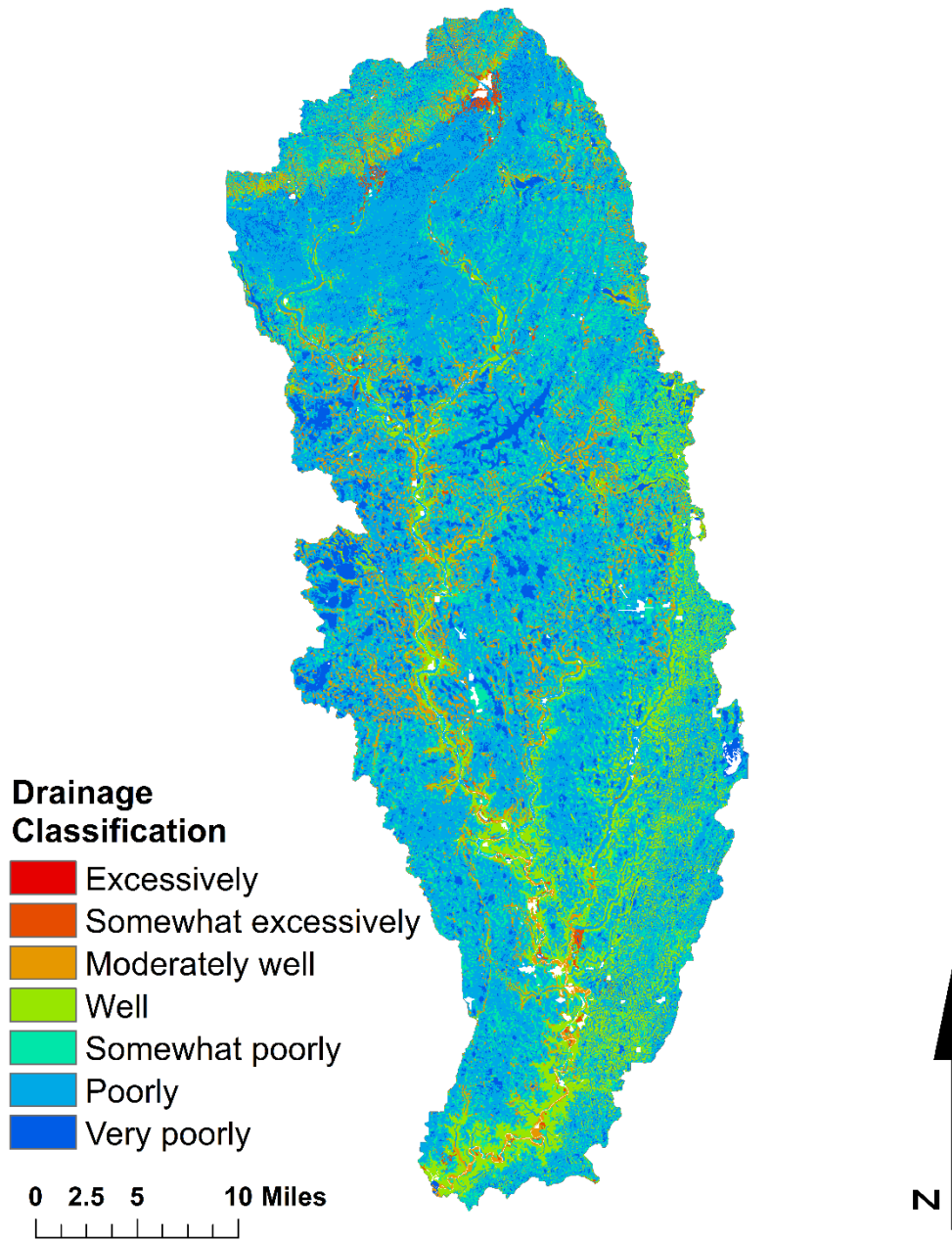
Figure 3-6: Soil Drainage Classification for the Boone River watershed.
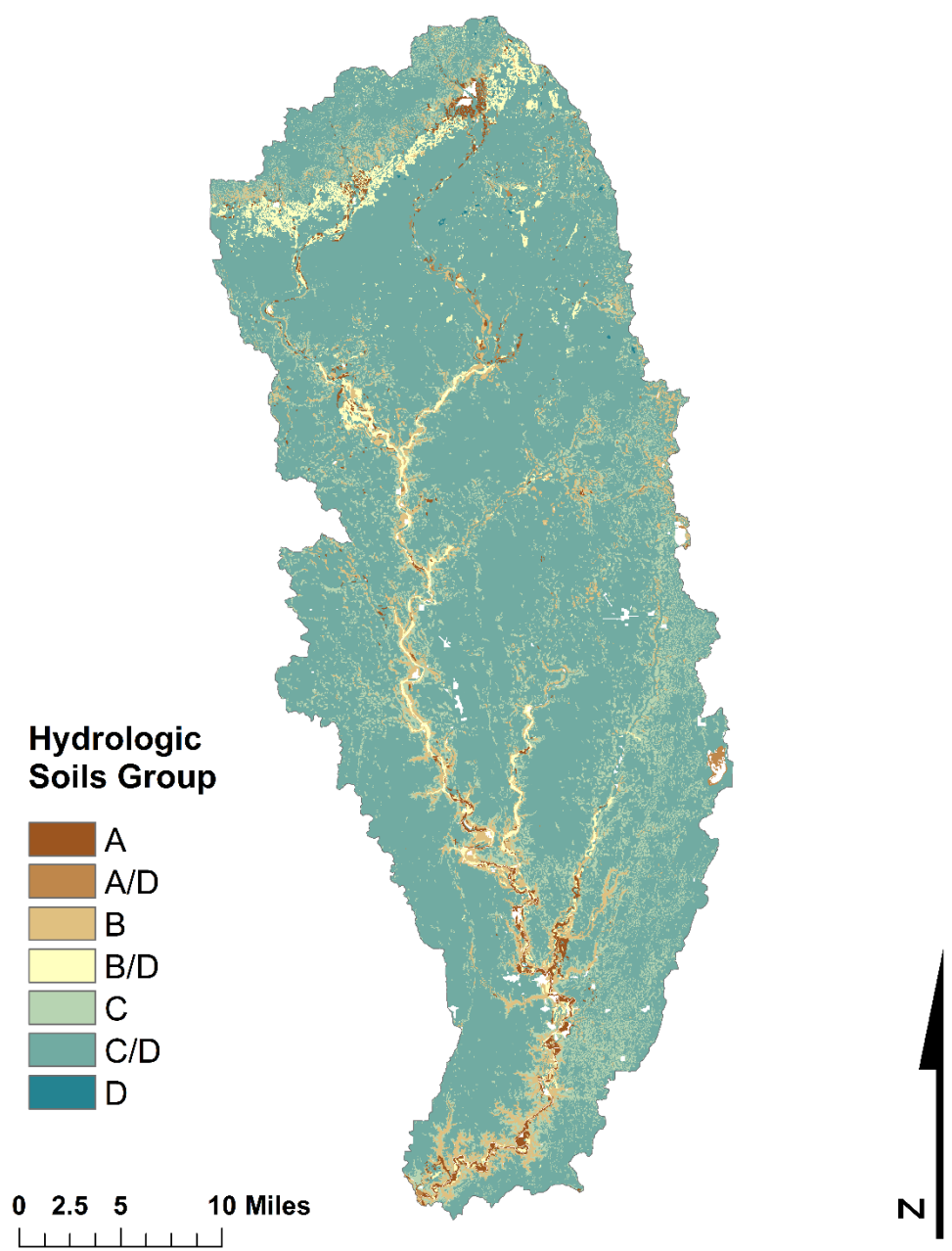
Figure 3-7: Hydrologic soils group for the Boone River watershed.

3.7 Hydrologic Alterations

      The Boone River watershed has undergone significant hydrologic alterations to make its landscape more amenable to conventional agriculture. These alterations were organized by drainage districts formed beginning in the early 1900s and include the installation of subsurface tile lines, the digging of ditches, and the straightening of existing channels (McCorvie & Lant, 1993; Thompson, 2002). Approximate public drainage district boundaries largely coincide with land in use for row crop agriculture (Figure 3-8)(Iowa Geodata, n.d.). The extent of these drainage districts covers more than 75 percent of the Boone River watershed. Largely excluding drainage tile due to lack of mapping, there are approximately 1,180 miles of drainage district infrastructure—including ditches, culverts, channelized streams, and limited amounts of tile lines (Figure 3-9)(Iowa Geodata, n.d.).
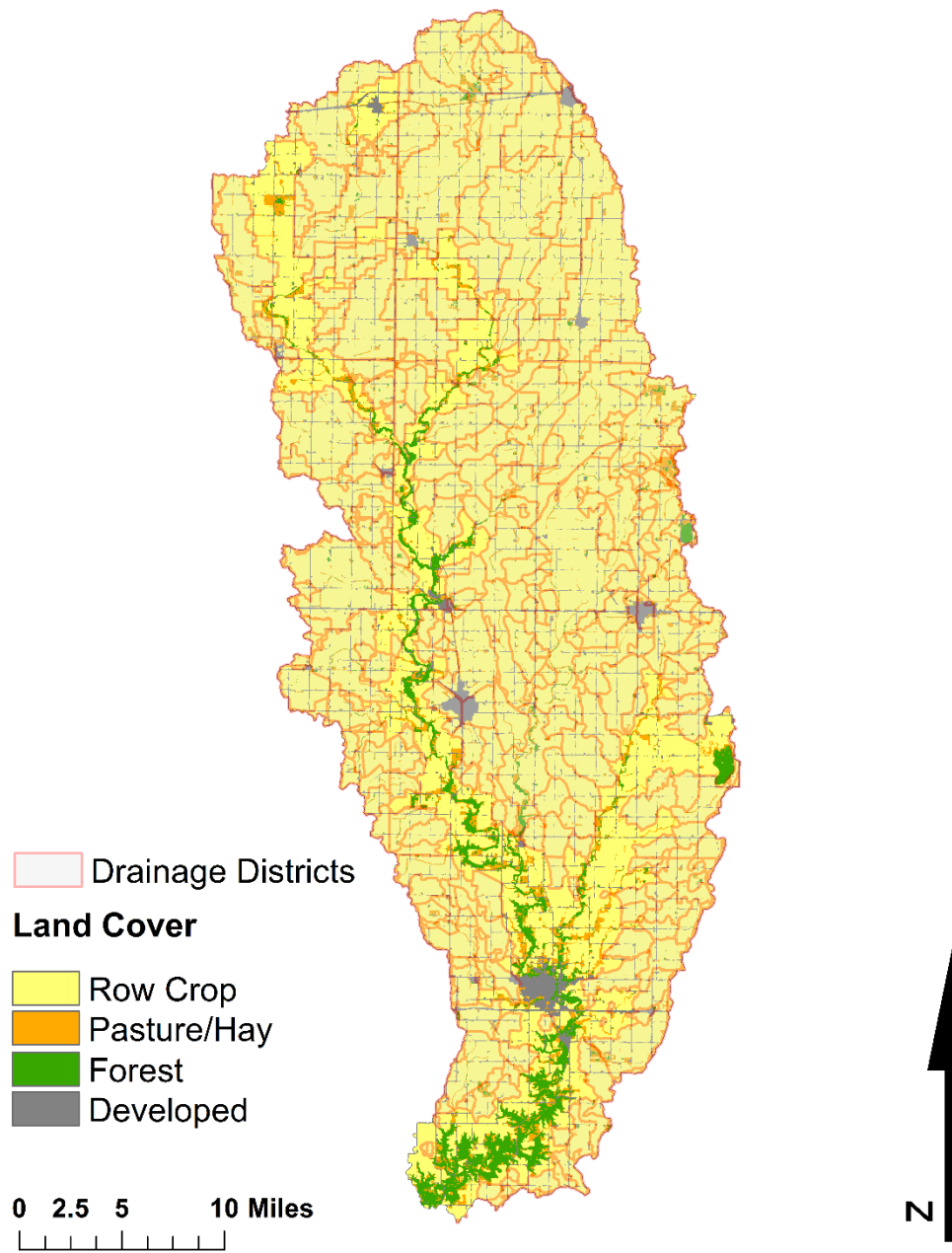
Figure 3-8: Approximate locations of drainage districts in the Boone River Watershed.
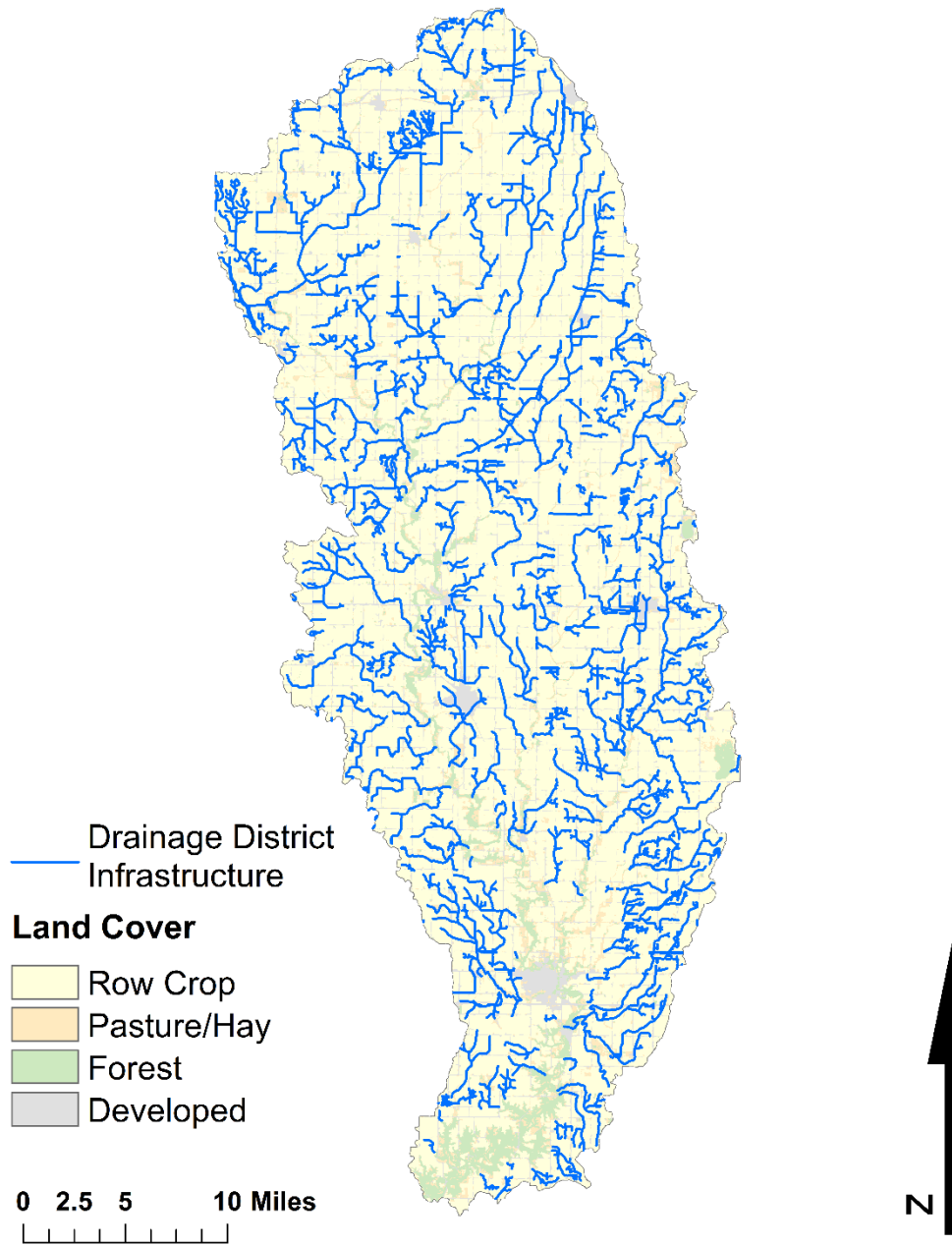
Figure 3-9: Approximate locations of drainage district infrastructure including drainage ditches, culverts, channelized streams, and limited amounts of tile lines.

3.8 Monitoring Network

The Boone River watershed currently has two currently operating USGS stream gages, two USGS sites with sparse peak flow observations, one Iowa Flood Center bridge sensor, three rain gages (two operated by the NWS as part of the HADS network, one operated by ISU), one soil moisture sensor operated by ISU (co-located with the ISU rain gage), and four water quality sensors (three operated by IIHR and one defunct operated by the USGS) (Table 3-1, Figure 3-10). Radar comes from the NWS and coverage for the Boone River watershed comes from the Des Moines station (DMX).

Table 3-1: Monitoring data sources for the Boone River watershed

Type	Source	Sensor ID	Location	Data Available	Start Date	End Date
Stream Gage	USGS	05481000	Webster City, Boone River	Discharge	10/1/1990	Present
				Gage Height	8/29/2017	Present
	USGS	05480820	Goldfield, Boone River	Discharge	10/01/2011	Present
				Gage Height	03/01/2009	Present
	USGS	05480993	Webster City, Brewers Creek Trib.	Peak Flow	6/17/1990	3/6/2017
				Annual Water-Data Report	2006	2013
	USGS	05480390	Clarion, White Fox Creek	Gage Height	10/29/2018	Present
	IIHR	BOONERV01	Goldfield, Boone River	Stage	--	Present
Rain Gage	NWS	GLDI4	Goldfield	Rainfall	--	Present
	NWS	WBCI4	Webster City	Rainfall	--	Present
	ISU	KNAI4	Near Kanawha	Rainfall	--	Present
Soil Sensor	ISU	KNAI4	Near Kanawha	Soil Moisture	--	Present

36

Table 3-2—Continued

				Soil Temperature	--	Present
Water Quality	USGS	05481000	Webster City, Boone River	Temperature (water)	11/22/2011	Present
				Nitrate and Nitrite	3/15/2012	10/2/2017
	IIHR	WQS0081	Webster City, Boone River	Nitrate and Nitrite as N	2018	Present
	IIHR	WQS0060	Webster City, Frye Oxbow	Dissolved Oxygen	2017	2017
				Nitrate and Nitrite as N	2017	2017
				pH	2017	2017
				Specific Conductance	2017	2017
				Temperature (water)	2017	2017
	IIHR	WQS0039	Goldfield, Boone River	N load, yield, and associated metrics	2016	Present
				Temperature (water)	2016	Present
				Turbidity	2016	Present
radar	NWS	DMX	Des Moines/Polk County	Rainfall	--	Present
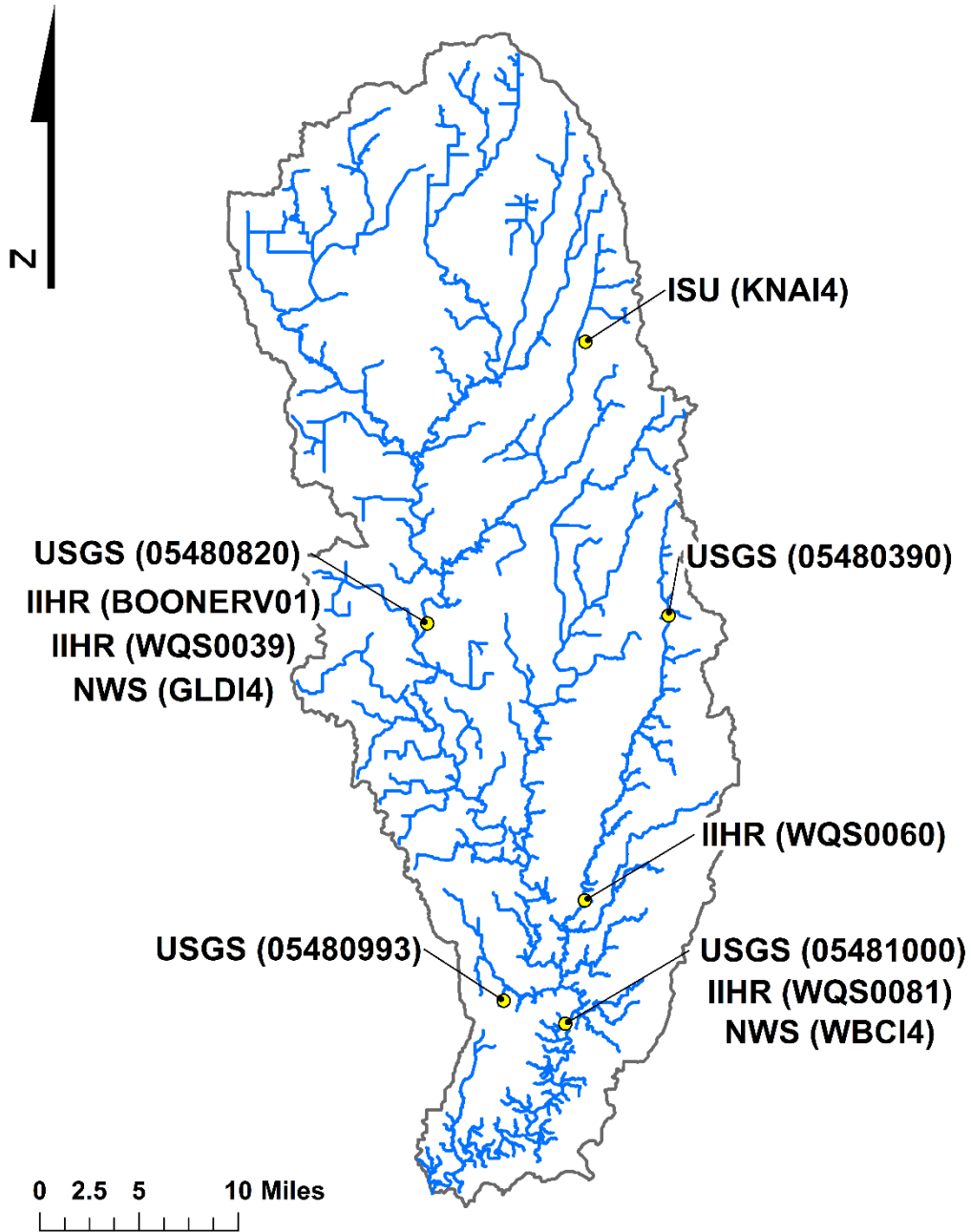
Figure 3-10: Locations, operating institutions, and sensor IDs of monitoring network sites in the Boone River watershed.

3.9 Hydrology

3.9.1 Annual Water Cycle

With USGS stream gage data from the Boone River watershed dating back to 1941 and PRISM long term annuals available through 2017, the annual water cycle can be well characterized through 77 years of record. Precipitation from PRISM's 30 year normal (1981 to 2010) show average annual precipitation in the Boone River watershed to be just over 34 inches (PRISM Climate Group, n.d.). Long term annuals from PRISM show a positive trend starting at ~30 inches in 1941 and increasing to ~34 inches in 2017 (Figure 3-11). Annual discharge is from the USGS gage on the Boone River at Webster City (05481000). Discharge also shows a positive trend, starting at ~300 cubic feet per second (cfs) in 1941 and climbing to ~750 cfs in 2017 (Figure 3-12). Using the assumption of long term balances between precipitation, runoff, and evapotranspiration (ET) and assuming net changes in groundwater to be near zero, discharge is subtracted from precipitation to estimate ET (Figure 3-13). ET shows a negative trend starting in 1941 at ~25 inches and decreasing to ~22 inches in 2017. For determining the annual runoff coefficient annual discharges from the USGS were divided by the annual rainfalls from PRISM. The trend for the period shows runoff coefficient being ~0.15 in 1941 and ~0.34 in 2017 (Figure 3-14). Baseflow was found using Purdue University's Web GIS Based Hydrograph Analysis Tool (WHAT) using the local minimum method (Jae Lim et al., 2005). Baseflow increases from ~160 cfs in 1941 to ~460 cfs in 2017 (Figure 3-15). Plotting baseflow as a fraction of discharge and performing a linear regression reveals increases in baseflow fraction from ~0.57 in 1941 to ~0.62 in 2017 (**Error! Reference source not found.**). From this water cycle assessment precipitation, discharge, runoff coefficient, baseflow, and baseflow fraction are all shown to be increasing while ET is decreasing.
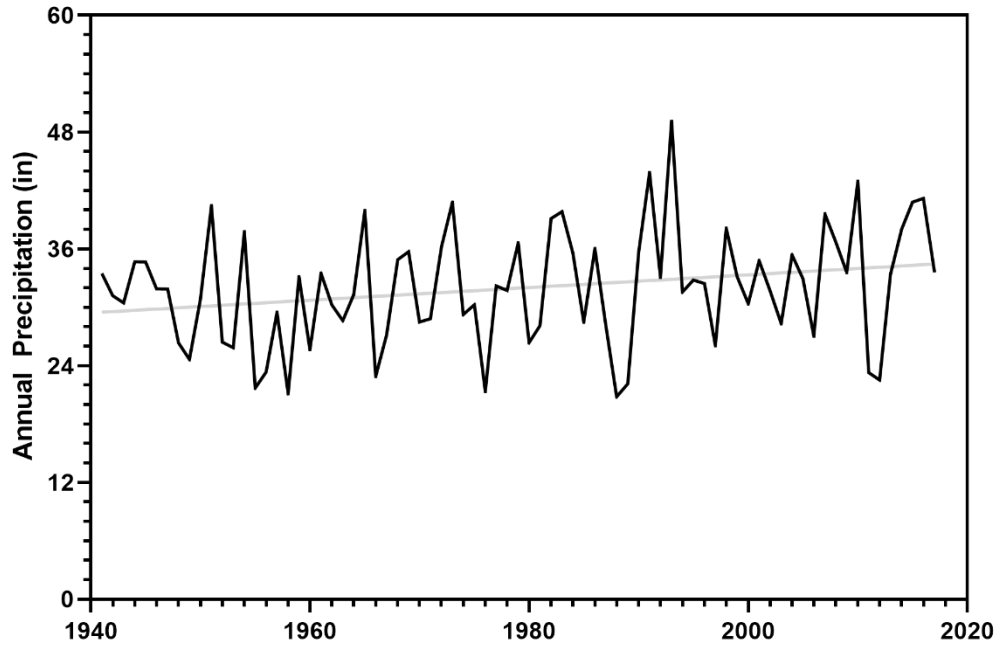
Figure 3-11: Annual precipitation in the Boone River watershed (black) and linear regression (grey).
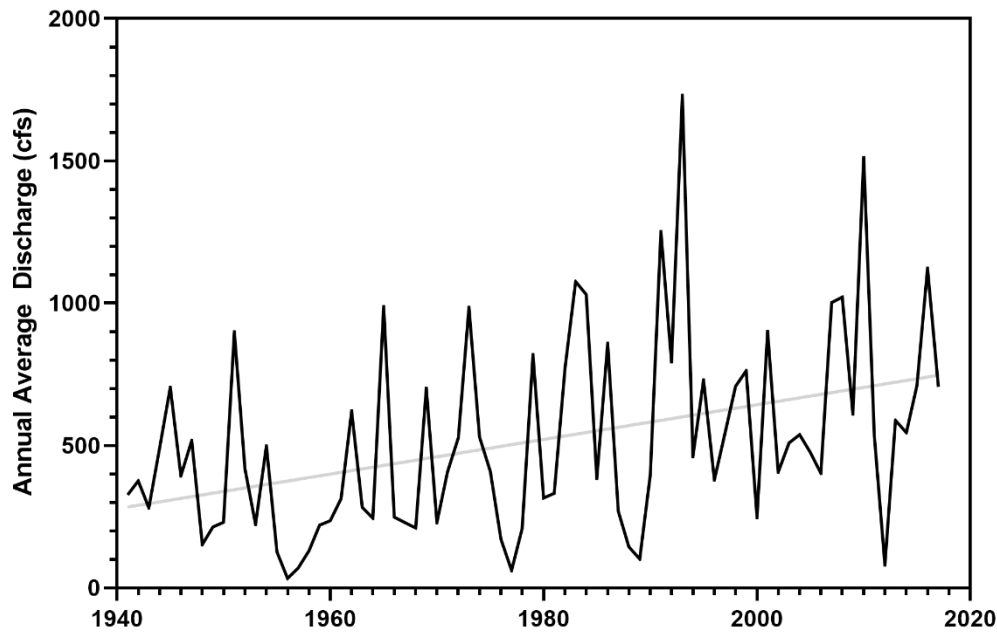
Figure 3-12: Average annual discharge from the Boone River at the Webster City USGS gage 05481000 (black) and linear regression (grey).

40
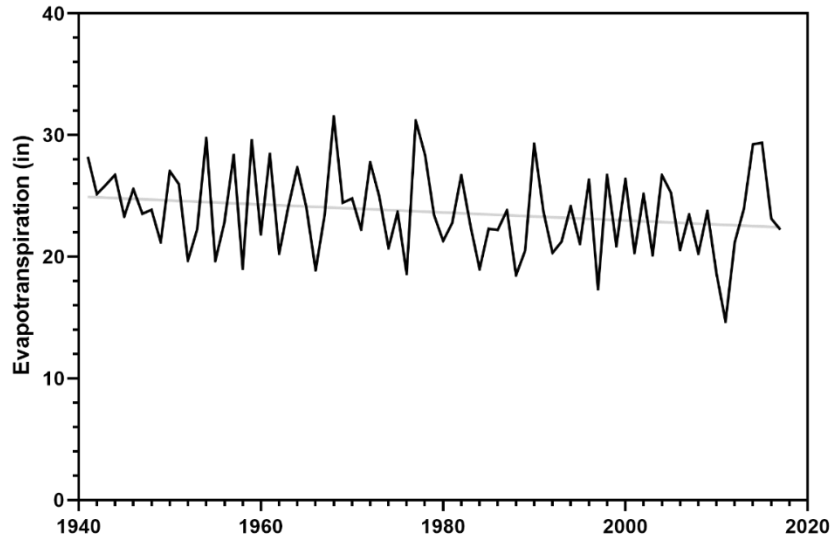
Figure 3-13: Estimated evapotranspiration for the Boone River watershed at the Webster City USGS gage 05481000 (black) and linear regression (grey).
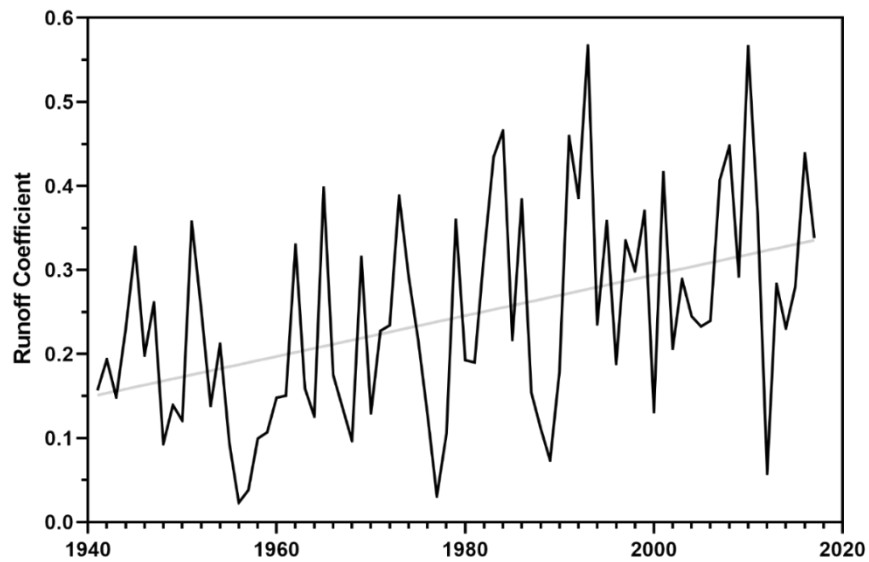
Figure 3-14: Annual baseflow for the Boone River at Webster City USGS gage 05481000 (black) and linear regression (grey).

41
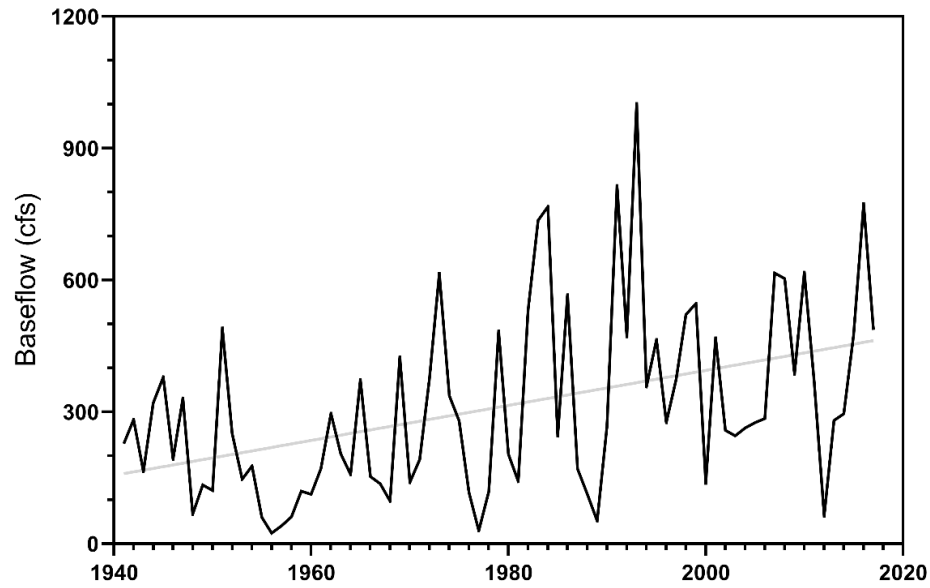
Figure 3-15: Annual baseflow for the Boone River at Webster City USGS gage 05481000 (black) and linear regression (grey).
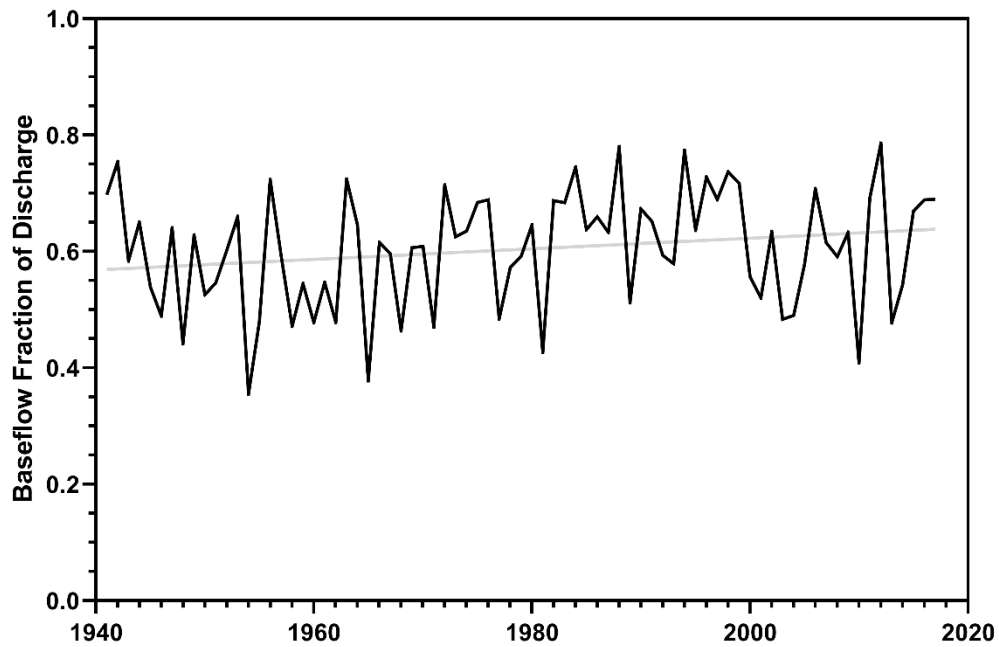
Figure 3-16: Baseflow as a fraction of discharge from 1941 to 2017 (black) and linear regression (grey).

42

USGS gaging station 05480820 is located on the Boone River watershed near Goldfield, Iowa. This station was installed in late 2011 and therefore the currently available USGS approved annual discharges are from 2012 to 2017. The station near Goldfield captures 418 of the Boone River watershed's 908 square miles (46.0 percent). Trends in the annual precipitation (Figure 3-17), annual discharge (Figure 3-18), runoff coefficient (Figure 3-19), baseflow (Figure 3-20), and baseflow to discharge ratio (Figure 3-21) are not meaningful due to the short period of record and the period starting in a drought year and including a relatively wet year as two of its 6 years.
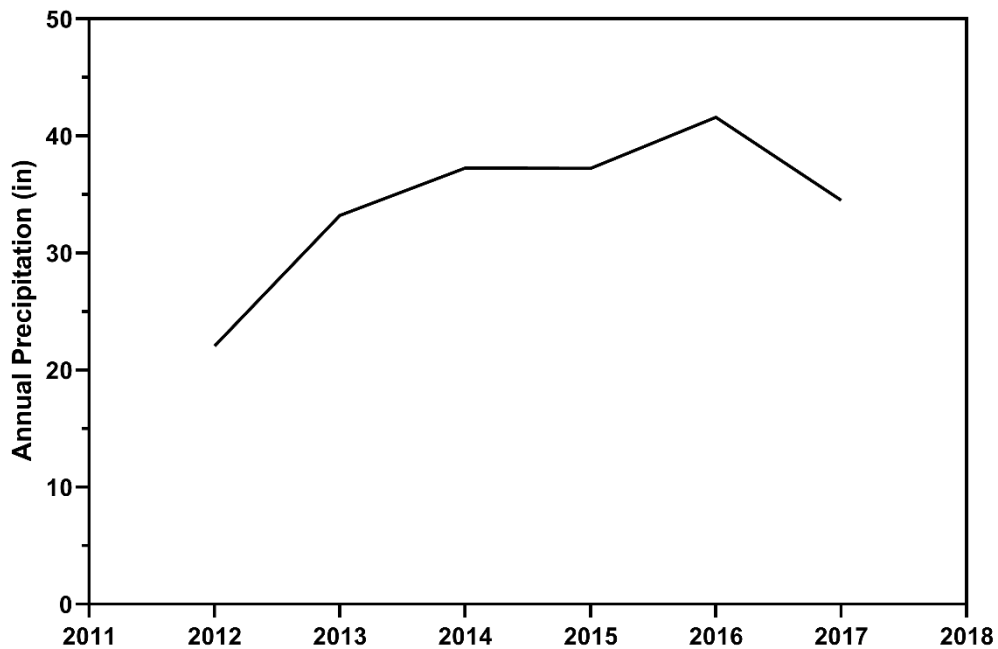
Figure 3-17: Annual precipitation for the watershed of the Boone River at Goldfield USGS gage 05480820.
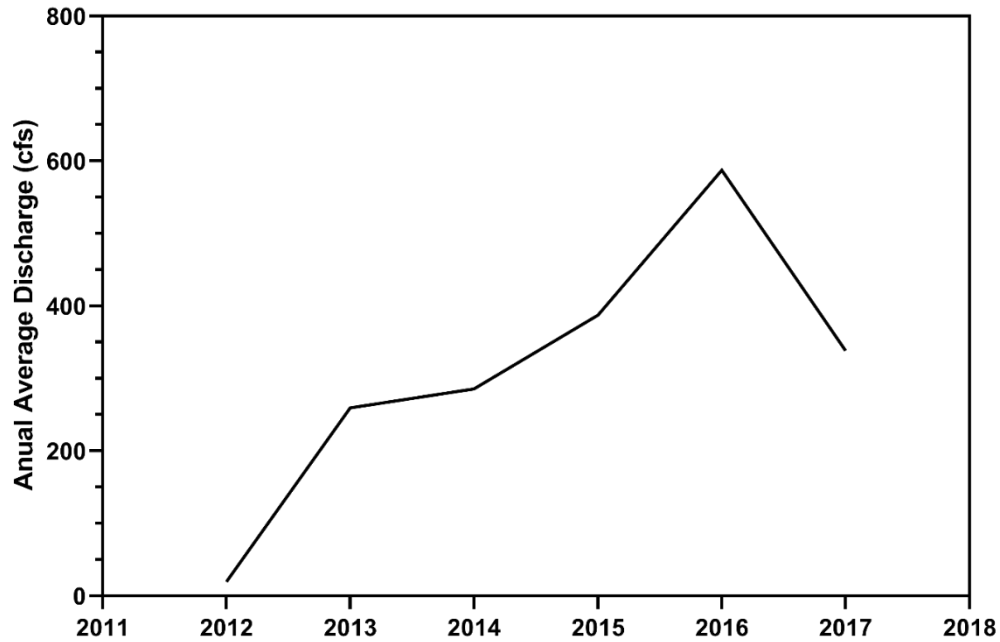
Figure 3-18: Annual average discharge of the Boone River at Goldfield USGS gage 05480820.
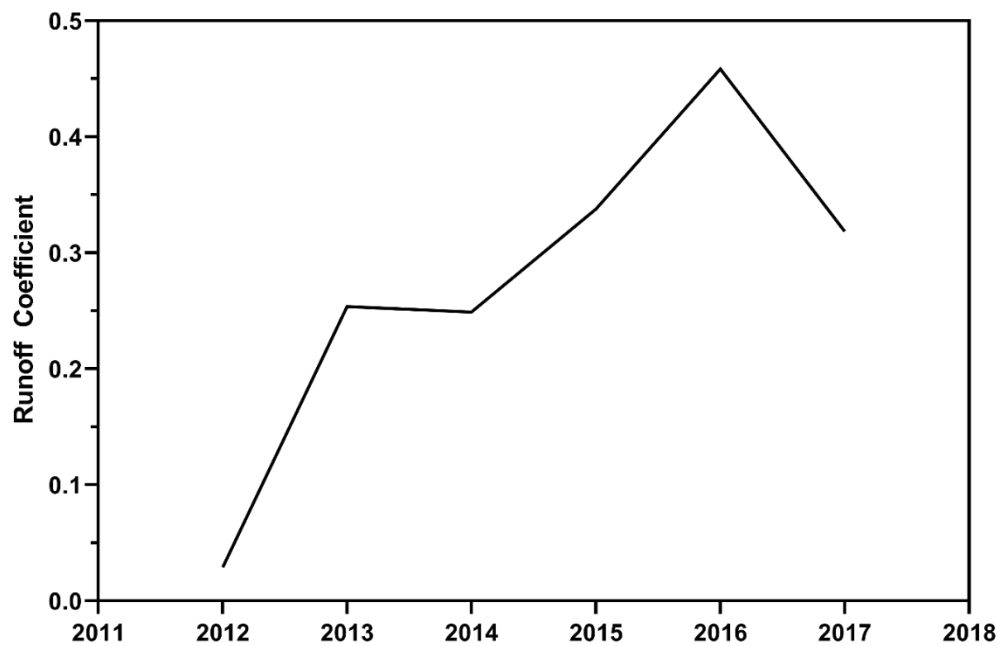
Figure 3-19: Annual runoff coefficient of the Boone River watershed at Goldfield USGS gage 05480820.

44
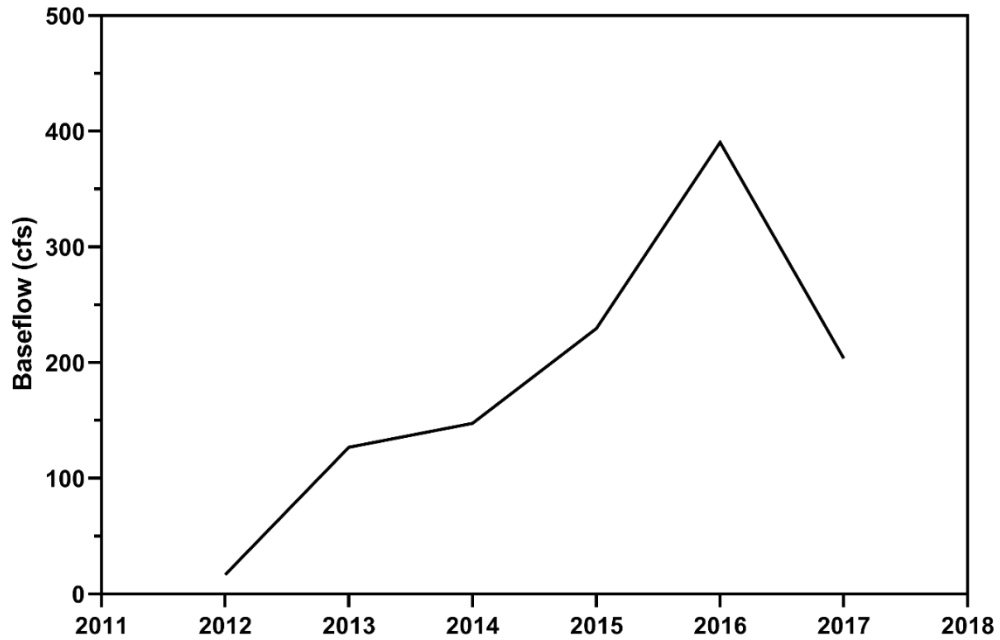
Figure 3-20: Annual baseflow of the Boone River at Goldfield USGS gage 05480820.
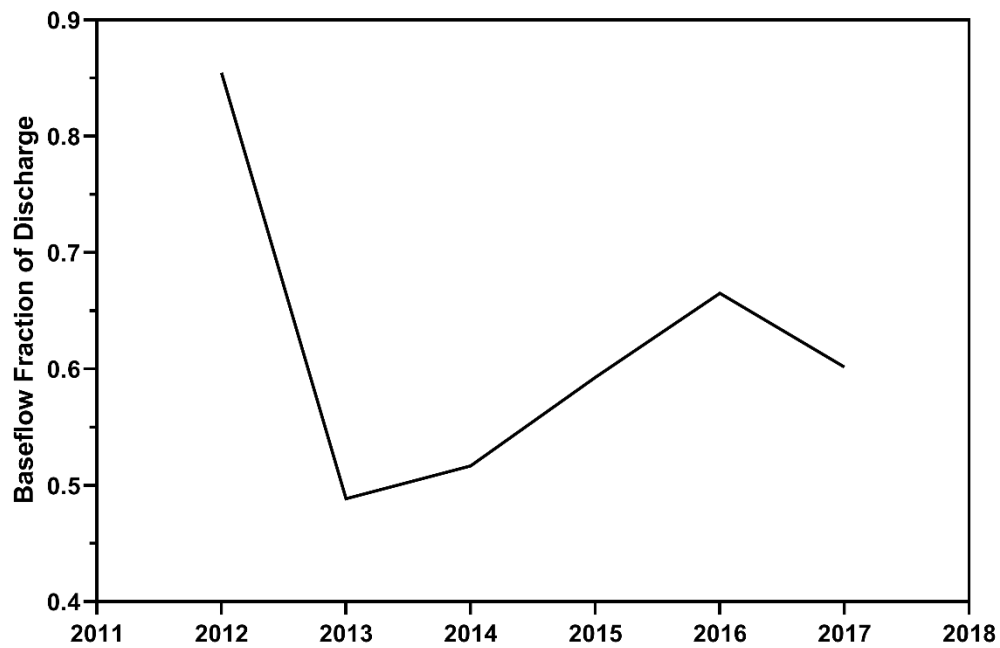
Figure 3-21: Annual baseflow fraction of discharge of the Boone River at Goldfield USGS gage 05480820.

45

3.9.2 Monthly Water Cycle

      The 30 year normal (1981-2010) monthly water cycle of the Boone River watershed is typical for the Midwest with the wet months—May, June, July, and August—delivering 19 of the 34 average inches of annual rainfall (PRISM Climate Group, n.d.). The month with the highest amount of rainfall is June and the month with the least amount of rainfall is January (Figure 3-22). Average monthly discharges over the same 30 year period deviate from the trends observed in precipitation (Figure 3-23). The four months with the highest average discharges are March, April, May, and June and account for more than 65 percent of the average annual discharge for the 30 year period. June has the highest average monthly discharge at 1680 cfs while January has the lowest at 140 cfs. The steady drop off seen in precipitation after the peak month is a comparatively precipitous plummet for discharge relative to precipitation with the months after June (1680 cfs) averaging just 395 cfs. The reason for this disparity between monthly precipitation and discharge is likely due to snow melt effects in spring and high temperatures paired with decreasing rainfall and high evapotranspiration rates in the late summer and fall.
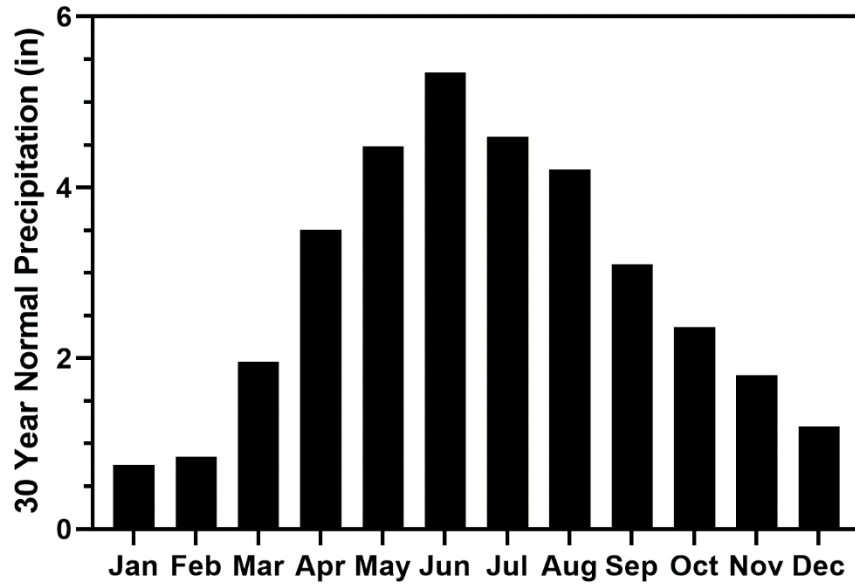
Figure 3-22: 30 year normal precipitation from 1981 to 2010 for the Boone River watershed at Webster City USGS gage 0541000.
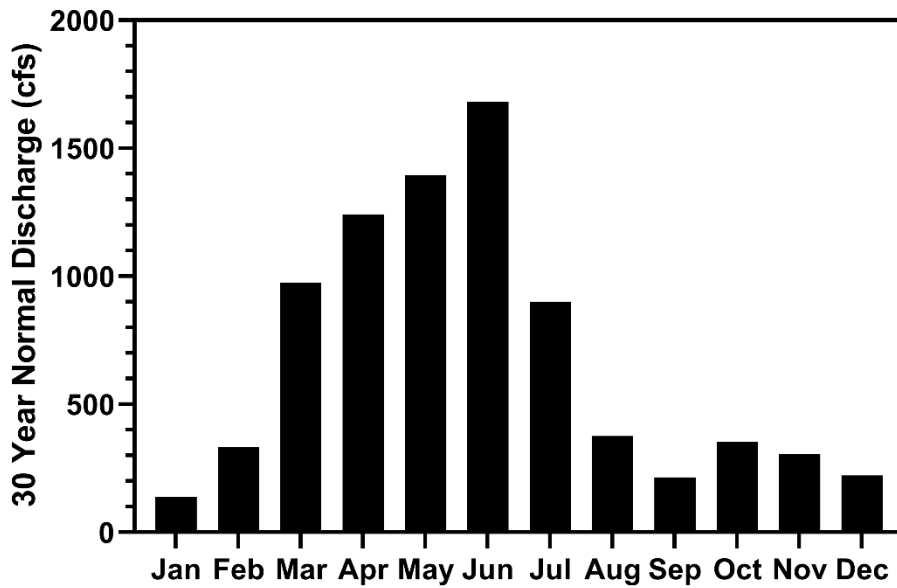
Figure 3-23: 30 year normal discharge from 1981 to 2010 for the Boone River watershed at Webster City USGS gage 0541000.

3.9.3 Flood Climatology

Characterizing the nature of flooding in a watershed is an important part of developing a better understanding of the processes which contribute to it. Peak flow frequency analysis was done using the USGS's PeakFQ tool version 7.1 for Bulletin 17B based estimates (Interagency Advisory Committee on Water Data, 1982) and version 7.2 for Bulletin 17C based estimates (England et al., 2018) (Figure 3-24 and Figure 3-25 respectively). Annual exceedance probabilities; return periods; and flows thresholds for the systematic record, Bulletin 17B, and Bulletin 17C are supplied in Table 3-3. In the period of record (1991 to present) for instantaneous data at the USGS gage at Webster City (05481000) there have been 50 identified peaks exceeding the 2-year food as defined by Bulletin 17B (Figure 3-26). Of these 50 peaks, ten have exceeded the 10-year food, and 2 have exceeded the 50 year flood. Peak flows in the Boone River watershed have a distribution peaking in early June. Of the 50 peaks exceeding the 2-year food, 14 (28 percent) have occurred in June followed by May with 9 (18 percent), April with 7 (14 percent), and July with 6 (12 percent) (Table 3-4). No analysis was done at the USGS gage 05480820 at Goldfield due to the short period of record.

48
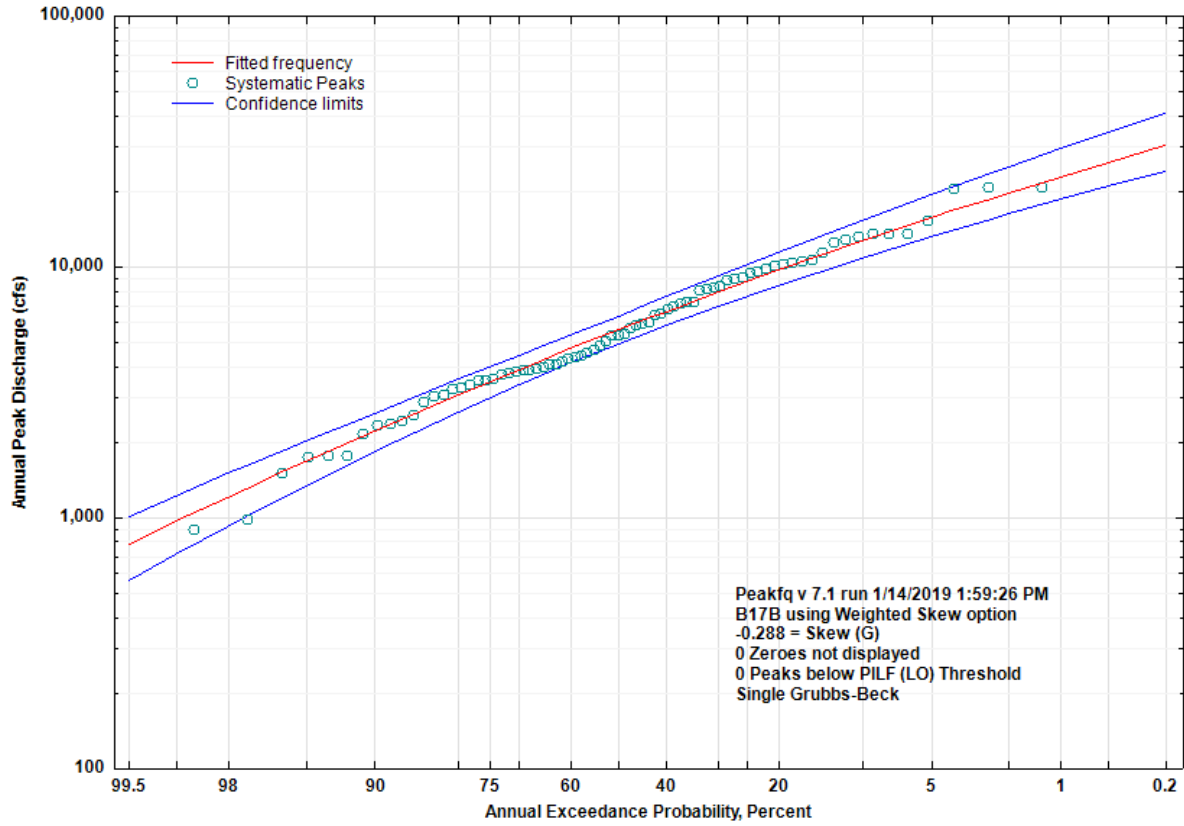
Figure 3-24: Annual Exceedance probability for the Boone River at Webster City USGS gage 0548100. Figure produced with the USGS PeakFQ tool version 7.1 using Bulletin 17B methodology.
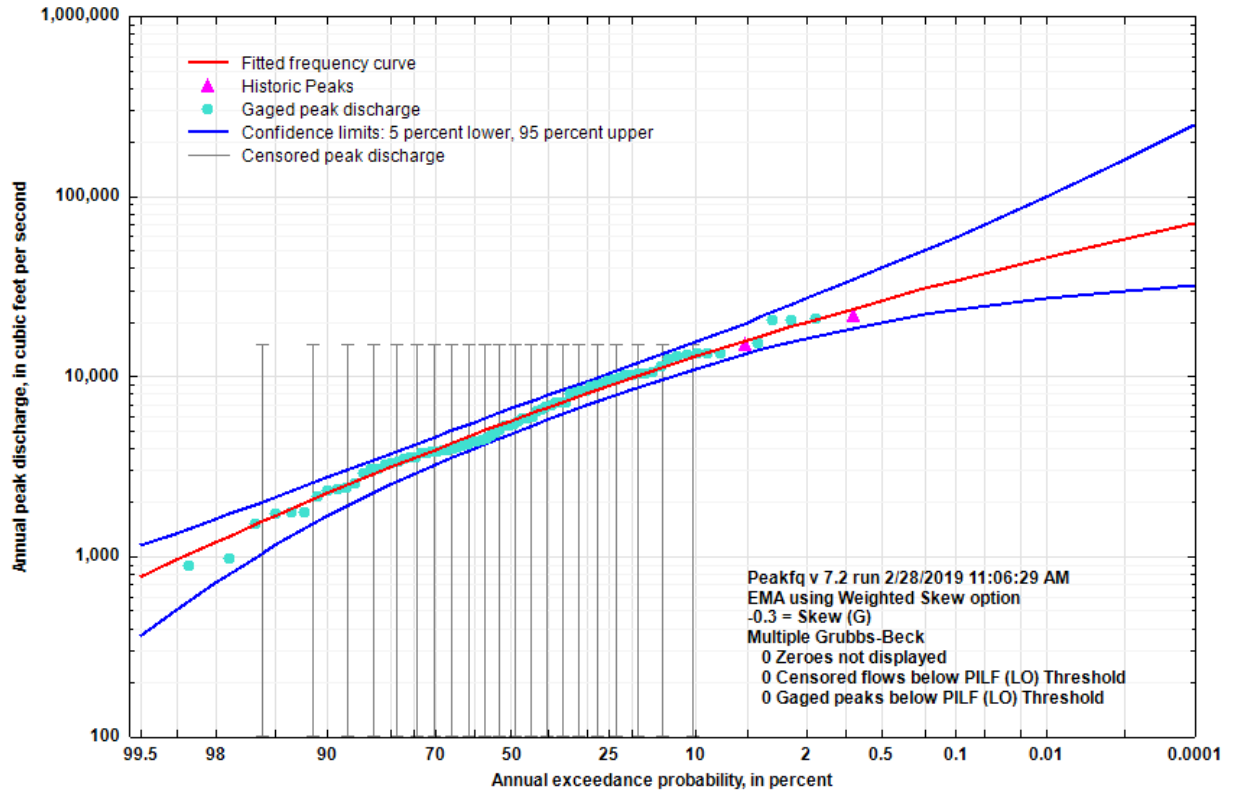
Figure 3-25: Annual Exceedance probability for the Boone River at Webster City USGS gage 0548100. Figure produced with the USGS PeakFQ tool version 7.2 using Bulletin 17C methodology.

Table 3-3: Annual exceedance probability, return period, Bulletin 17B flow thresholds, systematic record flow thresholds, Bulletin 17B flow thresholds, Bulletin 17C flow thresholds, and the lower and upper confidence intervals for the Bulletin 17C thresholds for the Boone River at Webster City USGS gage 05481000. Data from USGS PeakFQ tool versions 7.1 and 7.2.

Annual Exceedance Probability	Return Period (yr)	Systematic Record (cfs)	Bulletin 17B (cfs)	Bulletin 17C (cfs)	5% Lower Confidence Interval	95% Upper Confidence Interval
0.5	2	5,553	5,572	5,632	4,772	6,592
0.2	5	9,636	9,642	9,769	8,366	11,450
0.1	10	12,650	12,610	12,790	10,900	15,380
0.04	25	16,700	16,580	16,800	14,040	21,470
0.02	50	19,860	19,640	19,890	16,180	26,810
0.01	100	23,110	22,760	23,040	18,120	32,840
0.005	200	26,460	25,950	26,250	19,850	39,660
0.002	500	31,030	30,270	30,600	21,900	50,060
0.001	1,000	-	-	35,260	23,280	58,140
0.0001	10,000	-	-	45,500	27,050	98,830
0.00001	100,000	-	-	57,600	29,880	158,800
0.000001	1,000,000	-	-	70,070	32,050	249,000
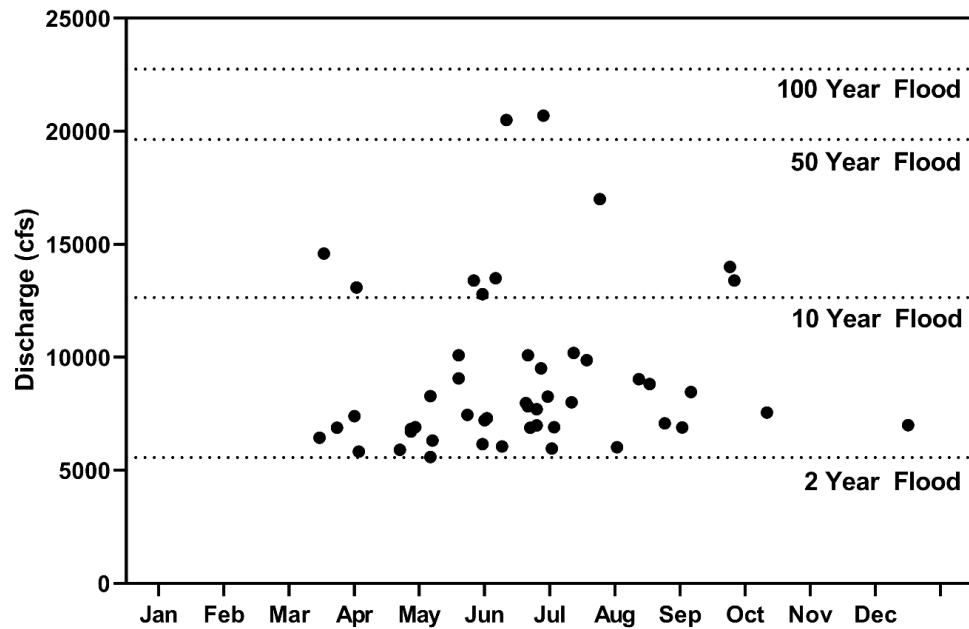
Figure 3-26: Flood peaks over the 2-year food threshold for the period 1991 to 2018 with the 2, 10, 50, and 100 year Bulletin 17B flood thresholds denotde with dotted lines.

Table 3-4: Number of peak, range of discharges, and mean flood peak by month for the period 1991 to 2018 at the USGS station 05481000 at Webster City, Iowa.

Month	Number of Floods	Percent of Floods (%)	Max discharge (cfs)	Mean Flood Peak (cfs)
Jan	0	0	-	-
Feb	0	0	-	-
Mar	3	6	14,600	9,313
Apr	7	14	13,100	7,531
May	9	18	13,400	8,800
Jun	14	28	20,700	10,041
Jul	6	12	17,000	9,665
Aug	5	10	9,040	7,612
Sep	4	8	14,000	10,693
Oct	1	2	7,560	7,560
Nov	0	0	-	-
Dec	1	2	7,010	7,010

52

3.9.4 Floods of Record

The National Weather Service has recorded 96 historic crests for the Boone River at Webster City over the 9 foot action stage (National Weather Service, 2019). Of these 96 historic crests spanning the period of 1918 to 2018, 47 have occurred after 1990. The highest recorded stage occurred on June 10th, 1918 and reached a height of 19.1 feet (Table 3-5). Two flood years stand out in Iowa's collective memory for their devastating, state-wide flooding: 1993 and 2008. In 1993, the Boone River set what would become its tenth all time flood peak and in 2008 it would set what would become its fourth.

Table 3-5: Top ten historic crests identified by the National Weather Service.

Rank	Stage (ft)	Peak Discharge (cfs)	Date
1	19.1	-	6/10/1918
2	18.55	-	6/22/1954
3	18.17	20,700	6/28/2010
4	17.74	20,500	6/10/2008
5	16	-	6/18/1932
6	15.94	17,000	7/23/2010
7	15.91	-	4/6/1965
8	15.63	13,500	6/5/1991
9	15.55	13,400	5/25/2004
10	15.32	13,100	4/1/1993

3.8 Summary

Located in North-Central Iowa, the 908 square mile Boone River watershed is a prototypical watershed of the Des Moines Lobe. The watershed owes its agricultural prowess to the recent glaciation, which deposited the tills which form its predominantly poorly draining clay loams and sand dominated soils. To achieve the agricultural productivity of the watershed,

53

significant alterations have been made. Drainage districts and their associated infrastructure are distributed throughout the watershed and undoubtedly play a large role in its hydrology.

On average, precipitation in the Boone River watershed has been increasing in the period from 1941 to 2017 at a rate of about one inch every fifteen years. Discharge has been increasing at a rate of about 100 cfs every fifteen years. Baseflow has been increasing in quantity by about 60 cfs every 15 years and in fraction of discharge has changed by about 5 percent over the 77 year period of record. Seasonally, precipitation reaches a maximum in June and a minimum in January and follows the prototypical distribution of the Midwestern United States. River discharge unsurprisingly also peaks in June and bottoms in January, but disproportionately higher discharges are seen in the spring due to the effects of snow melt and disproportionately lower discharges are seen in the late summer and fall due to high temperatures and evapotranspiration.

Flooding in the Boone River watershed is a frequent occurrence with eight 10-year floods and two 50-year floods happening in the 29 year period from 1991 to 2018. The 2-year flood threshold is 5,572 cfs, the 10-year flood is 12,610 cfs, the 50 year threshold is 19,640 cfs and the 100-year flood is 22,760. The majority of flooding in the Boone River watershed happens in the months of April through August. The peak flood month for the period from 1991 to 2018 is June for both number of floods and largest discharge. June is also the top month for historic crests; occupying six of the top ten spots.

CHAPTER 4: MODEL DEVELOPMENT

4.1 Introduction

The Generic Hydrologic Overland-Subsurface Toolkit (GHOST) is a continuous, physically-based, integrated, hydrologic model capable of simulating watersheds of varying scales and for long periods of time in a computationally and time efficient manner. GHOST was developed to address the needs of the Iowa Watershed Approach project to simulate watersheds 1,500 square miles in size and beyond, and to do so quickly. The model was based upon the open source MM-PIHM (Qu & Duffy, 2007; Yu, Bhatt, Duffy, & Shi, 2013). GHOST uses a triangular irregular network mesh for discretizing the domain to account for the spatial heterogeneities of Iowa and allows for the implementation of both field based and structural best management practices. Elements of the model which are necessary to understand the basic functions of the model and the changes made to represent conservation practices are reproduced here; for a full description of GHOST, see Politano (2018).

4.2 Mathematical Model Description

The model is built with three zones: the surface, the unsaturated zone, and the saturated zone (Kumar, Duffy, & Salvage, 2009). The boundary between the surface and the subsurface is static while the boundary between the two subsurface zones is dynamic and rises and falls with the water table. GHOST models surface flow, flow in the unsaturated zone, flow in the saturated zone, evapotranspiration from both the surface and the subsurface, and flow in the river network.

4.2.1 Climatological Forcing

GHOST uses meteorological forcing data to simulate precipitation and evapotranspiration. Precipitation is from hourly four-by-four kilometer radar rainfall from Nexrad Stage IV data (Lin, 2011). Whether precipitation falls as snow or rain is based upon the temperature transition preceding the precipitation. If the temperature drops from 1 °C to -3 °C, the precipitation falls as snow. Similarly, if the temperature rises through that same range, the

55

precipitation will be rain. Along with precipitation, the meteorological forcing data includes
surface temperature, long wave radiation, and pressure. These values drive the
evapotranspiration functions in the model. The meteorological forcing data are from the National
Land Data Assimilation Systems Phase 2 (NLDAS-2) dataset and come at a resolution of 11-by-
13 kilometers (Mitchell, 2004). The meteorological forcing for the GHOST model combines
these two products into a four-by-four kilometer grid with the NLDAS-2 data applied to multiple
grids.

4.2.2 Evapotranspiration

One of the largest parts of the hydrologic cycle modeled in GHOST is evapotranspiration
(ET). There are four forms of ET simulated in the model: canopy evaporation, surface
evaporation, soil evaporation, and transpiration. These four component ET sum in varying
proportions to the potential evapotranspiration as defined by the Penman-Montieth equation
after the FAO56 guidelines (Allen, Pereira, Raes, & Smith, 1998). These four ET components
are in a hierarchy where priority first goes to canopy evaporation, then surface evaporation, then
soil evaporation and transpiration. The progression from one form of ET to the next is dependent
on the availability of potential evapotranspiration.

Potential evaporation, or E_p is found using the Penman-Montieth equation (Allen et al.,
1998):

$$E_i^p = \frac{\left[\left(1 - f_i^S\right)R_i^S(1 - A_i) + R_i^l - G_i\right]\Delta_i + \frac{C_p\rho_a}{r_i^a}(e_i^* - e_i)}{\rho_w\lambda_i\left(\gamma_i\left(1 + \frac{r_i^S}{r_i^a}\right) + \Delta_i\right)}$$

(1)

where R_i^S is the incoming shortwave radiation, A_i is the albedo, R_i^l is the outgoing longwave
radiation, , G_i is the ground heat flux, C_p is the specific heat at constant pressure, ρ is the density,
r_i^a is the aerodynamic resistance, e_i is the vapor pressure, λ_i is the latent evaporation heat, and γ_i

56

is the psychrometric constant. For more on the calculations of potential evapotranspiration in GHOST, see Politano (2018).

Actual evapotranspiration is found using a reference ET. For the reference, GHOST uses an alfalfa-based ET:

$$ET_i^a = K_i^{crop} ET_i^R$$

(2)

where ET_i^a is the actual evapotranspiration, K_i^{crop} is the empirical crop coefficient relating actual evapotranspiration to ET_i^R, the alfalfa-based reference ET. For more on the calculations of potential evapotranspiration in GHOST, see Politano (2018).

Interception storage and canopy evaporation are modeled after Kristensen and Jensen (1975) and Panday and Huyakorn (2004) using a "bucket" model where leaf area index acts as an interception factor controlling the size of the bucket. Maximum interception storage in GHOST is defined as a function of an interception storage constant and the leaf area index (LAI):

$$\vartheta_i^{max} = C_{\vartheta i} LAI_i(t)$$

(3)

where ϑ_i^{max} is the maximum interception storage, C_ϑ is the interception storage constant, and $LAI_i(t)$ is the leaf area index of a type i at time (t). Intermediate interception storage is defined as the minimum between the max storage and the sum of the current storage and the precipitation from the next time step:

$$\vartheta_i^* = min\left(\vartheta_i^{max}, \vartheta_i^{t-\Delta t} + P_i \Delta t\right)$$

(4)

where ϑ_i^* is the intermediate interception storage, $\vartheta_i^{t-\Delta t}$ is the interception storage from the previous time step, and $P_i \Delta t$ is the additional precipitation in the current time step. Canopy evaporation is defined as the minimum between the intermediate canopy interception and the potential evapotranspiration:

$$E_i^{can} = min\left(\frac{\vartheta_i^*}{\Delta t}, E_i^p\right)$$

57

where E_i^{can} is the canopy evaporation. Interception storage is then modeled as the difference between the intermediate canopy storage and the canopy evaporation over the time step:

$$\vartheta_i = \vartheta_i^* - E_i^{can}\Delta t$$

(6)

If potential evapotranspiration is not depleted by canopy evaporation, evaporation from surface water occurs next and is defined as the minimum between the total amount of water on the surface and the difference between the potential evapotranspiration and canopy evaporation:

$$E_i^{surf} = min\left(\frac{y_i^{surf}}{\Delta t},\left(E_i^p - E_i^{can}\right)\right)$$

(7)

where E_i^{surf} is the surface evaporation and y_i^{surf} is the depth of water on the surface. For more on the functions of the canopy in GHOST, see Politano (2018).

Transpiration is found following Panday and Huyakorn (2004) and is activated in the model if potential evapotranspiration has not been depleted by canopy or surface water evaporation. Transpiration is modeled as the max between the product of three functions (f_1 and f_2 described below) and zero:

$$T_i = max\left(f_1(LAI_i)f_2(\theta_i)f_R\left(ET_i^a - E_i^{can} - E_i^{surf}\right),0\right)$$

(8)

where $f_1(LAI_i)$ is defined using Beer Lambert law as the fraction of incident radiation absorbed by the canopy:

$$f_1(LAI_i) = \left(1 - e^{-k_i^{ext}LAI_i}\right)$$

(9)

where k_i^{ext} is the canopy extinction coefficient. The second function, $f_2(\theta_i)$, is the effect water content has on the transpiration rate:

58

$$f_2(\theta_i) \begin{cases} 0 & if\ 0 < \theta_i \leq \theta_i^{WP} \\ 1 - \left(\dfrac{\theta_i^{FC} - \theta_i}{\theta_i^{FC} - \theta_i^{WP}}\right)^{C_3/ET_i^a} & if\ \theta_i^{WP} < \theta_i \leq \theta_i^{FC} \\ 1 & if\ \theta_i^{FC} < \theta_i \leq \theta_i^{O} \\ \left(\dfrac{\theta_i^{FC} - \theta_i}{\theta_i^{FC} - \theta_i^{WP}}\right)^{C_3/ET_i^a} & if\ \theta_i^{O} < \theta_i \leq \theta_i^{AN} \\ 0 & if\ \theta_i^{O} < \theta_i \end{cases}$$

(10)

where θ_i is the soil water content, θ_i^{WP} is the soil water content at the wilting point, θ_i^{FC} is the soil water content at field capacity, θ_i^{O} is the soil water content at the oxic limit, θ_i^{AN} is the soil water content at the anoxic limit, and C_3 is a dimensionless fitting parameter. Transpiration in the unsaturated region is calculated as the product of the transpiration and the minimum between one and the difference between the soil depth and height of groundwater divided by the root depth:

$$T_i^{uns} = T_i min\left(1, \frac{D_i^{soil} - y_i^{GW}}{R_i}\right)$$

(11)

where T_i^{uns} is the transpiration in the unsaturated zone, T_i is transpiration, D_i^{soil} is the element depth, y_i^{GW} is the height of groundwater, and R_i is the root depth.

Soil evaporation occurs simultaneously with transpiration and is found following Panday and Huyakorn (2004). The evaporation rate from the soil is defined as the max between the product of three functions (f_3 and f_E described below) and zero:

$$E_i = max\left((1 - f_1(LAI_i))f_3(\theta_i)f_E\left(ET_i^a - E_i^{can} - E_i^{surf}\right), 0\right)$$

(12)

where $f_3(\theta_i)$ is a function of soil water contents at the saturation limiting and energy limiting stages of evaporation:

$$f_3(\theta_i) \begin{cases} 0 & if\ \theta_i < \theta_i^{e2} \\ \left(\dfrac{\theta_i - \theta_i^{e2}}{\theta_i^{e1} - \theta_i^{e2}}\right) & if\ \theta_i^{e2} < \theta_i \leq \theta_i^{e1} \\ 1 & if\ \theta_i^{e1} < \theta_i \end{cases}$$

(13)

59

where θ_i^{e2} is the soil water content below which evaporation is zero and θ_i^{e1} is the soil water content at the end of the energy limiting stage of evaporation. For more on evaporation in the subsurface in GHOST, see Politano (2018).

4.2.3 Surface

The surface zone is where overland flow (runoff, stormflow) take place. Water depth of flow in the surface zone is calculated by the 2-D diffusive wave-approximation of the St. Venant equation given by Politano (2018) as:

$$\frac{\partial y^{surf}}{\partial t} + \nabla(\vec{u}^{surf} y^{surf}) = S^{surf} - q^{surf-uns} + q^{GW-surf}$$

(14)

where y^{surf} is the water depth at the surface, $\vec{u}^{surf}$ is the water velocity from the momentum equation of the diffusive wave and Manning equation, $q^{surf-uns}$ is the mass flux to the unsaturated zone, $q^{GW-surf}$ is exfiltration from the subsurface to the surface, and S^{surf} is the source term containing precipitation, drainage from the canopy, snowmelt, surface evaporation, and a flexible source term defined by the user. For more on the source and surface velocity terms in GHOST, see Politano (2018).

Overland flow is a function of surface water depth, surface elevation, average roughness of the surrounding elements, the gradient of the surface, and mesh geometries and is given by Politano (2018) as:

$$q_{ij}^{surf} = \frac{\left(y_{ups}^{surf} + z_{ups}^{ground}\right)^{2/3}}{n_{ij}} sign\left(|G_{ij}^{surf}|\right)\left(G_{ij}^{surf}\right)^{1/2}\left(y_f^{surf} + z_{ups}^{ground}\right)L_{ij}$$

(15)

where q_{ij}^{surf} is the mass flux at the surface, y_{ups}^{surf} is the water depth upstream, z_{ups}^{ground} is the elevation of the model surface upstream, n_{ij} is the average Manning's roughness of the surrounding elements, , G_{ij}^{surf} is the gradient of the total head, y_f^{surf} is the average water depth of the surrounding elements, and L_{ij} is the element edge length. The 1-D stream network connects to the mesh at the surface and the through the subsurface. Surface flow is routed over a

broad crested weir before entering the stream to approximate the effects of the riparian zone (Panday & Huyakorn, 2004). Flow in the subsurface passing from the subsurface to the channel is subjected to a user specified hydraulic conductivity to simulate the effects of alluvial sediments. Flow in the 1-D channel is governed by a 1-D approximation of the St. Venant equation (Politano, 2018).

4.2.4 Fluxes Between Zones

Mass flux from the surface to the subsurface is given by Politano (2018) as:

$$q_i^{surf-uns} = \begin{cases} Z_i^{surf}\Gamma_i & if\ \Delta h_i > 0\ (infiltration) \\ \begin{cases} \dfrac{y_i^{uns}}{y_i^{soil}}\Gamma_i & if\ |\Gamma_i^{uns}| < |\Gamma_i| \\ \Gamma_i & if\ |\Gamma_i^{uns}| > |\Gamma_i| \end{cases} & if\ \Delta h_i > 0\ (infiltration) \end{cases}$$

(16)

where $q_i^{surf-uns}$ is the flux from the surface to the subsurface, Z_i^{surf} is a sigmoid function which reduces infiltration when ponded water on the surface approaches the depression storage:

$$Z_i^{surf} = \left(\frac{\left(y_i^{surf}\right)^3}{\left(y_i^{surf}\right)^3 + \left(D_i^{strg}\right)^3} \right)$$

(17)

where y_i^{surf} is the depth of water on the surface and D_i^{strg} is the depression storage or the depth water at the surface must reach before leaving an element.

where Γ_i^{surf} is the maximum mass flux from the surface to the subsurface and is a function of vertical hydraulic conductivity, the coupling length, and the head in the element which is a function of the capillary head from van Genuchten (van Genuchten, 1980).

When the subsurface is fully saturated exfiltration can occur from the saturated zone to the surface. The flux from the saturated zone to the surface is defined as the minimum between the difference between the maximum mass flux from the surface to the unsaturated zone and the flux from the surface to the unsaturated zone and zero:

$$q_i^{GW-surf} = -min\left(\Gamma_i^{uns} - q_i^{surf-uns}, 0\right)$$

61

where Γ_i^{uns} is the maximum mass flux from the subsurface to the surface and $q_i^{surf-uns}$ is the mass flux from the surface to the subsurface.

Mass flux from the unsaturated zone to the saturated zone (recharge) is modeled as the maximum between the product of the surface-unsaturated zone mass flux and a sigmoid function and zero:

$$q_i^{uns-GW} = max\left(Z_i^{rech} q_i^{surf-uns}, 0\right)$$

(19)

where $q_i^{surf-uns}$ is the surface to subsurface mass flux and Z_i^{rech} is a sigmoid function defined as:

$$Z_i^{rech} = \left(\frac{s_{ni}^m}{s_{ni}^m + s_n^{*m}}\right)$$

(20)

where s_n is a constant and s_n^* and m are model parameters. For more information on the coupling between zones in GHOST, see Politano (2018).

4.2.5 Subsurface Zone

Flow in the subsurface is a 2-D mass flux between two elements i and j and is a function of saturated hydraulic conductivity, height of groundwater upstream, the gradient of the total head, and the edge length of the element:

$$q_{ij}^{GW} = k_{ij}^{sat} y_{ups}^{GW} G_{ij}^{GW} L_{ij}$$

(21)

where q_{ij}^{GW} is the groundwater flux between two adjacent elements, k_{ij}^{sat} is the average saturated hydraulic conductivity between two adjacent elements, L_{ij} is the length of the shared edge, and G_{ij}^{GW} is the gradient of the total head defined as:

$$G_{ij}^{GW} = \frac{y_i^{GW} + z_i^{bed} - y_j^{GW} - z_j^{bed}}{d_{ij}}$$

(22)

where y_i^{GW} and y_j^{GW} are the heights of groundwater and z_i^{bed} and z_j^{bed} are the bed elevations of elements i and j respectively and d_{ij} is the distance between element centers. For more on the modeling of groundwater in GHOST see Politano (2018).

4.2.6 Boundary Conditions and Retention Basins

Two types of boundary conditions exist in GHOST; 1-D and 2-D. The 2-D boundary condition is a no-flow boundary along the watershed boundary. This boundary condition stands for both surface and subsurface flows. For the 1-D river network there is a boundary condition applied at the outflow of the model—for a description, see Politano (2018).

GHOST has the ability to model retention basins built in to the 1-D stream network model. These basins have a stage storage relationship with the flux through them modeled with a project rating curve and project storage:

$$q_{kl}^{chan} = f\left(S_k^{chan}\right)$$

(23)

where q_{kl}^{chan} is the flux through the retention basin between river segments k and l and S_k^{chan}, the project storage, is defined as:

$$S_k^{chan} = \left(S_k^{chan}\right)^{t-\Delta t} + \left(\sum_{j=1}^{2} q_{kj}^{chan} + \sum_{j=1}^{2} q_{ik}^{surf-chan}\right)^{t-\Delta t} \Delta t$$

(24)

where the first term is the change in storage for the time step, and the second term is the change in flow through the channel over the time step.

4.2.7 Limitations

Perhaps the most apparent limitation of the GHOST model in its current formulation and in this particular application is the lack of a representation of the effect of subsurface tile drainage. Much of the Boone watershed is influenced by artificial drainage (Figure 3-8, Figure

63

3-9) and while there is ongoing research into the impacts tile drainage has on hydrology, (Arenas Amado, Schilling, Jones, Thomas, & Weber, 2017; Schilling & Helmers, 2008; Sloan, Mantilla, Fonley, & Basu, 2017; Thomas, Arenas, Schilling, & Weber, 2016) that it has an impact is well understood.

The accuracy of the representation of the watershed by the model mesh depends on the steps taken during mesh construction to limit the mesh to known characteristics of the watershed. Currently, the mesh is built off of the river network, and watershed boundary and elevation values are assigned at triangle nodes by overlaying the TIN on a DEM. There is potential for meshes to be constructed based off of other surface features such internal sub-basin boundaries, regions of distinct land cover, pedology, and geology. Mesh building could also benefit from mesh geometry being constrained by topography in a way that optimizes the representation of the topography of a watershed rather than reading it at points alone (Bates et al., 2003).

4.3 Model Construction

4.3.1 Mesh

GHOST utilizes a triangular irregular network (TIN) populated by Delaunay triangulation. GHOST's mesh construction is based upon the mesh construction established for PIHM and as a result still utilizes the QGIS derived PIHMgis (Qu & Duffy, 2007). PIHMgis is capable of creating a model mesh from only a DEM, but is prone to crashing for some of the beginning steps when using large, fine resolution DEMs. For the work presented here, ArcGIS and some of the tools of the ACPF were used to generate equivalent products, namely the flow direction raster, flow accumulation raster, and river network shapefile. Using this method, the only thing the user must supply are a DEM and a watershed boundary. For the work presented here, a 2 meter, hydro-enforced DEM from the ACPF was used (ISU GISF, n.d.). The river network can be generated using the ACPF toolbox in ArcGIS using the 1.a. and 1.b. tools titled *D8 Terrain Processing* and *Flow Network Definition – Area Threshold* respectively. The resulting river network shapefile is passed onto PIHMgis along with the DEM. In PIHMgis, the

Vector Processing tools are run and the results are manually checked and edited to eliminate small angles and features with the potential to generate smaller than desired elements. This process includes the conversion of the river network and watershed boundary from complex shapes with intricate topology to simplified versions made up of larger elements to facilitate the fitting of elements to them. Next, the *Domain Decomposition* tools are run. The TIN is inspected for flaws or computationally prohibitively small elements and edited as needed to correct. Then only the *Generate MeshFile* and *Generate RivFile* sub-tools of the *DataModel Loader* tools of PIHMgis are run.

In this process there are decisions to be made which will affect the qualities of the final mesh (Table 4-1). First, during the flow network building in ArcMap, there is a flow accumulation threshold the user must specify which controls how far into the watershed the river network will "reach." Next, in the PIHMgis *Vector* Processing tool, the user must specify a tolerance for the maximum distance between the river network generated from the DEM and the simplified network the tool generates as well as for the watershed boundary. The next decision is made in the *Domain Decomposition* tool and sets limits for minimum element interior angle and maximum element area. After the TIN is made, a desired minimum area threshold may be identified by the user and they may go back and manually edit the river or watershed boundaries to achieve it (see Table 4-2 for a summary of the properties of the mesh and river network generated from this process).

65

Table 4-1: Mesh building geometry controls.

Flow Accumulation Threshold (ac)	River Network Deviation (m)	Watershed Boundary Deviation (m)	Minimum Element Interior Angle (°)	Maximum Element Area (m²)	Minimum Element Area (ac)	Mesh Depth (m)
500	75	150	25	150,000	7	20

Table 4-2: Summary of mesh and river network attributes

Statistic	Mesh Element (ac)	River Segment (ft)
Count	12,728 (number)	1579 (number)
Total	908 (mi²)	608 (mi)
Minimum	7	677
Maximum	74	4181
Mean	46	2036
Standard Deviation	12	648

4.3.2 River Smoothing

In order for GHOST to run, there can be no negatively sloping segments of the river file. Due to mesh construction techniques and properties inherent to the DEMs used to construct GHOST meshes, the mesh as it comes out of PIHMgis often contains negative slopes. This is resolved in a two-step process. First, the river network as it exists in the mesh contains nodes that

66

do not fall upon the un-simplified river network as produced by the ACPF tools. These nodes are reassigned elevation values in the mesh file of the nearest points along the un-simplified river network. Second, the altered mesh and river files produced from PIHMgis and the first step are run through a script developed by Marcela Politano to average out the slopes of the river profile to ensure no negative slopes remain. The first step is accomplished in ArcMap, the second in Matlab. The finished product is a mesh altered only along the river network and which stays as true as possibly to the original river profiles while ensuring the river network maintains a positive slope.

4.3.3 Model Attributes and Inputs

GHOST has attributes which are assigned to individual elements and river segments. Element attributes include soil type, land cover type, meteorological forcing, and leaf area index. The soil attribute an element is assigned links to a table of soil types including infiltration rate, saturated hydraulic conductivity, maximum and minimum soil moisture content, alpha and beta van Genuchten parameters, and recharge sigmoid parameters. All of these parameters can be customized to meet the modeling needs. The land cover element attribute links an element to a table which specifies a number of land cover and model surface parameters such as Manning's roughness and the interception coefficient. Land cover is taken from the National Agricultural Statistical Service's 2016 Crop Data Layer, grouped into similar land cover types, and the maximum land cover type per element is assigned (Figure 4-1) (National Agricultural Statistics Service, 2016). Since the hydrologic properties of the soils of the Boone River watershed are relatively uniform, soils were assigned based on land cover under the assumption that land cover was a larger control on the hydraulic properties of soils than minute differences in type. The meteorological element attribute links each element to the nearest four-by-four kilometer meteorological forcing time series which correlates to a Nexrad Stage IV pixel. The forcing is derived from Nexrad Stage IV gage corrected radar rainfall and NLDAS-2 data sets. There are 161 of these meteorological time series for the Boone River watershed (Figure 4-2). The leaf

area index element attribute corresponds to four vegetation-linked time series—leaf area index, crop coefficient, vegetation height, and root depth—for the four vegetative cover types in the model: row crop, hay/pasture, forest, and developed. River attributes can be set both by segment and by Strahler stream order (Figure 4-2) including depth, width, Manning's roughness, and the parameters that affect the flow from the 2D model mesh to the 1D river network

Other significant model inputs are the parameters for evapotranspiration and snowmelt. ET parameters include extinction coefficient, C_3, θ_{WP}, θ_{FC}, θ_O, and θ_{AN} for use in Equation 10, θ_{e1} and θ_{e2} for use in Equation 13, and B_{soil} for the depth over which soil evaporation acts. Snowmelt is determined by a simple millimeter per degree Celsius rate which can be set by month.
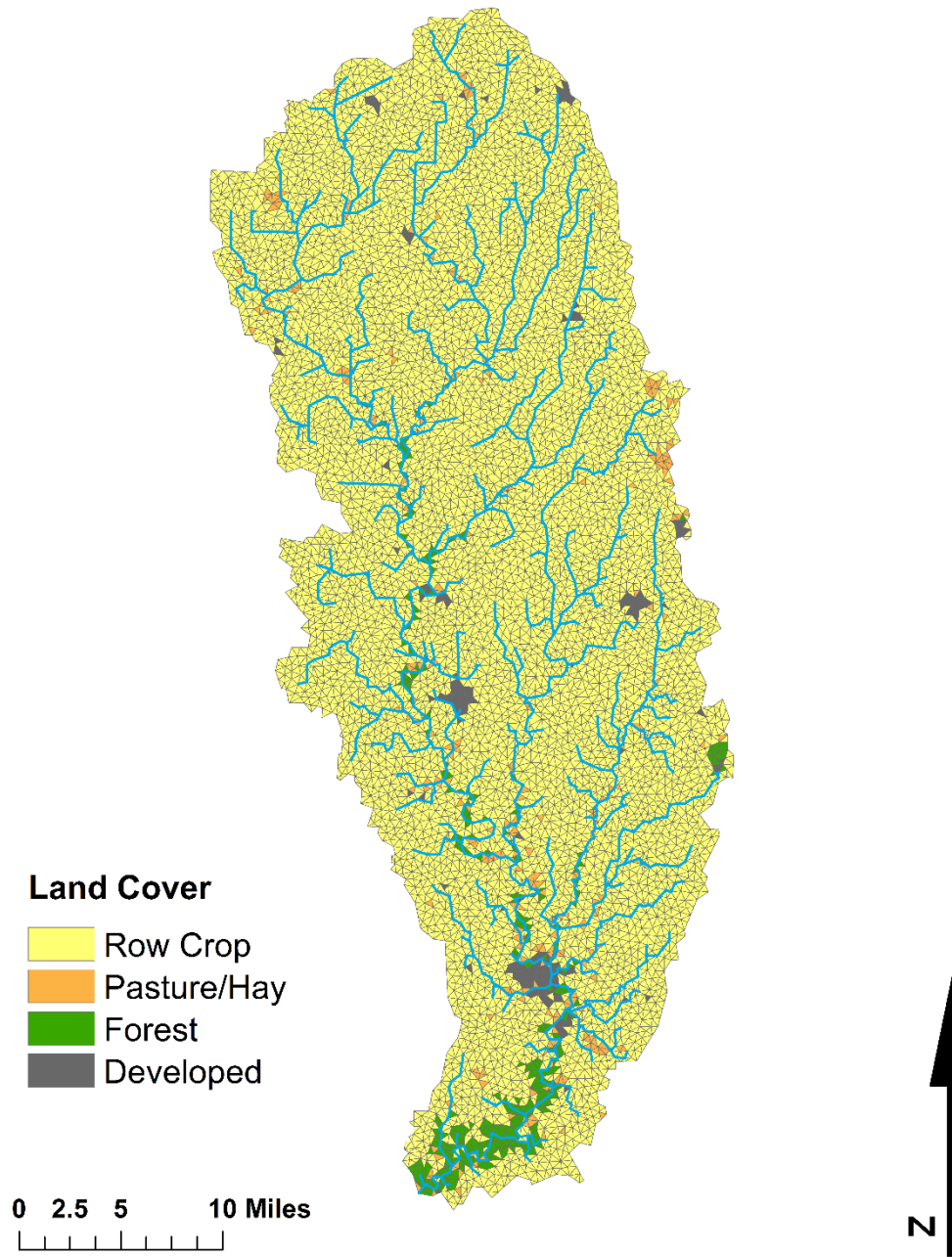
Figure 4-1: The Boone River model mesh and river network with land cover by element.
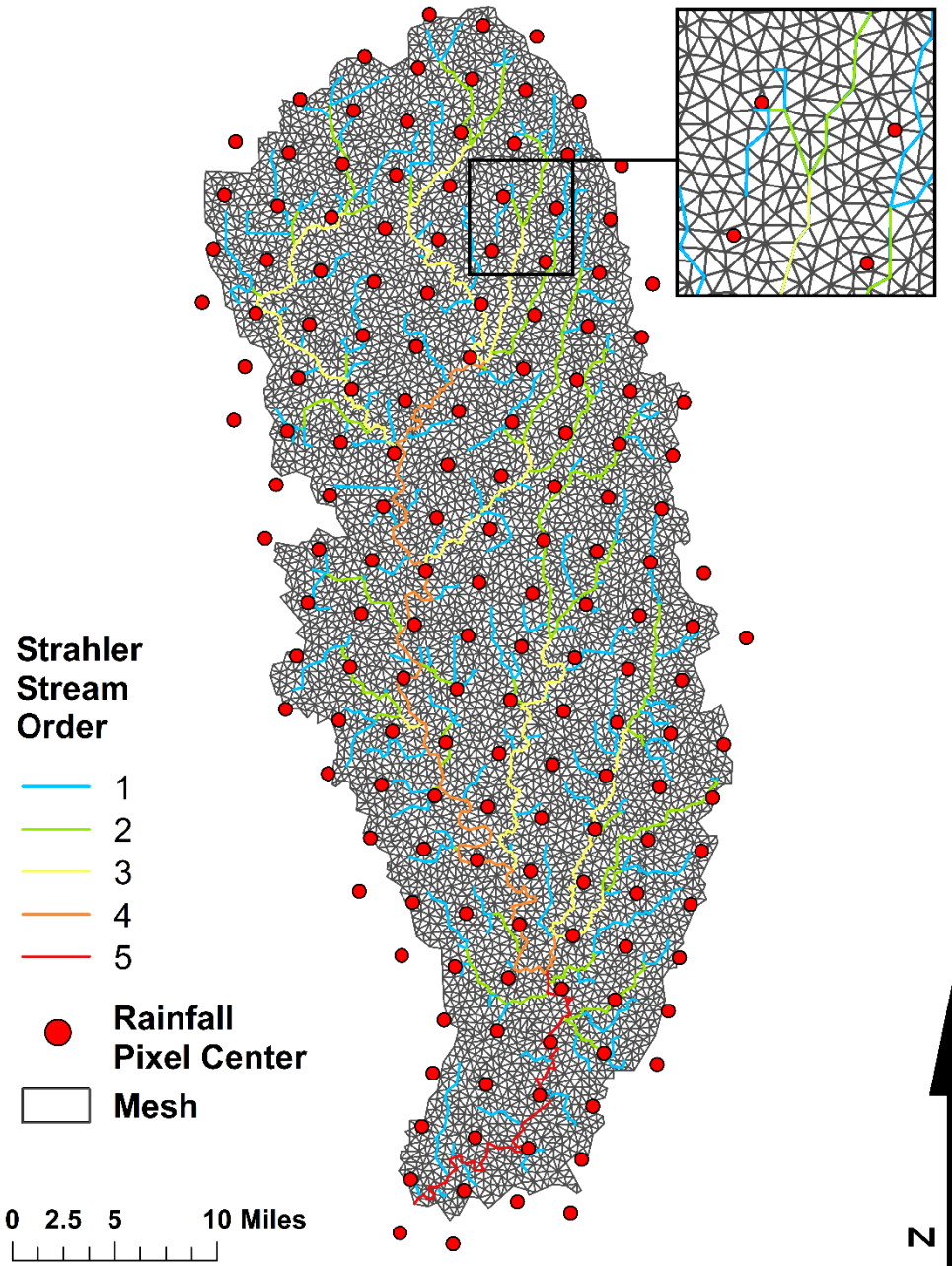
Figure 4-2 The Boone river mesh and river network colored by Strahler order and rainfall pixel centers.

4.4 Summary

The GHOST hydrologic model was constructed to accurately simulate large watersheds in Iowa while representing the spatial heterogeneities of watersheds and remaining computationally efficient. To do this, GHOST makes use of common, physically-based approaches and equations to govern its internal processes. The construction of the model allows for high degrees of customization for the needs of individual watersheds.

The Boone River model was built with the ability to model conservation practices in mind. Average element size was kept small to be able to represent field and sub-field level changes to land cover within the model. The river network was populated at an accumulation threshold high enough to slightly surpass known river extents to be able to simulate wetlands placed in the further reaches of the stream order one drainage basins. The Boone River model was built to allow for computational efficiency while still retaining a high level of detail to accurately capture the characteristics of the watershed.

CHAPTER 5: MODEL CALIBRATION

5.1 Introduction

In order to use the Boone River GHOST model to evaluate the conservation scenarios, first the model must be able to accurately simulate the known hydrology of the watershed. This ability is honed and demonstrated through model calibration Hydrologic models can be calibrated different ways which can broadly be categorized into manual and automated. For the work presented here, the model was calibrated manually using an iterative procedure of parameter estimation and refinement.

5.2 Model Initialization

GHOST has the ability to initialize one of two ways: with uniform values for water depth at the surface, water depth in the river, water content in the unsaturated zone, depth to groundwater, and project storage or with these values defined from a previous model state. For the calibrated model, the second option was chosen as the option that produced the best calibration. Soil moisture for the initial condition ranges from 0.73 to 0.99 and varies based upon both proximity to the river network and topography (Figure 5-1). The height of the unsaturated zone (also depth to water table) ranges from 1.0 to 13.8 meters and similarly mirrors the river network (Figure 5-2).
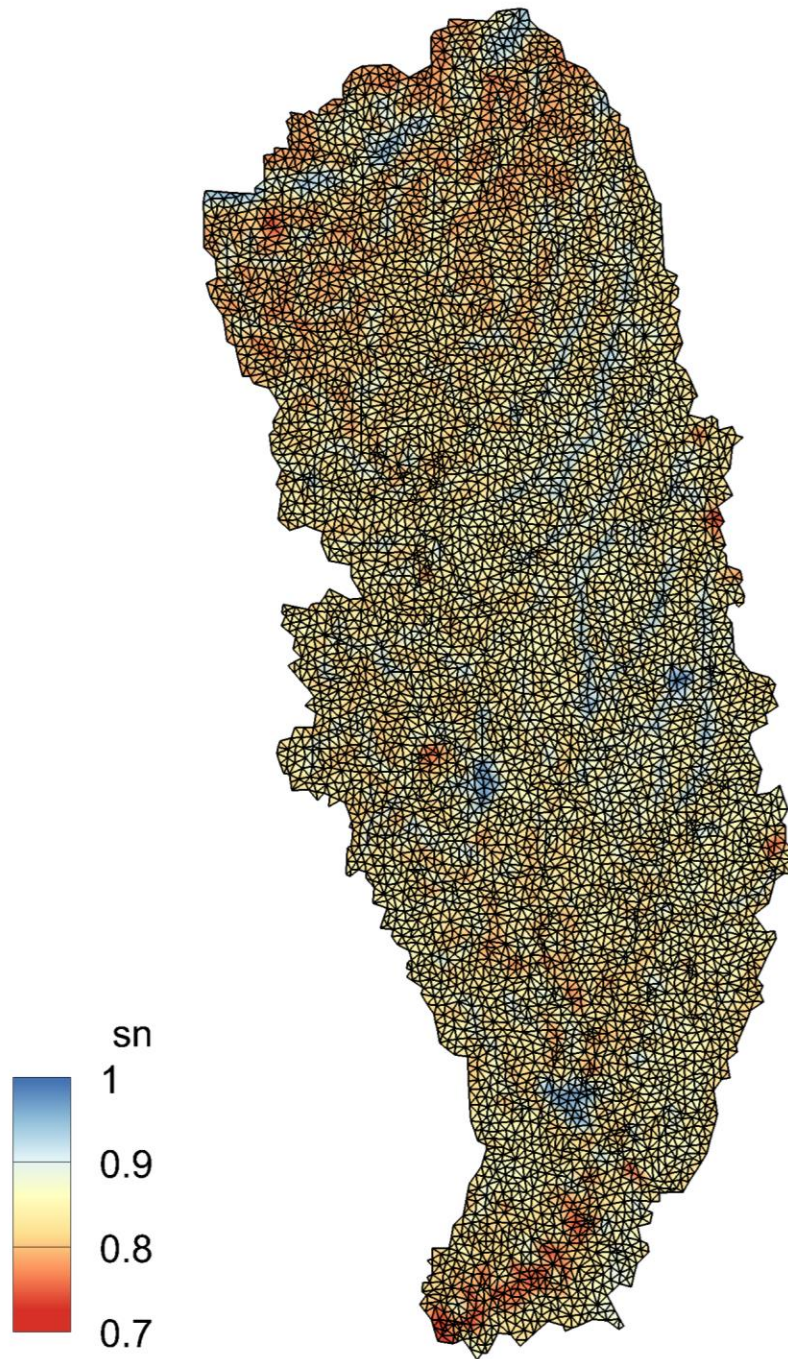
Figure 5-1: Soil moisture for the initial condition of the Boone River model.
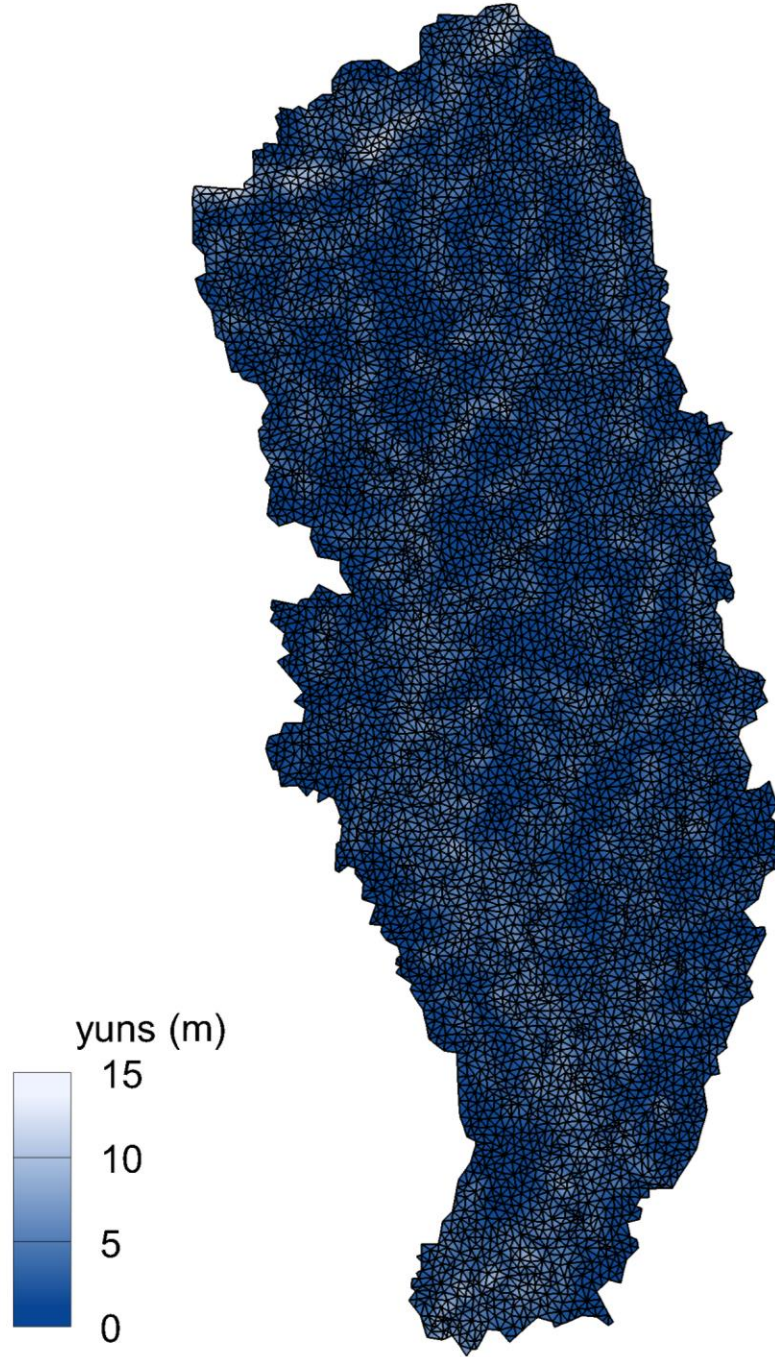
Figure 5-2: Height of the unsaturated zone (yuns) or depth to water table for the initial condition of the Boone River model.

74

5.3 Calibration Targets

In a series of papers which reflect on the field of hydrologic and water quality modeling Moriasi et al. (2007, 2015, and 2012) have established guidelines for model calibration and validation through a number of performance metrics and methods. Moriasi et al. (2007) investigated performance evaluation for streamflow, sediment, and nutrient modeling and established thresholds for satisfactory performance for each. In a 2012 paper, Moriasi et al. reviewed 22 articles on 25 hydrologic and water quality models to establish their functions and the important aspects of calibration and validation for each. Moriasi et al. (2015) established thresholds for not satisfactory, satisfactory, good, and very good performance for annual simulations at the watershed scale. For this thesis, performance must be evaluated both on the 17 year continuous simulation and for the simulation of individual flood peaks during the continuous simulation. For the continuous 15 years, the targets for calibration follow Moriasi et al. (2015) thresholds for satisfactory performance for annual simulations at the watershed scale with a Nash Sutcliffe efficiency > 0.50, percent bias $\leq \pm 15$ percent, and an $R^2 > 0.60$.

5.4 Calibrated Model Performance

The model's performance is evaluated using daily discharge data on three scales: a 17 year, whole simulation, annual, and monthly. Calibration was done against observed discharge data from the USGS gaging station 05481000 near Webster City, Iowa. This USGS gage captures 93.0 percent of the drainage area of the Boone River watershed. The flow duration curves for the USGS gage at Webster City and the model outputs for the same location reveals varying model performance across the range of exceedance probabilities with the flow duration curves for low exceedance probabilities showing the most agreement. For the whole 17 year simulation, the calibration achieved an NSE of 0.79, PBIAS of -6.0 percent, and an R^2 of 0.80. According to Moriasi et al. (2015), the level of performance attained for these metrics achieved the highest threshold of "Very Good" for both NSE and R^2 and "Good" for PBIAS. Annual model performance ranged from an NSE of 0.31 to 0.94 (Figure 5-4), PBIAS ranged from -48 to

31 percent (Figure 5-5), and R^2 ranged from 0.46 to 0.94 (Figure 5-6). By month, NSE ranged

from -0.25 to 0.91 (Figure 5-7), PBIAS ranged from -44.7 to 35.5 percent (Figure 5-8), and R^2

ranged from 0.35 to 0.92 (Figure 5-9). Analyzing the average monthly runoff depths (Figure

5-10), there is good agreement in general with March and July having larger discrepancies.

March is under-predicted by 0.52 inches which amounts to 45 percent. One possible explanation

for this is the lack of ground freeze dynamics in the current formulation of the GHOST model

leading to erroneously low late winter-early spring peaks. Early 2010 is a candidate for an event

that is likely driven by a combination of rainfall on frozen ground and snow melt due to

changing model average temperature (Figure 5-12). Adversely, July is over predicted by 0.36

inches (35 percent). This over prediction in discharge is attributed to an under prediction in

evapotranspiration and therefore leading to systematically higher recession curves and baseflow

(Figure 5-11).
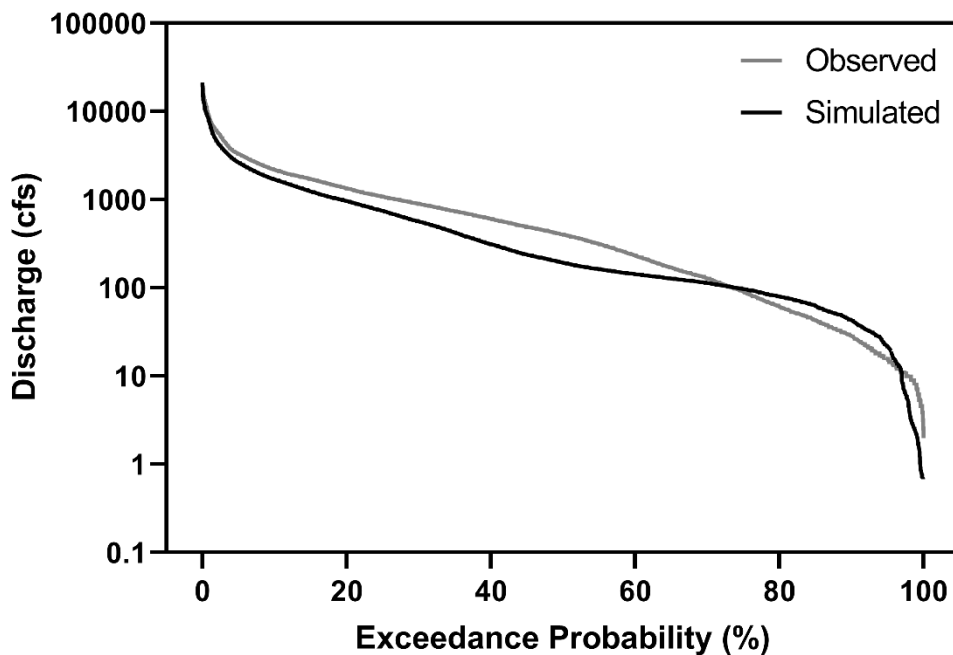
Figure 5-3: Discharge versus exceedance probability for the observed data from the USGS gaging station 05481000 near Webster City, Iowa and the calibrated model.

76
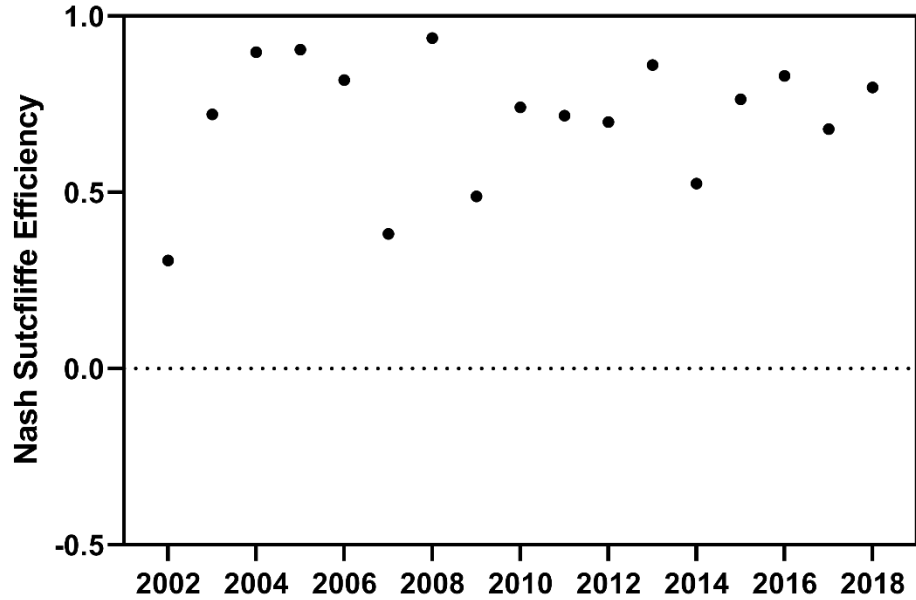
Figure 5-4: Annual Nash Sutcliffe efficiency for the calibrated model. Dotted line indicates NSE reference value for performing better (positive values) or worse (negative values) than the mean.
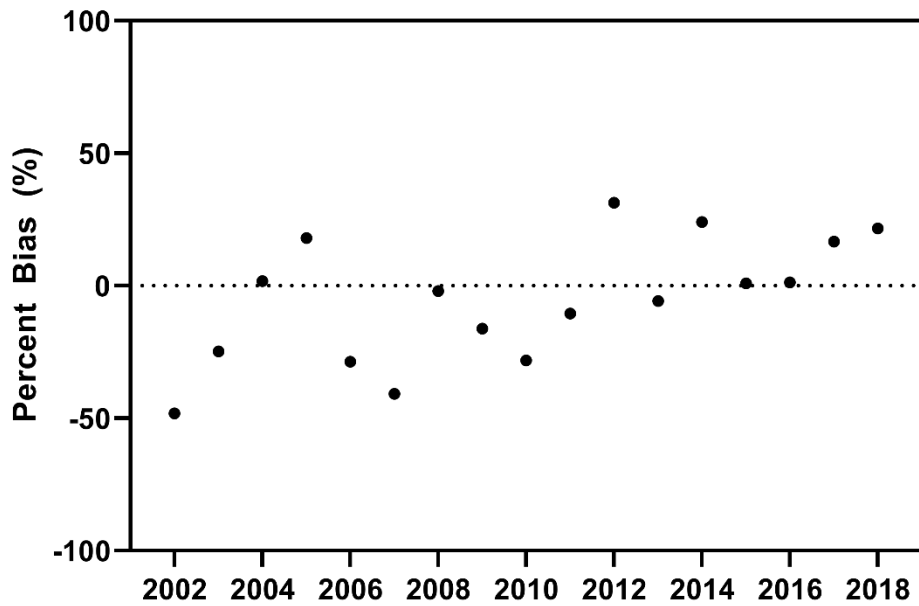
Figure 5-5: Annual percent bias for the calibrated model. Dotted line indicates the ideal performance value.
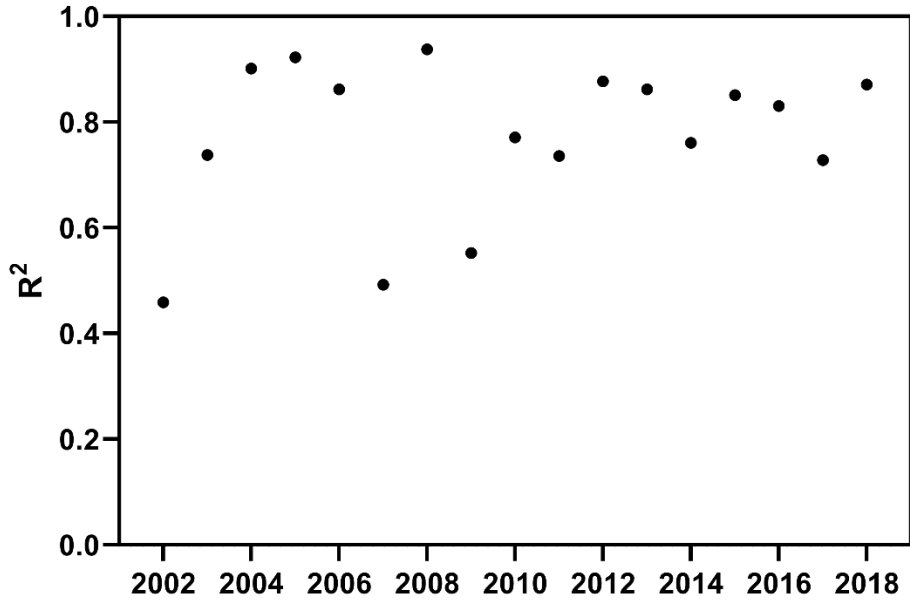
Figure 5-6: Annual R^2 for the calibrated model.
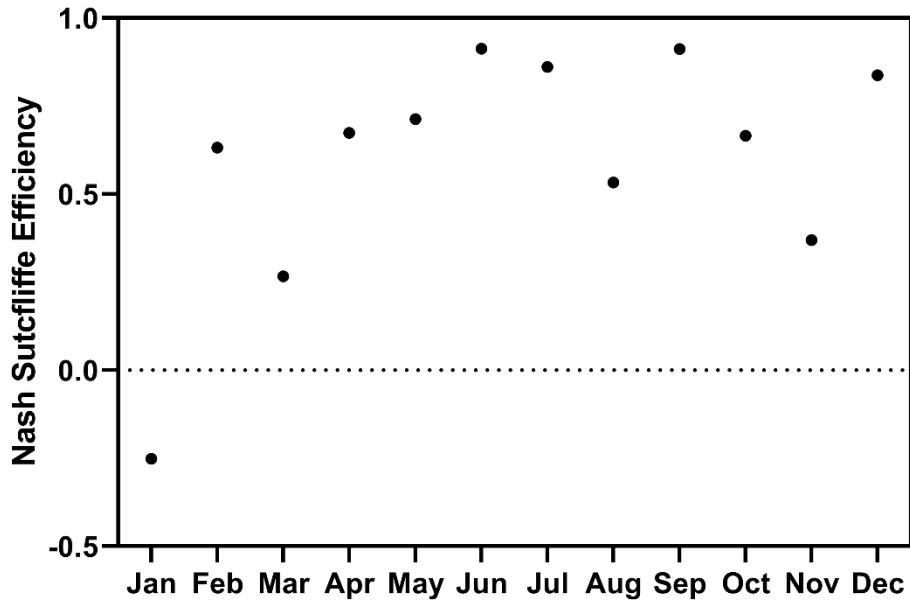
Figure 5-7: Monthly Nash Sutcliffe efficiency for the calibrated model. Dotted line indicates NSE reference value for performing better (positive values) or worse (negative values) than the mean.
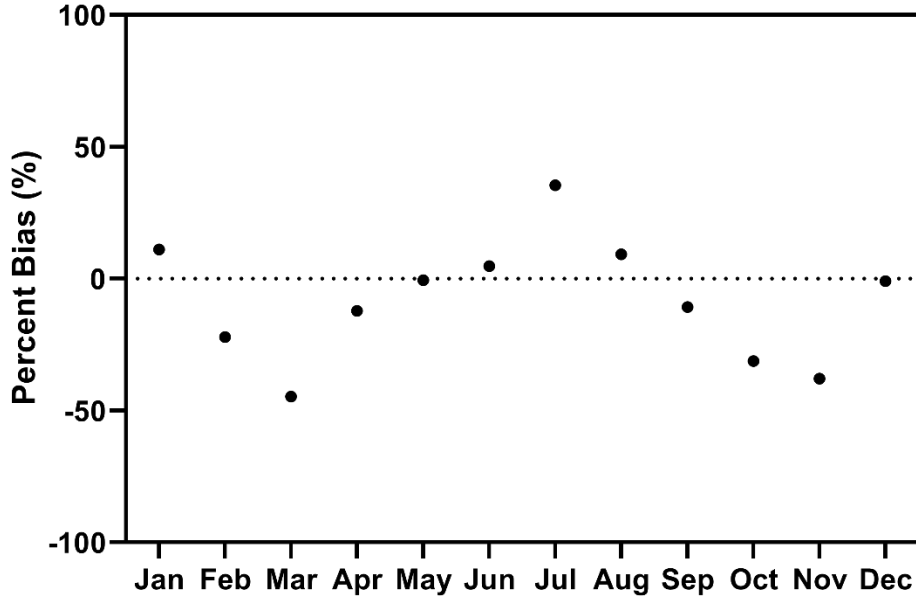
Figure 5-8: Monthly percent bias for the calibrated model. Dotted line indicates the ideal performance value
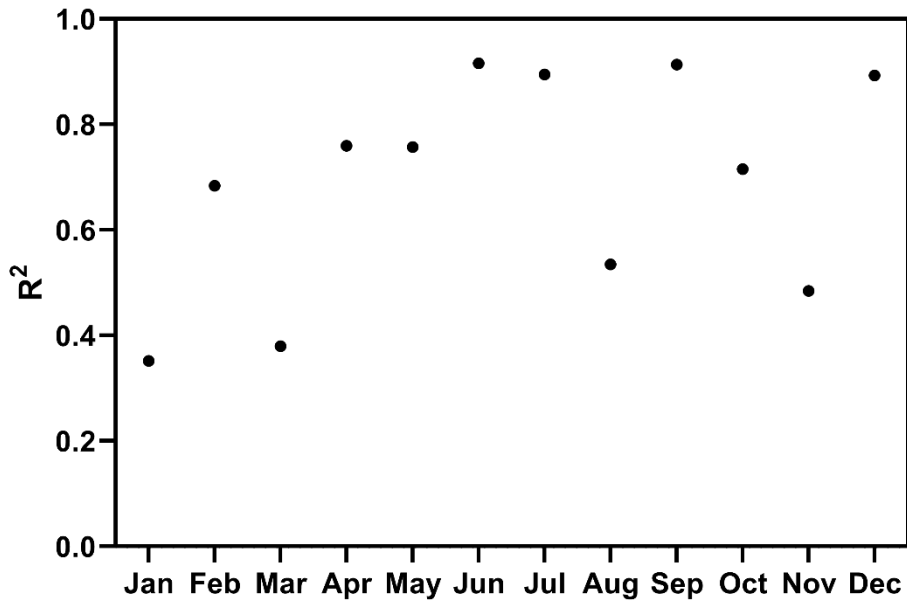
Figure 5-9: Monthly R^2 values for the calibrated model.

79
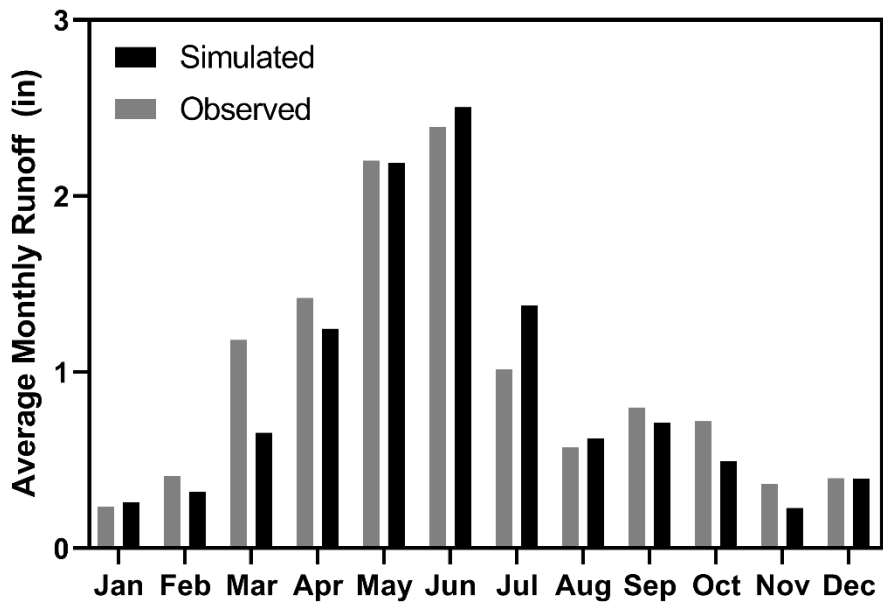
Figure 5-10: Simulated and observed average monthly runoff depths for USGS gage 0541000 on the Boone River near Webster City, Iowa.
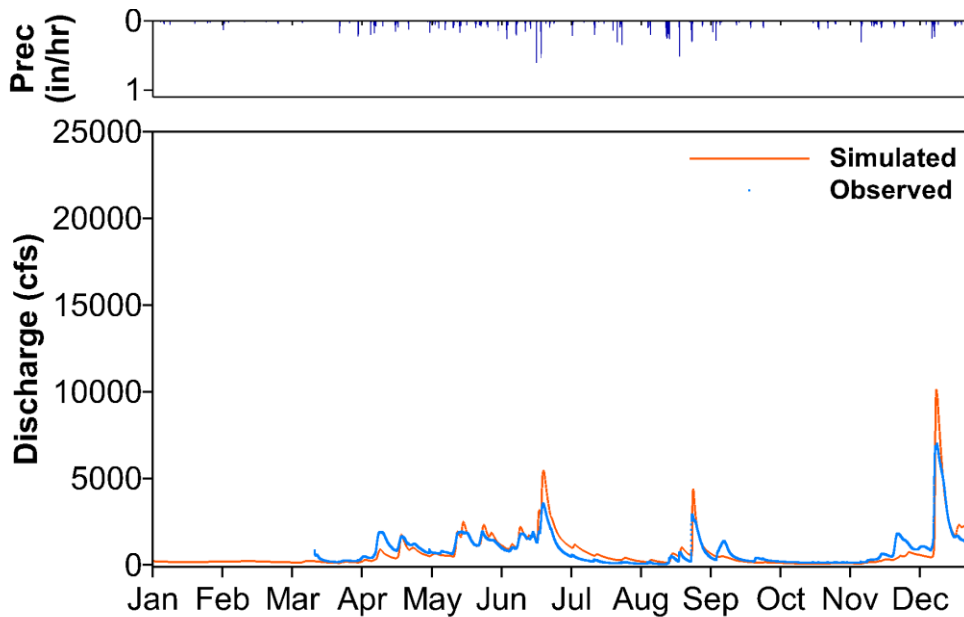
Figure 5-11: Simulated and observed discharge at USGS gaging 05481000 near Webster City, Iowa with watershed average precipitation forcing (Prec) for 2015 showing an over prediction on the recession curve during the month of July.
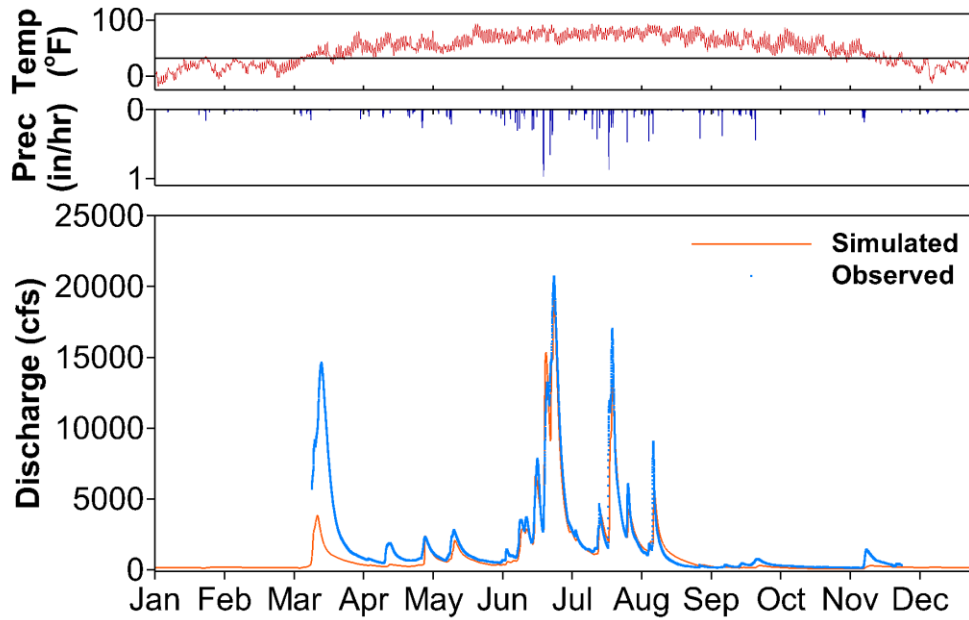
Figure 5-12: Simulated and observed discharge at USGS gaging 05481000 near Webster City, Iowa with watershed average precipitation forcing (Prec) and temperature forcing (Temp) for 2010. Showing a missed peak during the month of March in relation to the temperature and precipitation timing.

Two methods are used for evaluating the performance of the model in its ability to accurately simulate the magnitudes of peak flows: annual maximums and peaks-over-threshold (POT). For the annual maximums, R^2 for the comparison of simulated to observed peaks is 0.88 (Figure 5-13). 2007 stands out for poor performance. The annual maximum for 2007 occurs in mid-August where the USGS has recorded a peak of 6,900 cfs and GHOST has simulated a peak of 1,390 cfs (Figure 5-14). For the POT method, a threshold of the 2-year flood (5,572 cfs) is used as a representative value for bankfull conditions (Leopold, 1994). R^2 for the comparison of simulated to observed peaks over threshold is 0.54 (Figure 5-15). The poorest model performance for a peak identified by the POT method is for the peak identified in March 2010 where the USGS reported a discharge of 14,600 cfs and GHOST simulated a discharge of 3,850 cfs. This is likely due to this event being driven by rainfall on frozen soil—a conclusion supported by the model average temperature and rainfall preceding the March 2010 event (Figure 5-12).
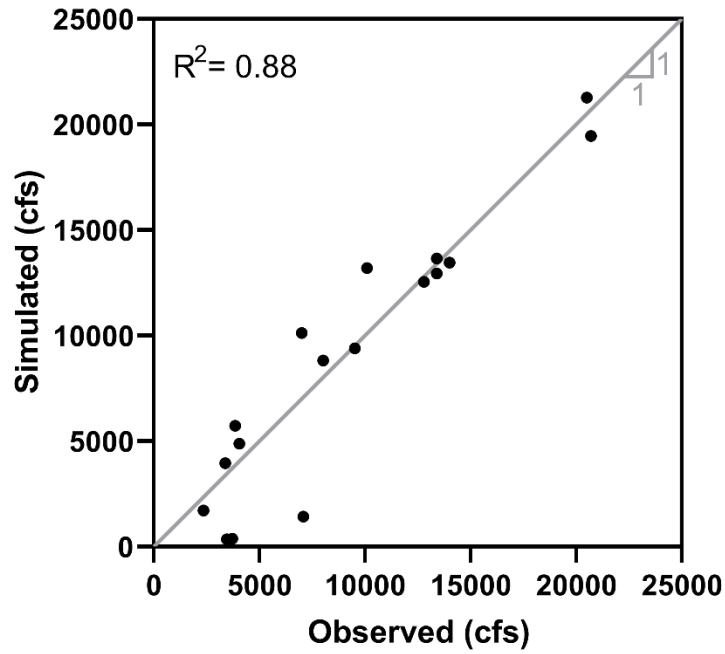
Figure 5-13: Simulated versus observed annual maximums for the 17 years of the model run using instantaneous (15 minute) data.
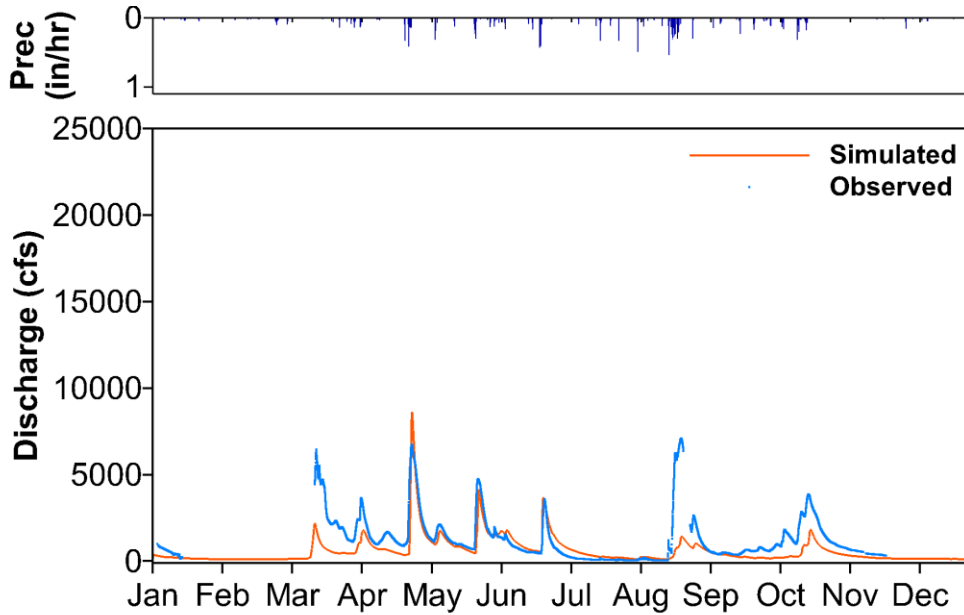
Figure 5-14: Simulated and observed discharge at USGS gaging 05481000 near Webster City, Iowa with watershed average precipitation forcing (Prec) for 2007 showing an under prediction on the annual maximum discharge in August.

82
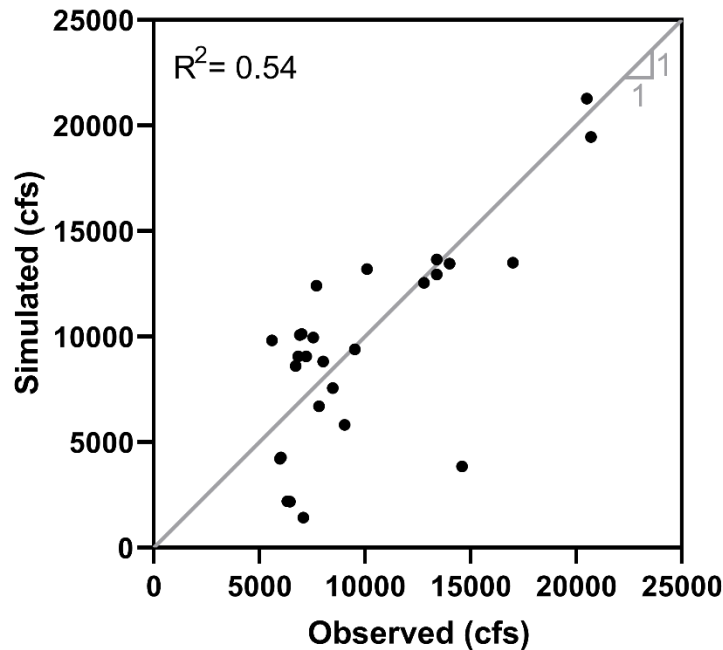
Figure 5-15: Simulated versus observed identified by POT (threshold of 5,572 cfs, 27 identified) for the 17 years of the model run using instantaneous (15 minute) data.

5.5 Summary

Overall, the calibration for the Boone River model achieved remarkable levels of success. For the entire 17 year period, calibration achieved levels of performance which qualify by the thresholds laid out by Moriasi et al. (2015) for both very good and good performance. Since the objective of this thesis is to characterize the changes conservation practices induce in peak flows, the model was also evaluated for its ability to accurately simulate both annual maximums and POT where it is found to do very well and satisfactory. With a well-calibrated model, the effects on peak discharges from changes made to represent conservation scenarios can be better characterized.

83

CHAPTER 6: SIMULATED CONSERVATION PRACTICE SCENARIOS

6.1 Introduction

Most practices sited by tools like the ACPF have hydrologic benefits, but many of these practices are targeted at small scales and therefore difficult to model on a watershed scale. Here a selection was made of scenarios that were practically feasible to simulate within the spatial resolution of the Boone River GHOST model. These scenarios include complete conversion of row crop acres to native vegetation, complete adoption of cover crops/no-till/soil health practices (cover crops), wetlands, and two scenarios assessing the importance of native vegetation in the riparian corridor. These scenarios are run with two different sets of meteorological forcing: the standard observed precipitation and an edited version that accentuates extreme events in a simplistic attempt to simulate the anticipated effects of climate change on precipitation alone. The discharge reductions produced by the scenarios are assessed against the calibrated model by both the annual maximum discharges (Table 6-1) and the peaks identified by the peaks-over-threshold method using a threshold of 5,572 cfs (the 2-year flood) (Table 6-2).

Table 6-1: Exceedance probability, date of occurrence, and discharge of simulated annual
maximum discharges of the baseline model.

Exceedance Probability (%)	Date	Discharge (cfs)
94.4	5/7/2012	2,381
88.9	8/6/2002	2,850
83.3	4/3/2006	3,961
77.8	5/28/2009	4,387
72.2	5/21/2017	4,883
66.7	5/26/2011	5,740
61.1	4/26/2007	8,617
55.5	7/9/2003	8,821
50.0	6/26/2005	9,406
44.4	12/15/2015	10,129
38.9	5/28/2013	12,560
33.3	5/24/2004	12,940
27.8	6/19/2014	13,208
22.2	9/22/2018	13,459
16.7	9/24/2016	13,660
11.1	6/27/2010	19,460
5.6	6/9/2008	21,285

Table 6-2: Exceedance probability, date of occurrence, and discharges identified by peaks-over-threshold of 5,572 cfs. Asterisks denote peaks also identified as annual maximum discharges.

Exceedance Probability (%)	Date	Discharge (cfs)
96.3	9/17/2016	5,639
92.6	5/26/2011*	5,740
88.9	8/11/2010	5,820
85.2	4/23/2018	6,088
81.5	5/13/2014	6,407
77.8	6/19/2010	6,702
74.1	5/3/2013	7,104
70.4	9/6/2018	7,567
66.7	4/26/2007*	8,617
63.0	7/9/2003*	8,821
59.3	5/31/2008	9,061
55.6	4/26/2008	9,076
51.2	6/26/2005*	9,406
48.1	5/5/2018	9,824
44.4	10/10/2018	9,967
40.7	7/2/2018	10,084
37.0	12/15/2015*	10,129
33.3	6/22/2018	12,480
29.6	5/28/2013*	12,560
25.9	5/24/2004*	12,940
22.2	6/19/2014*	13,208
18.5	9/22/2018*	13,459
14.8	7/23/2010	13,508
11.1	9/24/2016*	13,660
7.4	6/27/2010*	19,460
3.7	6/9/2008*	21,285

86

6.2 Increased Precipitation

A simple approach is taken to model the effects of increased precipitation—just one of the anticipated consequence of climate change (Hoegh-Guldberg et al., 2018). For the increased precipitation (IP) scenarios, meteorological forcing is edited to reflect increases in precipitation from extreme events alone. To do this, hourly precipitation was increased by 10 percent for the wettest 5 percent of days with rainfall; consistent with Hoegh-Guldberg et al. (2018). This method preserves the spatial and temporal patterns of rainfall for the storms over the 17 year period while have slightly higher average values of annual precipitation. Using 2008 as an example, the effects of this method can be seen for both precipitation (Figure 6-1) and discharge (Figure 6-2).
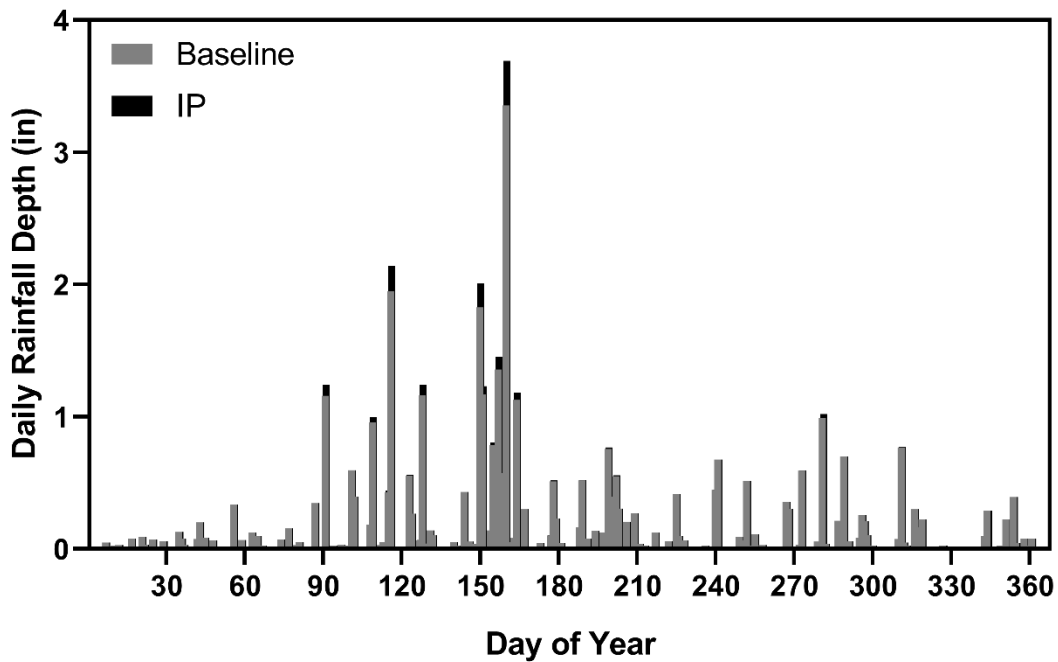
Figure 6-1: Baseline and IP scenario model average daily precipitation depths for 2008 by day of year.
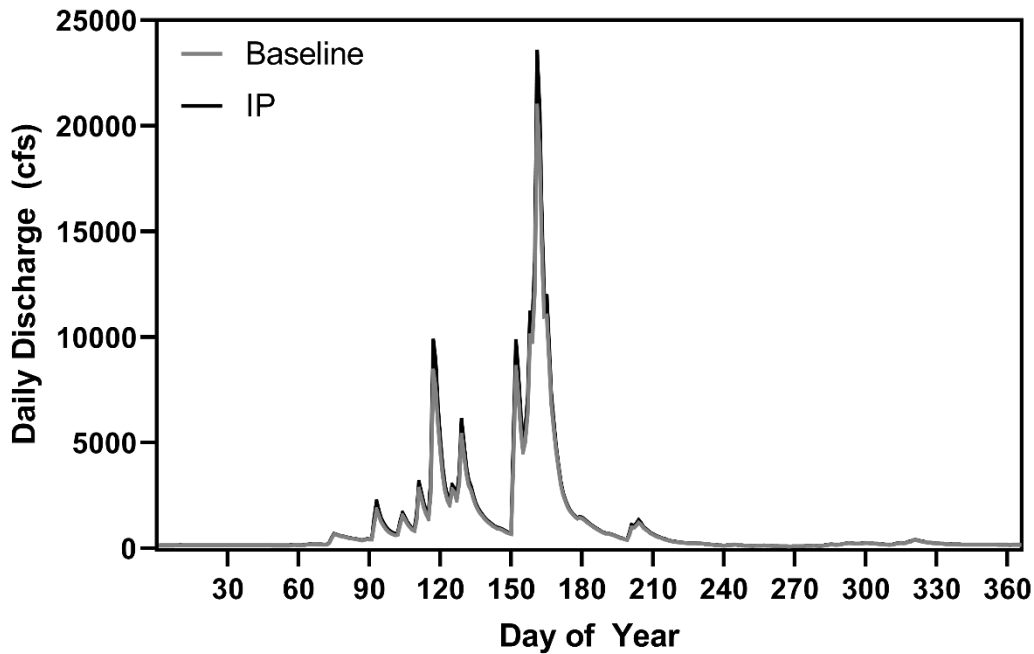
Figure 6-2: Baseline and IP scenario daily discharge versus day of year for 2008 at the USGS gage near Webster City.

For the baseline condition of the model, the increased precipitation scenario produces increased discharges for all discharges with larger increases at lower exceedance probabilities (Figure 6-3). Increases in annual maximum discharges due to the IP scenario range from 260 to 2,680 cfs and average 1,440 cfs with larger increases seen at lower exceedance probability discharges (Figure 6-4). Increases in the annual maximum discharge by percent range from 6.3 to 28.8 and average 13.0 percent. For the peaks identified by POT, increases range from 300 to 2,680 cfs and average 1,440 cfs (Figure 6-5). By percent, increases in POT peaks due to the IP scenario range from 3.0 to 20.3 and average 12.3 percent. The larger increases at high discharges are reflective of the changes made to the meteorological forcing being made only for the already wettest 5 percent of days with rainfall.
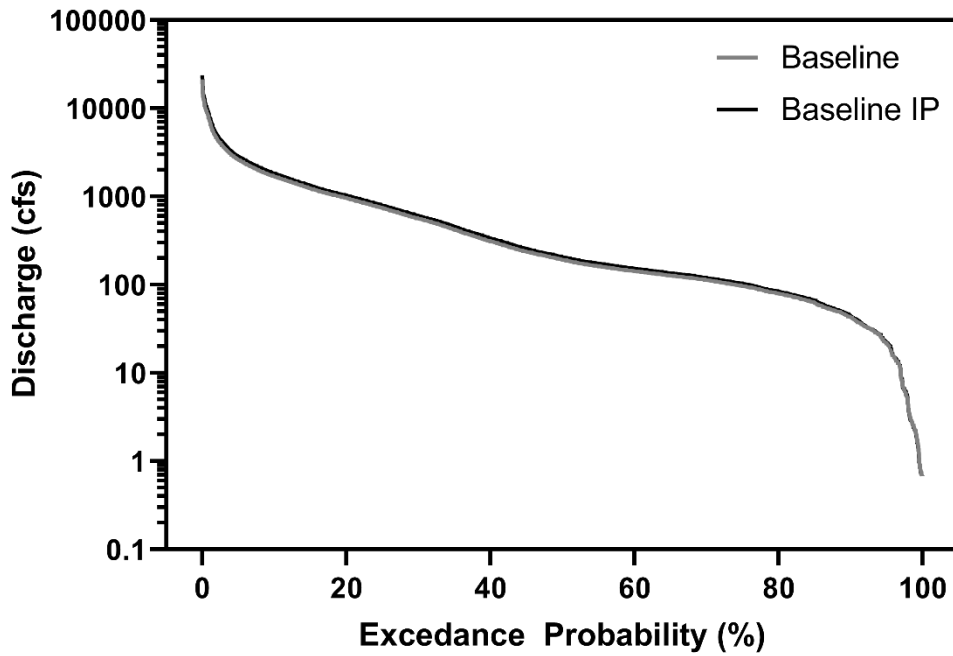
Figure 6-3: Discharge versus exceedance probability for the baseline and increased precipitation scenario (Baseline IP).
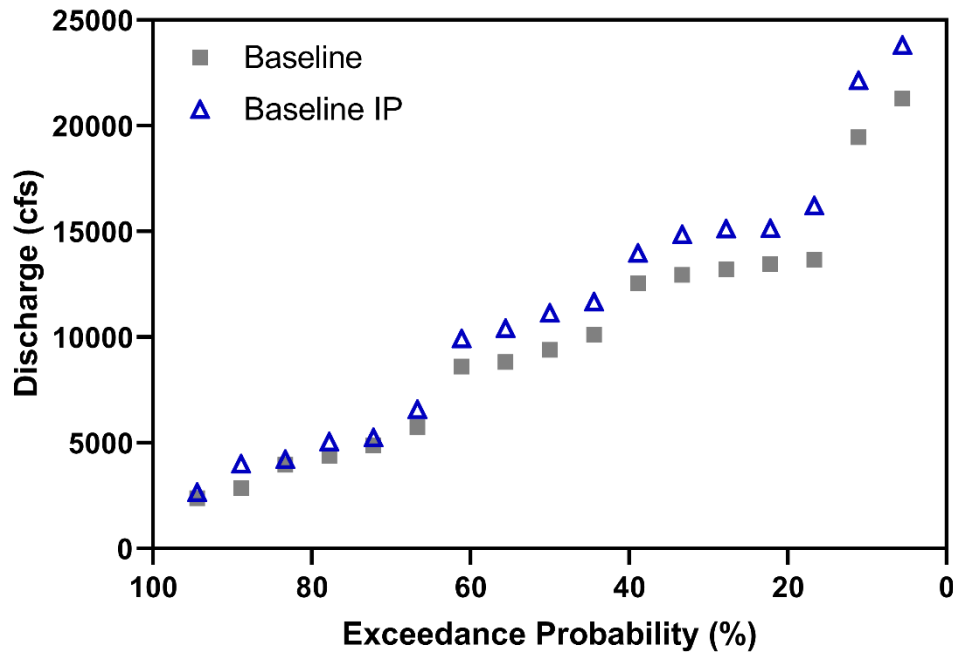
Figure 6-4: Discharge versus exceedance probability for the annual maximums of the baseline and IP baseline.

89
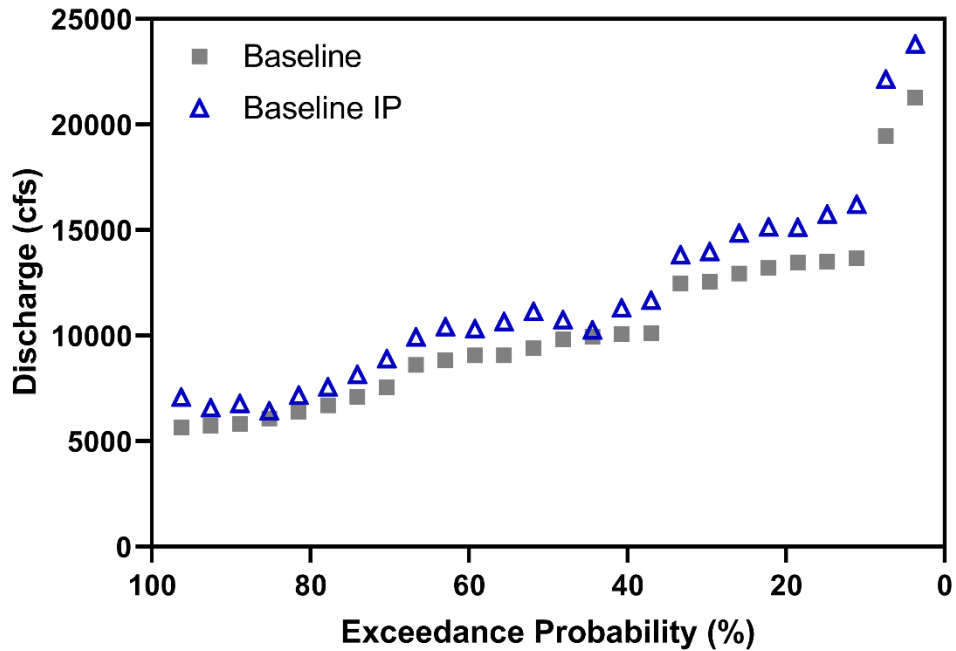
Figure 6-5: Discharge versus exceedance probability for the peaks identified by POT for the baseline and IP baseline.

6.3 Native Vegetation

The first scenario considered is converting all row crop acres in the model to native vegetation—which consisted primarily of perennial vegetation in tallgrass prairie. This scenario is intended to represent an idealized state of the watershed for the maximum application of areal conservation practices and is intended to inform on theoretical maximum flood reduction benefits that can be attained with conservation practices. The changes made in the model to reflect the transition from row crops to native vegetation are in the leaf area index (LAI), crop coefficient (kc), and root depth (rd) time series, changes made in the soil characteristics to reflect changes in the infiltration rate and unsaturated zone water holding capacity, and changes to the row crop land cover attributes.

90

6.1.1 Changes to the Model

One common, well studied native prairie species is switchgrass. While variable, existing literature indicates switchgrass has higher LAI values and a longer growing season compared to conventional row crops (Heaton, Dohleman, & Long, 2008; Zeri et al., 2011). The LAI time series implemented in the model is consistent with these attributes (Figure 6-6). The crop coefficient for tallgrass native prairie has higher values year-round and similar peak values during the summer growing period (Hutchinson, Koelliker, & Knapp, 2007). Studies also identify the dormancy period for existing prairie in Iowa as from December through March (Larson et al., 2011; Scasta, Engle, Harr, & Debinski, 2014)The kc time series for native vegetation is consistent with these observations (Figure 6-7). Due to their perennial nature, root depths of native prairies are assumed to be constant at their maximum reported depths of 2 meters (Jackson, Canadell, Ehleringer, Mooney, & Sala, 1996; Tufekcioglu, Raich, Isenhart, & Schultz, 1999) (Figure 6-8). In their review, Basche (2017) identified 40 studies in which infiltration rates for perennial vegetation were found to be about 60 percent higher than row crop infiltration rates. Another study found infiltration rates in a perennial, multi-species riparian buffer as high as 5 times that of comparable row crops (Bharati, Lee, Isenhart, & Schultz, 2002). To reflect these findings, the infiltration rate (k_{inf}) was changed from 1×10^{-6} to 1.6×10^{-6}, the parameter s_n^* in the sigmoid function which controls the flow from the unsaturated zone to the saturated zone was changed from 1.33 to 1.395 to reflect greater soil water holding capacity (which corresponds to an increase in model average soil moisture by 10.5 percent), and the Manning's roughness for overland flow was changed from 0.1 to 0.4 (Mohamoud, 1992).

91
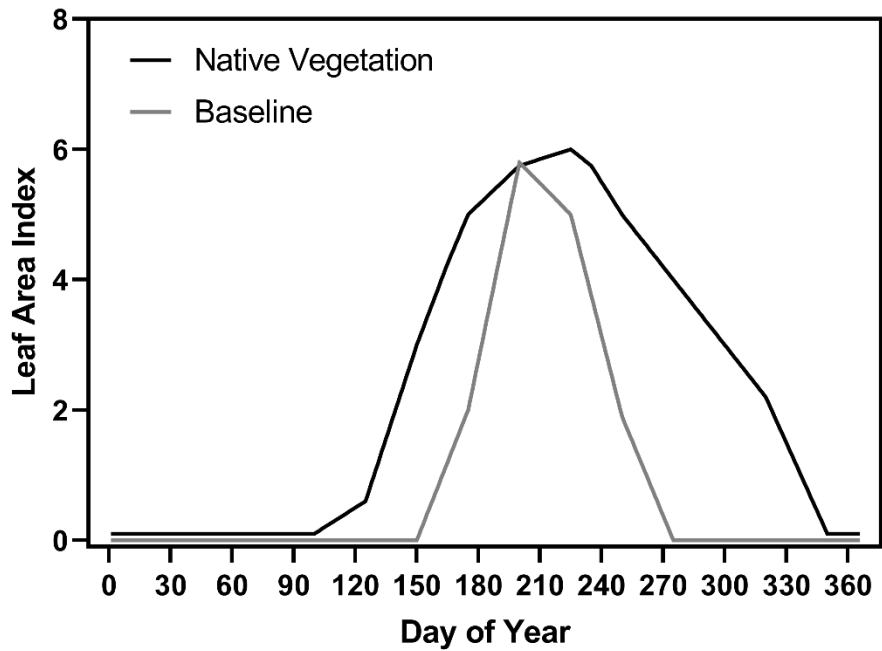
Figure 6-6: Leaf area index annual time series for native vegetation land cover and the row crop baseline.
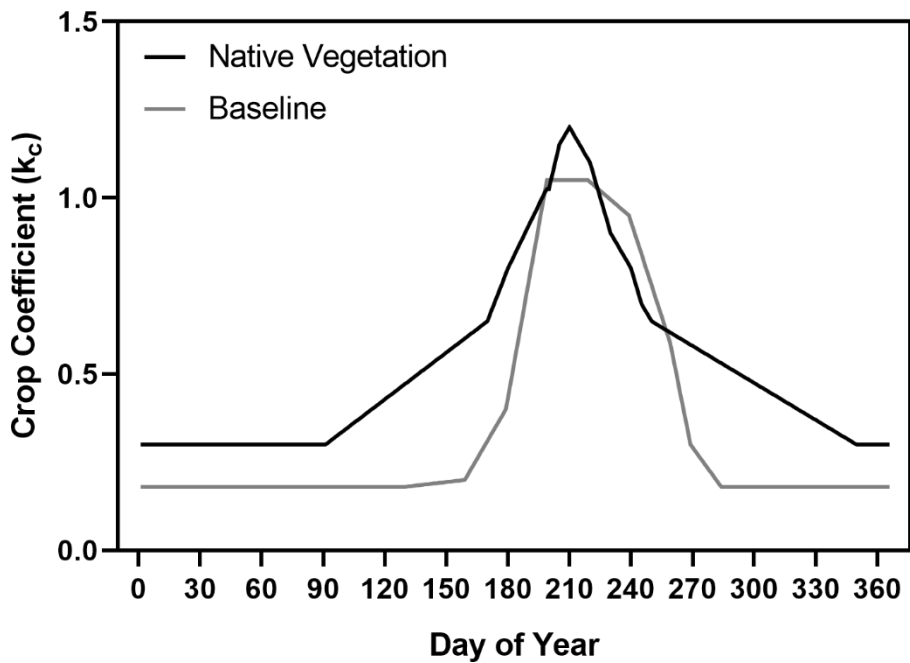
Figure 6-7: Crop coefficient annual time series for native vegetation land cover and the row crop baseline.
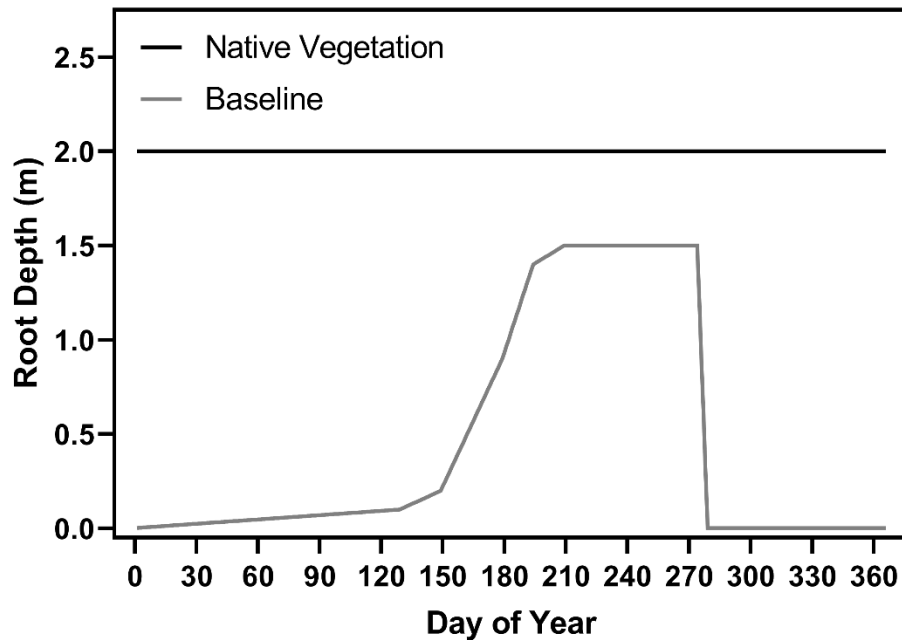
Figure 6-8: Root depth annual time series for native vegetation land cover and the row crop baseline.

6.1.2 Native Vegetation Results

The native vegetation scenario represents the largest deviation from the baseline in terms of both vegetation properties and soil characteristics. The flow duration curves for the baseline and native vegetation scenarios show large reductions at high and middling scales of flow, but little change occurs for low flows (Figure 6-10). Peak flow reductions from native vegetation are the largest of any scenario (Figure 6-9). The annual maximum discharges show high percent reductions for the high exceedance probability flows and smaller reductions for the lower exceedance probability flows (Figure 6-11). The reductions range from 2,000 to 15,330 cfs and average 7,700 cfs while percent reductions range from 14.9 to 95.7 and average 82.4 percent. The native vegetation scenario is able to mitigate the effects of the increased precipitation maintaining an average reduction of 6,930 cfs (76.3 percent). Seasonal trends from the reductions of annual maximum discharges are unclear (Figure 6-12).

93
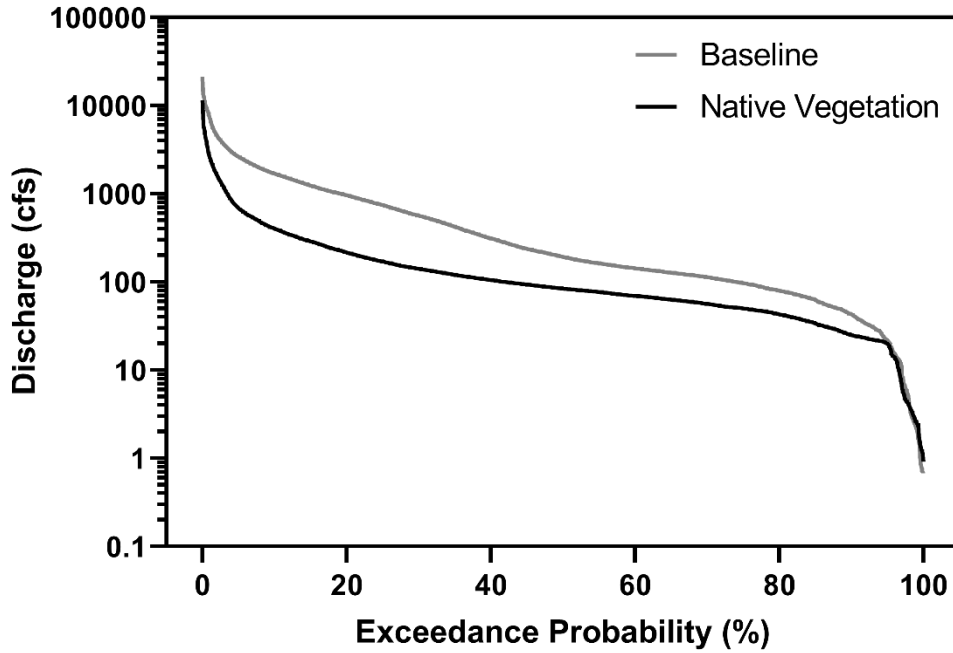
Figure 6-10: Discharge versus exceedance probability for the baseline and native vegetation scenario.
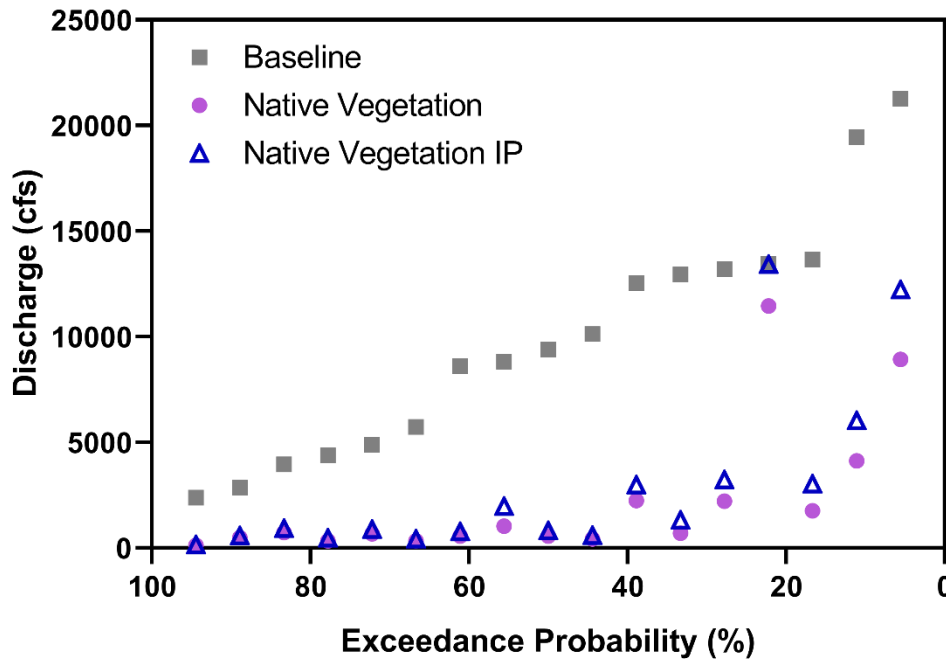
Figure 6-9: Maximum annual discharge versus exceedance probability for the baseline, native vegetation, and native vegetation with increased precipitation.

94
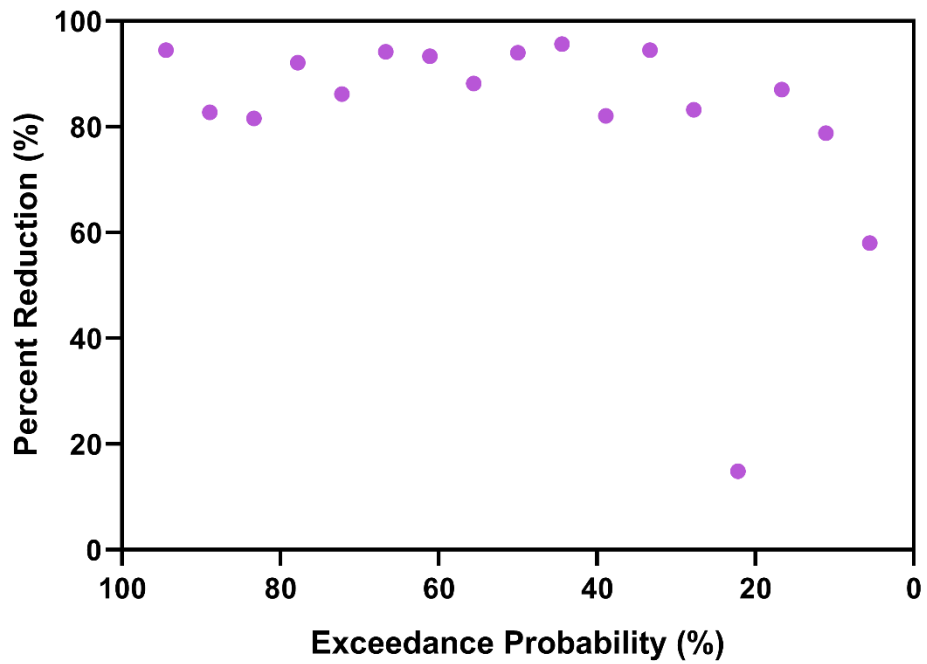
Figure 6-11: Percent reduction versus exceedance probability for the native vegetation scenario.
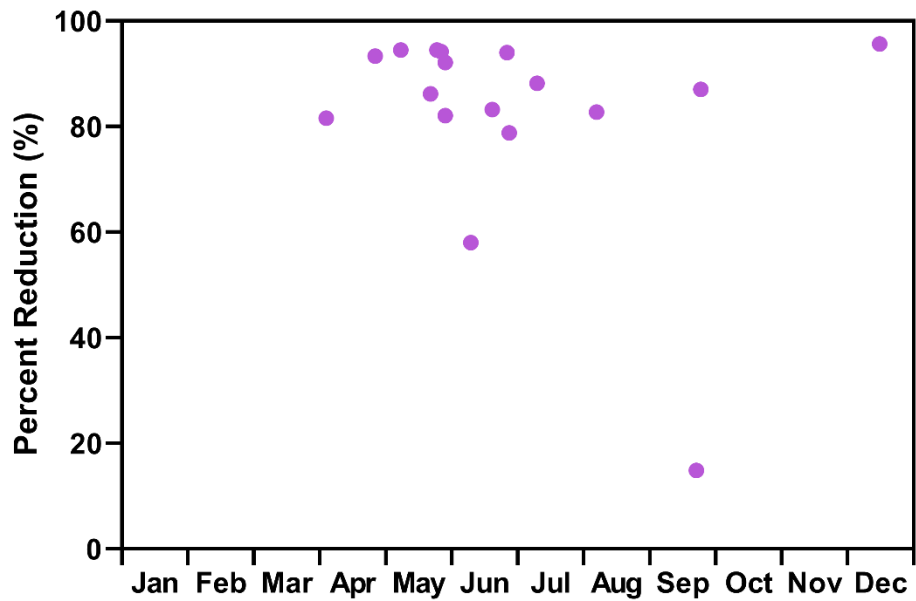
Figure 6-12: Percent reduction versus the month of the annual maximum discharge for the native vegetation scenario.

95

The clear outlier in the analysis of the annual maximums is the 2018 event with exceedance probability of 22 percent that occurs in September. Reductions produced by the native vegetation scenario for this event were the lowest in terms of both magnitude and percent. The 2016 event with exceedance probability of 17 percent is similar in magnitude and also occurs in September, yet the native vegetation scenario produced a much larger reduction for this annual maximum. What differs for these two events is the soil moisture states of the model in the week preceding the 2018 and 2016 events (Figure 6-13). 2018 is a wetter year overall and the 2018 annual maximum is preceded by a large event in late August that left soils in the model highly saturated (Figure 6-14).
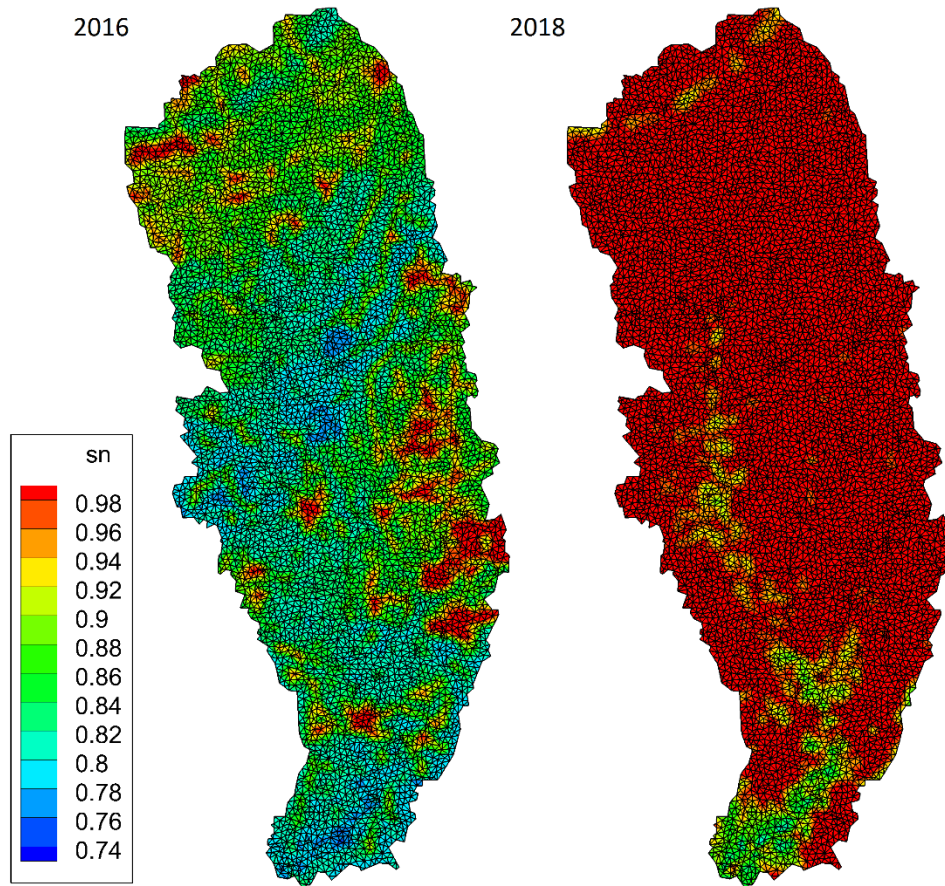
Figure 6-13: Soil moisture in the model in the week before the September 2016 event (left) and September 2018 events (right).
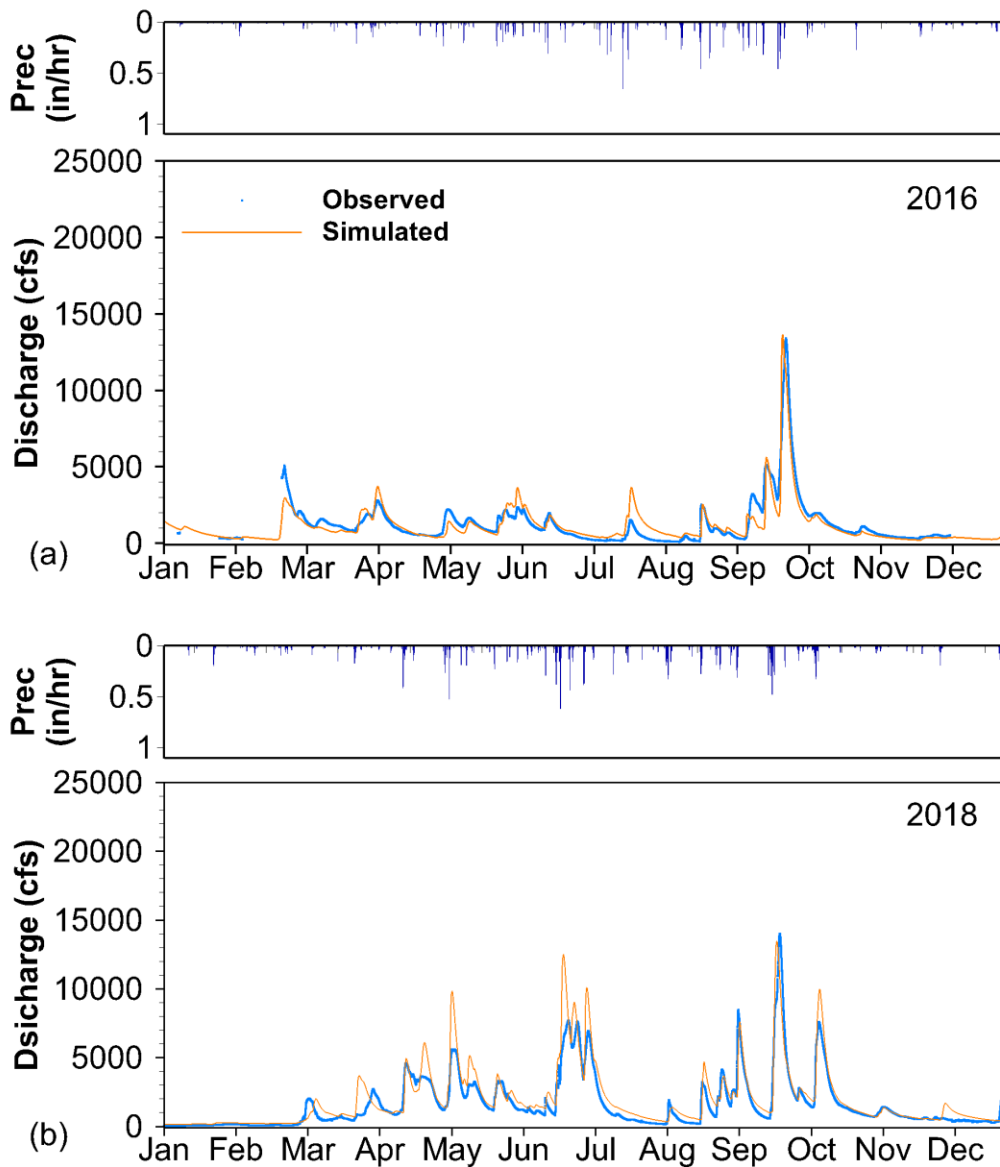
Figure 6-14: Observed and simulated flows for the calibrated model for 2016 (a) and 2018 (b).

Using the POT method, the maximum discharge reduction is 15,330 cfs, while the minimum reduction is 2,000 cfs, and the average is 7,540 cfs (Figure 6-15). Analysis using POT reveals more variation in discharge for the native vegetation scenario and subsequently more variation in percent reduction (Figure 6-16). The maximum percent reduction is 96.4 percent, while the minimum is 14.9 percent and the average is 74.9. Average reductions for the increased

97

precipitation native vegetation scenario fall to 6,600 cfs (66.5 percent). Peaks span the months of April through October and December with the majority of peaks occurring in May and June. Using POT allows for the characterization of a broader spectrum of higher peaks than using the annual maximum peaks alone. Because of this, comparing the seasonal timing of the annual maximums (Figure 6-12) with that of the POT (Figure 6-17) reveals the percent reduction of discharge for the native vegetation scenario is seasonally dependent. During the months of April and May the percent reductions of peaks are consistently higher on average than those during the months of July, August, September and October (Table 6-3). These seasonal differences are primarily attributed to the changes made in the LAI, kc, and rd time series that reflect the perennial nature of the native vegetation versus the annual nature of the row crop baseline. Since the crop coefficients between the native vegetation scenario and the row crop baseline are more similar late in the growing period, there is a lower degree of difference between the peaks of the two during this period.
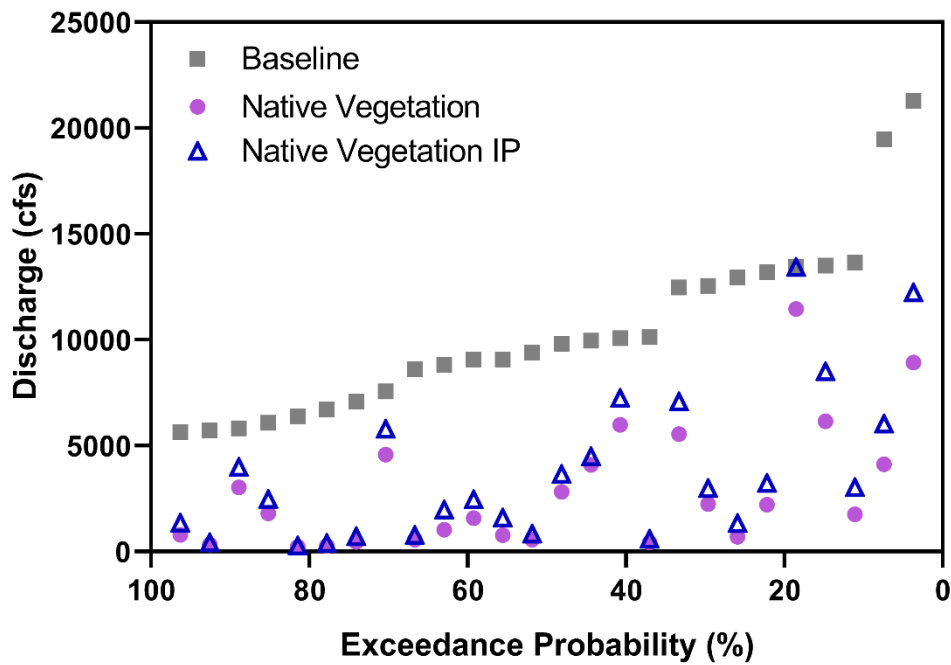
Figure 6-15: Peak discharges identified by POT vs exceedance probability for the baseline, native vegetation scenario, and native vegetation with increased precipitation.

98
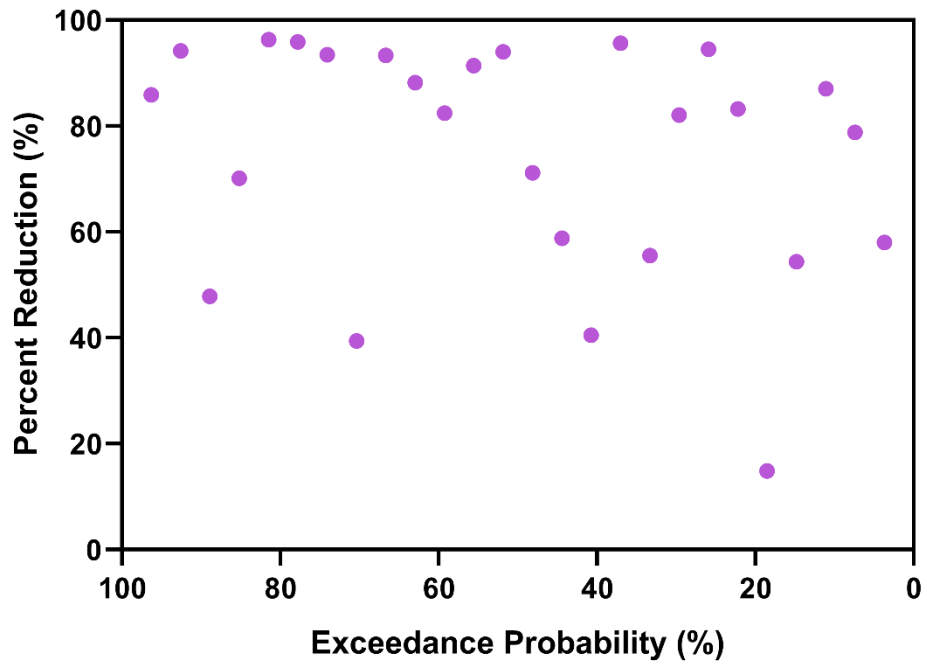
Figure 6-16: Peak discharges identified by POT versus exceedance probability for the native vegetation scenario.
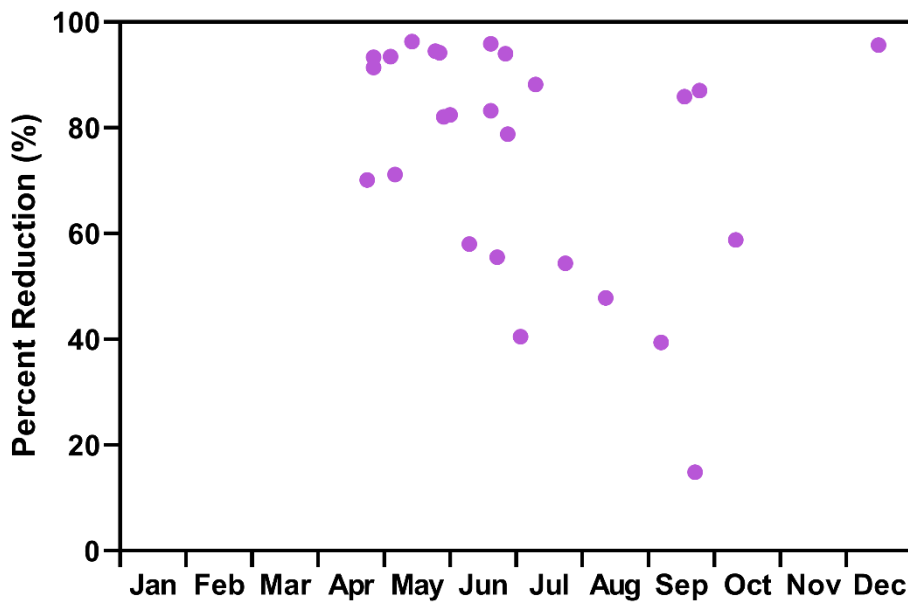
Figure 6-17: Peak discharges identified by POT versus month of occurrence for the native vegetation scenario

99

Table 6-3: Peaks-over-threshold count and average percent reduction of discharge by month for the native vegetation scenario.

Month	Count	Average Reduction (%)
January	0	-
February	0	-
March	0	-
April	3	85.0
May	7	87.8
June	6	77.6
July	3	61.1
August	1	47.9
September	4	56.8
October	1	58.8
November	0	-
December	1	95.7

6.1.3 Comparison to Literature

The results presented here for the native vegetation scenario show dramatic reductions in both year round and peak flows. While these results are highly dependent on the changes made to the model to represent native vegetation and these changes merit scrutiny, there is precedent in the literature for similar reductions being observed at the field scale. In a study done at the Neil Smith National Wildlife Refuge in Jasper County, Iowa, Hernandez-Santana et al. (2013) found similar scales of reductions in surface runoff (Figure 6-18, Figure 6-19). For the 2009 study period from Hernandez-Santana et al. (2013), the percent difference between the 100 percent row crop watersheds (100RC) and the 100 percent native prairie vegetation (100NPV) shows a greater than 95% reduction in surface runoff. The Boone River watershed model shows a 96.7 percent reduction in surface runoff for the equivalent period in 2009. For the 2010 study period from Hernandez-Santana et al. (2013), the percent difference between the 100RC and 100NPV sites shows a greater than 75% reduction in surface runoff. For the equivalent period, the Boone River watershed model shows a 74.7 percent reduction in surface runoff.

100
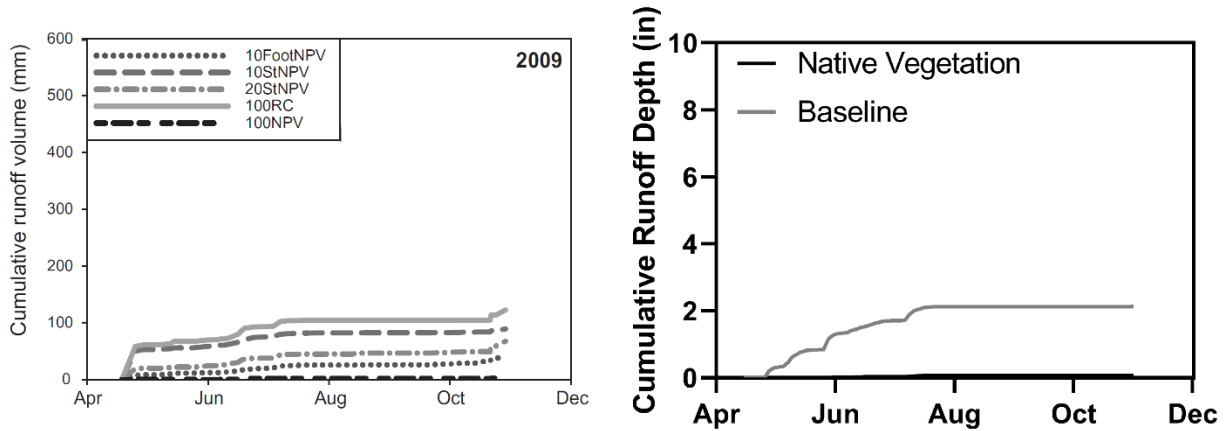
Figure 6-18: Left: Figure adapted from Hernandez-Santana et al. (2013) of cumulative surface runoff volume versus month for the year 2009. Each line is the average for three different field-scale sites. 100RC correlates with the baseline from the Boone River model and 100NPV correlates with the native vegetation scenario. Right: cumulative surface runoff depth for the baseline (agriculture acres in 100 percent row crop) and native vegetation (agriculture acres 100 percent native vegetation) for the Boone River model.
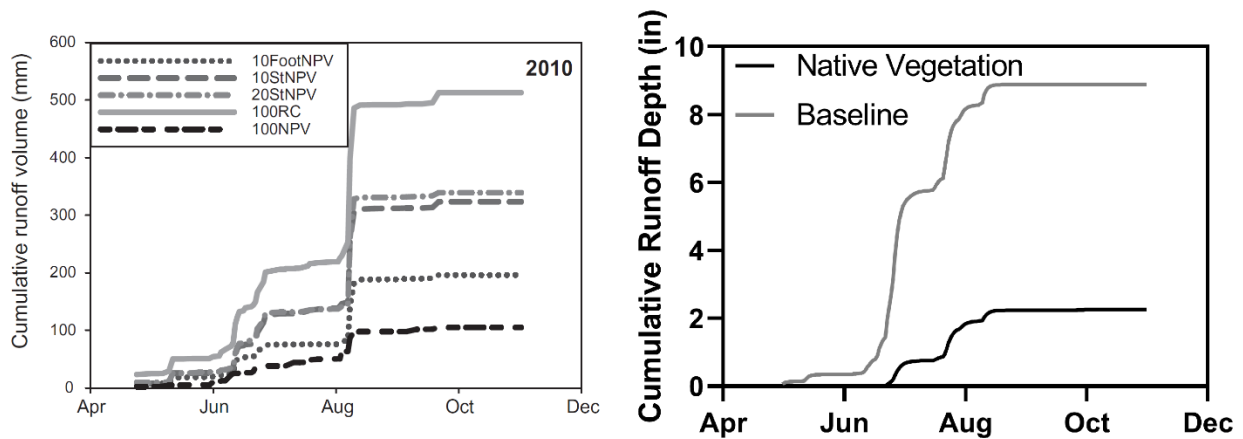
Figure 6-19: Left: Figure adapted from Hernandez-Santana et al. (2013) of cumulative surface runoff volume versus month for the year 2010. Each line is the average for three different field-scale sites. 100RC correlates with the baseline from the Boone River model and 100NPV correlates with the native vegetation scenario. Right: cumulative surface runoff depth for the baseline (agriculture acres in 100 percent row crop) and native vegetation (agriculture acres 100 percent native vegetation) for the Boone River model.

101

6.2 Cover Crops/No-Till/Soil Health

There is much interest in modern, conservation-minded agriculture in cultivating healthier soils to benefit crops and reduce soil loss. These practices have the serendipitous accompanying benefit of improving the hydrologic properties of the soils in the fields they are implemented in—infiltration rate has been identified as an indicator of good soil health (Radke & Berry, 1993). Cover crops and no-till practices are both areal and can be viewed as a limited version of the native prairie scenario. Where the two differ is in the seasonality and degrees of changes made to model inputs. Cover crops are planted in the Fall and either harvested, tilled under, or killed with herbicide in the spring (Sustainable Agriculture Research and Education, 2012). As a result, changes to the baseline to reflect the growth of cover crops are limited to the late fall, winter, and early spring when regular cash crops are not growing and fields would otherwise be bare. Like the native vegetation scenario, model parameters describing evapotranspiration, soil characteristics, and surface roughness were changed to reflect the implementation of cover crops and no till practices on all row crop land.

6.2.1 Changes to the Model

A number of studies have assessed LAI for cover crops (Baron, Najda, Salmon, & Dick, 1993; Blaser, Singer, & Gibson, 2011; Kang, Gu, Du, & Zhang, 2003). Due to the regions where they were done (Canada and semi-arid parts of the US and China) and some not being grown as winter cover crops, these studies are limited in their applicability can still inform the general behavior of cover crop LAI. Fang et al. (2008) reported year-round mean LAI of cereal crops for North America and Qi and Helmers (2010) reported the maximum LAI they observed for a winter rye cover crop of 1.78. The cover crop LAI implemented in the model is consistent with the findings of Fang et al. (2008) and Qi and Helmers (2010) (Figure 6-20).

Crop coefficients for cover crops are not well reported. Kang et al. (2003) and Kjaersgaard et al. (2008) reported crop coefficients for winter wheat, but the applicability of these studies is tenuous due to their being conducted in China and Denmark respectively. A

102

recent duo of papers determined the crop coefficients of a variety of mixtures of cover crops and found the crop coefficients of these plantings for the winter months to be variable with the crop mixture studied and highly variable in time (Sharma & Irmak, 2017; Sharma, Irmak, Sharma, Djaman, & Odhiambo, 2017). Allen et al. (1998) reported winter crop coefficients for winter wheat in frozen soils to be 0.4. The cover crop kc time series takes into consideration the observations of Kang et al. (2003) and Kjaersgaard et al. (2008) and is in agreement with the findings of Sharma & Irmak (2017) and Allen et al. (1998) with higher kc than the row crop baseline for the non-growing season (Figure 6-21).

Root depths have been reported for cover crops (Thorup-Kristensen & Rasmussen, 2015) and winter wheat in particular (Rasmussen & Thorup-Kristensen, 2016; Thorup-Kristensen, Cortasa, & Loges, 2009). Root growth starts in the fall increasing in depth at a rate that is consistent with Rasmussen & Thorup-Kristensen (2016) and Thorup-Kristensen et al. (2009). Root depth then is constant through winter to reflect dormancy and increases again in the spring to reach a max of 3.3 feet (1 meter). The rest of the year, root depth is identical to the baseline (Figure 6-22).

In addition to cover crops, this soil health scenario also includes the adoption of no-till practices. No-till has been shown to improve soil structure and health in ways which improve hydrologic properties (Basche, 2017; Edwards et al., 1988; Lee, 1985). As a result, no-till help increases soil infiltration rates by as much as an order of magnitude. No-till practices also affect the soil surface by effectively increasing Manning's roughness from 0.048 to 0.114 (Mohamoud, 1992). In light of these findings the infiltration rate (k_{inf}) for cover crops increases from 1×10^{-6} to 1.4×10^{-6}, the parameter s_n^* in the sigmoid function which controls flow from the unsaturated to the saturated zone was changed from 1.33 to 1.36 to reflect greater soil water holding capacity (which corresponds to an increase in model average soil moisture by 1.0 percent), and the Manning's roughness for overland flow was changed from 0.1 to 0.3.

103
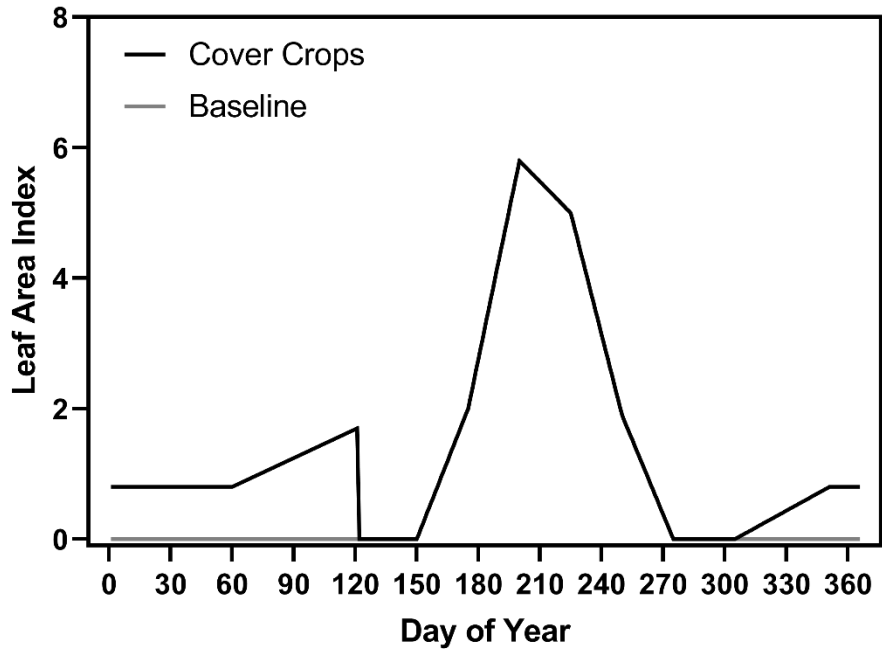
Figure 6-20: Leaf area index annual time series for cover crop land cover and the row crop baseline.
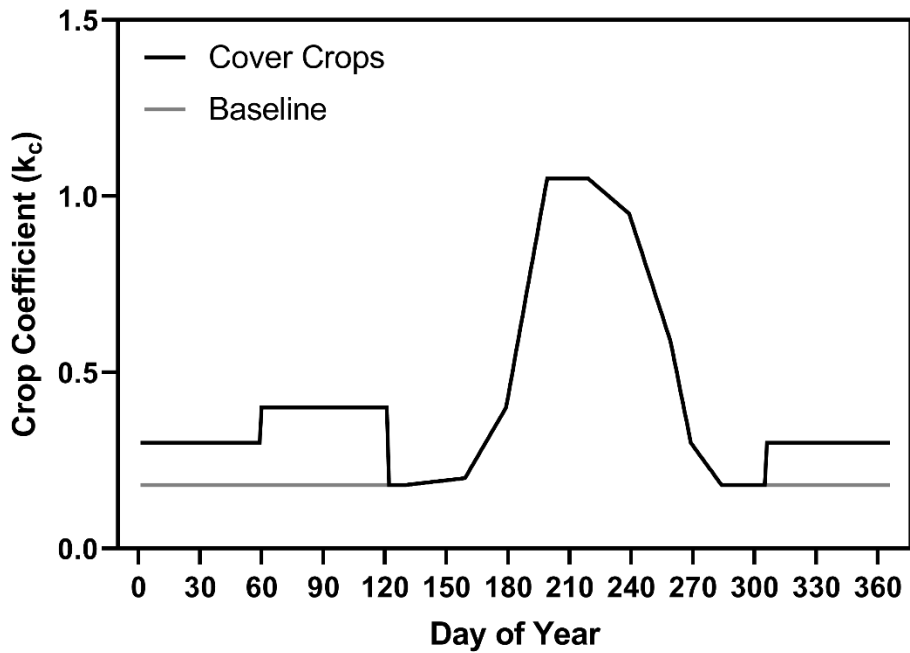
Figure 6-21: Crop coefficient annual time series for cover crop land cover and the row crop baseline.

104

www.manaraa.com
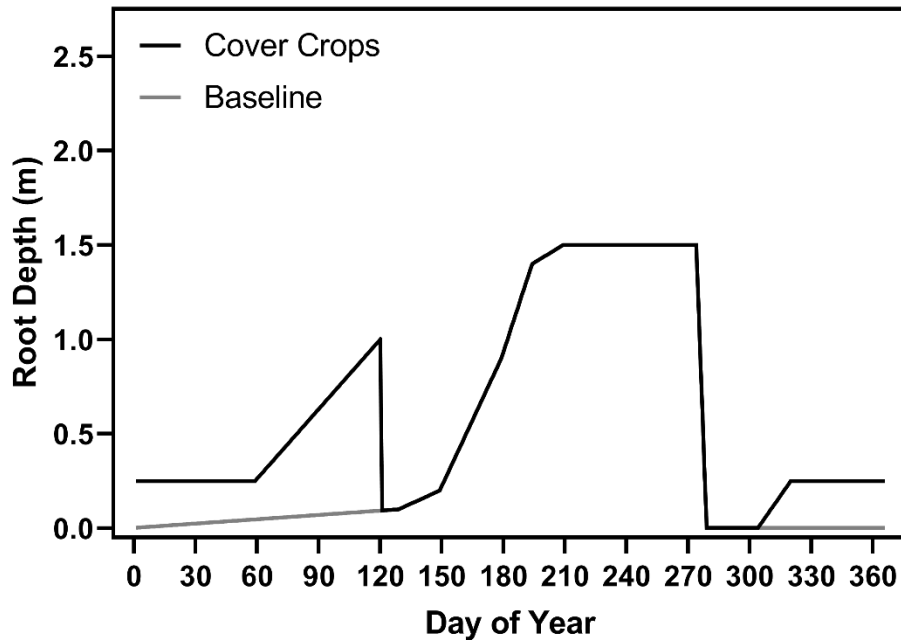
Figure 6-22: Root depth annual time series for cover crop land cover and the row crop baseline.

6.2.2 Cover Crops/No-Till/Soil Health Results

Since the changes to the model to represent the cover crops scenario in terms of LAI, Kc, and rd are limited to the non-growing season and the changes to the soil parameters are less drastic than those made to represent the native vegetation scenario, it is anticipated the discharge reductions will be lessened. The flow duration curve for the cover crop scenario closely mirrors that of the baseline with reductions at all scales of flow except the highest exceedance probability flows (Figure 6-23). Annual maximum discharge reductions for this scenario range from 1,300 to 6840 cfs and average 2,970 cfs (Figure 6-24); annual maximum discharge percent reductions range from 9.7 to 88.4 and average 38.5 percent (Figure 6-25). The cover crop scenario is able to offset the effects of the increased precipitation scenario maintaining an average reduction of 1,750 cfs (27.0 percent). Seasonally, percent reductions are most significant for events occurring in April and early May with mid to late May through July seeing

105

significantly lower percent reductions (Figure 6-26). This effect is likely due to the events in mid to late May through July being the highest discharge events.

Figure 6-23: Discharge versus exceedance probability for the baseline and cover crop scenario.

Figure 6-24: Annual maximum discharges versus exceedance probability of discharge for the baseline model, cover crop scenario, and the cover crop scenario with increased precipitation.

Figure 6-25: Annual maximum discharge percent reduction versus exceedance probability for the cover crop scenario

107

Figure 6-26: Annual maximum discharges versus month of occurrence for the cover crop
scenario.

The peak flow reductions for POT for the cover crop scenario range from 580 to 6,840
cfs and average 2,770 cfs (Figure 6-27). Percent reductions for the POT peaks range from 9.7 to
63.6 percent and average 29.3 percent (Figure 6-28). On average, cover crops maintain their
ability to offset the impacts of increased precipitation with an average reduction of 1,530 cfs
(17.5 percent). Analyzing the percent reductions plotted by month of occurrence for POT reveals
a clear decreasing trend from April through October which reflects how the effects of the cover
crops diminish as the growing season progresses and the model is further removed from the
vegetation changes (Figure 6-29).
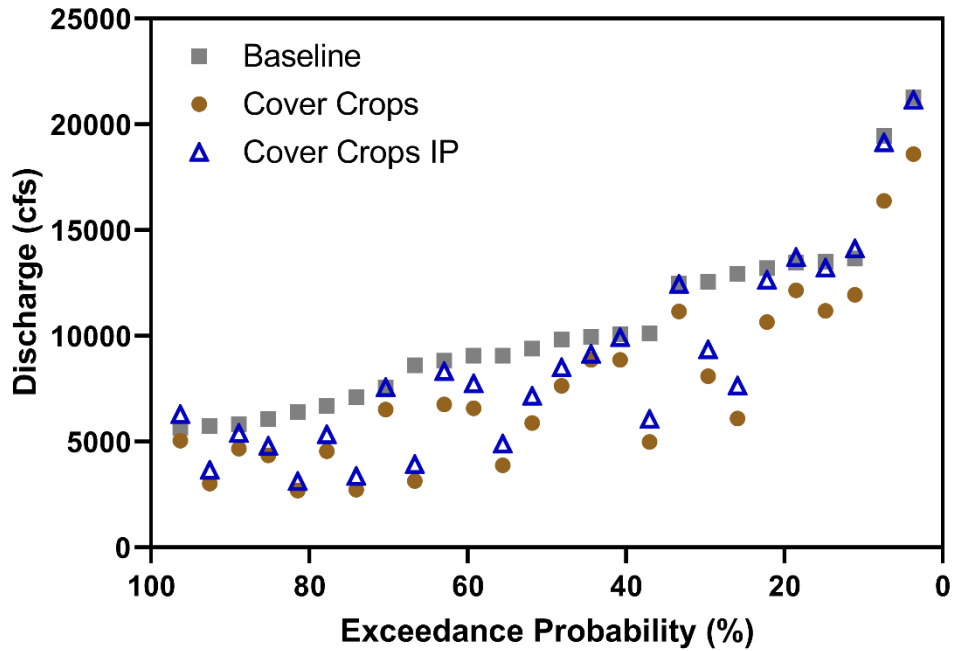
Figure 6-27: Peaks identified by POT versus exceedance probability for the baseline model, cover crops scenario, and cover crops with increased precipitation.

Figure 6-28: Percent reductions of peak discharges identified by POT versus exceedance probability.

109

Figure 6-29: Percent reductions of peak discharges identified by POT versus month of occurrence.

Table 6-4: Peaks-over-threshold count and average percent reduction of discharge by month for the cover crops scenario.

Month	Count	Average Reduction (%)
January	0	-
February	0	-
March	0	-
April	3	49.7
May	7	43.5
June	6	21.3
July	3	17.5
August	1	19.7
September	4	11.6
October	1	11.0
November	0	-
December	1	50.7

110

6.3 Wetlands

In GHOST, wetlands are simulated as a stage-storage-discharge relationship built into river segments. Therefore, the wetlands are not sited at specific locations, but rather aggregated so that a number of them are sited for a particular river segment to simulate wetlands in the drainage area up-watershed of the segment. The design of the stage-storage-relationship is meant to reflect a typical wetland. To represent multiple wetlands sited in one drainage area, the stage-storage-discharge relationship for each is summed. Design metrics for a typical wetland include a storage of 20 acre-feet, a principal spillway pipe that is 6 inches in diameter with discharge calculated using an orifice equation, and an emergency spill way that is 10 feet wide with flow over the emergency spillway calculated by a weir equation.

6.3.1 Changes to the Model

The ACPF sites wetlands in agricultural watersheds using 3 criteria: they must be located along runoff flow paths, they must drain at least 60 acres, and their pooled area to drainage area ratio must be between 0.5 and 2 percent. These metrics and the siting rates in the HUC-12 watersheds of the Boone River watershed for which ACPF work was completed informed the number of wetlands simulated in this scenario. For the work presented here, wetlands were sited on the third segment from the ends of stream order one streams (Figure 6-30). To do this, these stream segments were assigned stage-storage-discharge relationships that were dependent on the area that drained into them with larger drainage areas being assigned stage-storage-discharge relationships that correspond to more wetlands. The total number of wetlands sited in the Boone River watershed is 411 in 103 drainage areas with a maximum of 7, minimum of 3 and average of 4.0 wetlands per drainage area. These 103 drainage areas make up approximately 31 percent of the area of the Boone River watershed. NRWs are implemented in the model via a user specified stage-storage relationship attached to river segments near the sited wetlands. Segments get assigned stage storage relationships that reflect the number of wetlands sited in the drainage

111

areas. Within the limits of wetland design constraints, the wetlands being built could have whatever stage storage relationship the user specifies.

It is important to note that in contrast to the native vegetation and cover crops scenarios, the wetlands scenario should not be viewed as a 100 percent implementation scenario or even an optimal implementation of the 411 wetlands sited. As such, the results should not be interpreted as the maximum possible benefit possible from wetlands. Although the number and distribution wetlands in the model is informed by the outputs of the ACPF, the distribution could be further optimized to move areas with more wetland storage than they need to areas with less storage than they need. Additionally, the number and distribution of wetlands that would represent the maximum possible benefit is difficult to define.
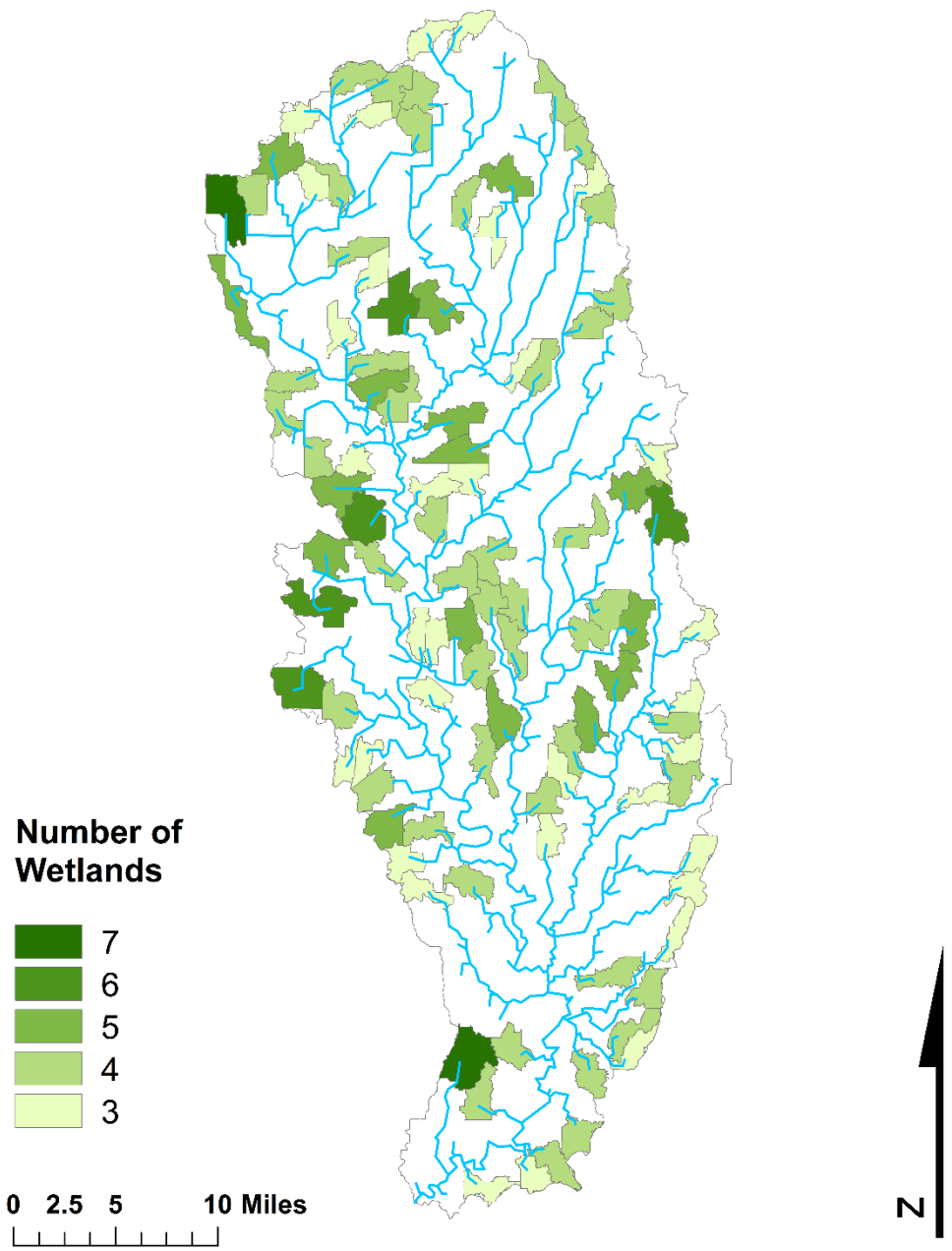
Figure 6-30: Approximate drainage areas where wetlands are sited and the number of wetlands in each drainage area.

6.3.2 Wetlands Results

Reductions produced by wetlands are modest in magnitude, but induce unique changes. The flow duration curve for the wetlands scenario closely follows the baseline and is lower for most exceedances except for the lowest flows where the wetlands scenario produces higher flows than the baseline (Figure 6-31). Annual maximum peak reductions range from 150 to 1300 cfs with an average reduction of 810 cfs and vary little with exceedance probability (Figure 6-32). Percent reductions for the annual maximum peak discharges range from 3.8 to 19.9 percent with an average reduction of 9.1 percent (Figure 6-33). Wetlands are not able to fully mitigate the effects of the increased precipitation scenario resulting in an average increase of 560 cfs (5.2 percent) over the baseline model. By month of occurrence, the percent reductions show no strong seasonality (Figure 6-34).
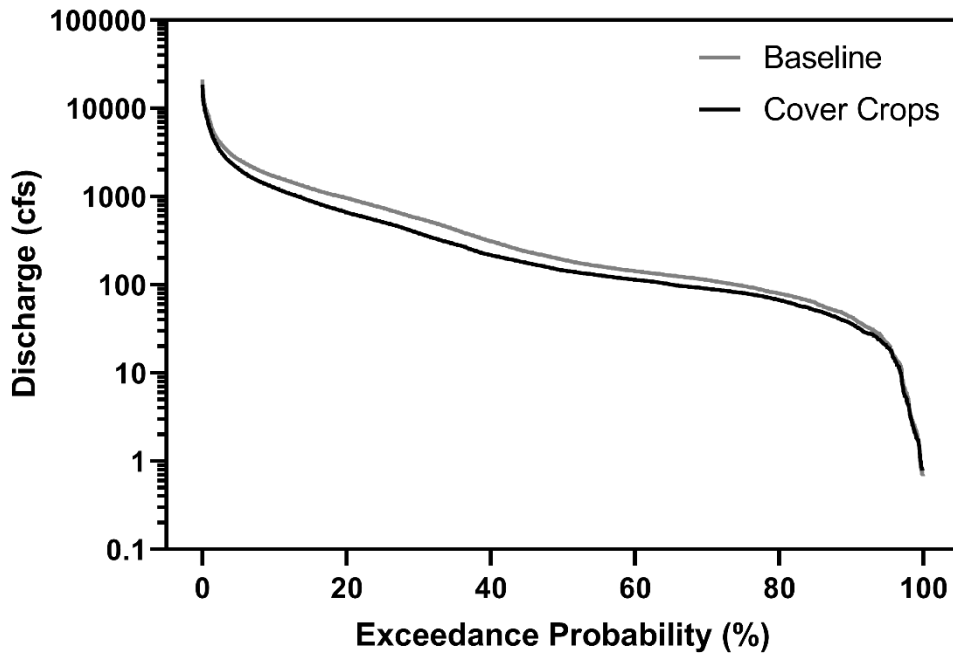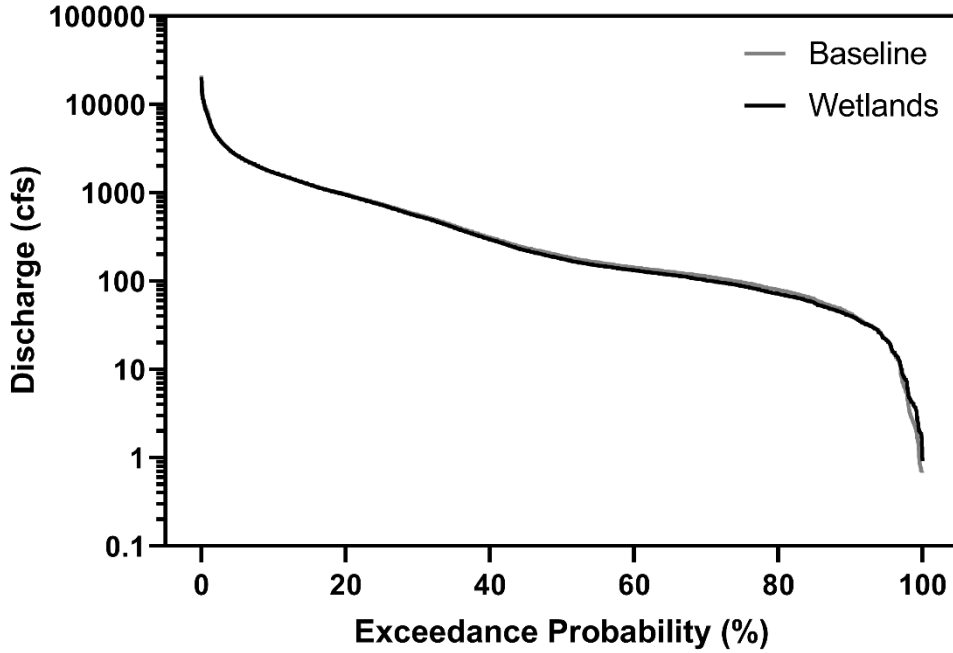
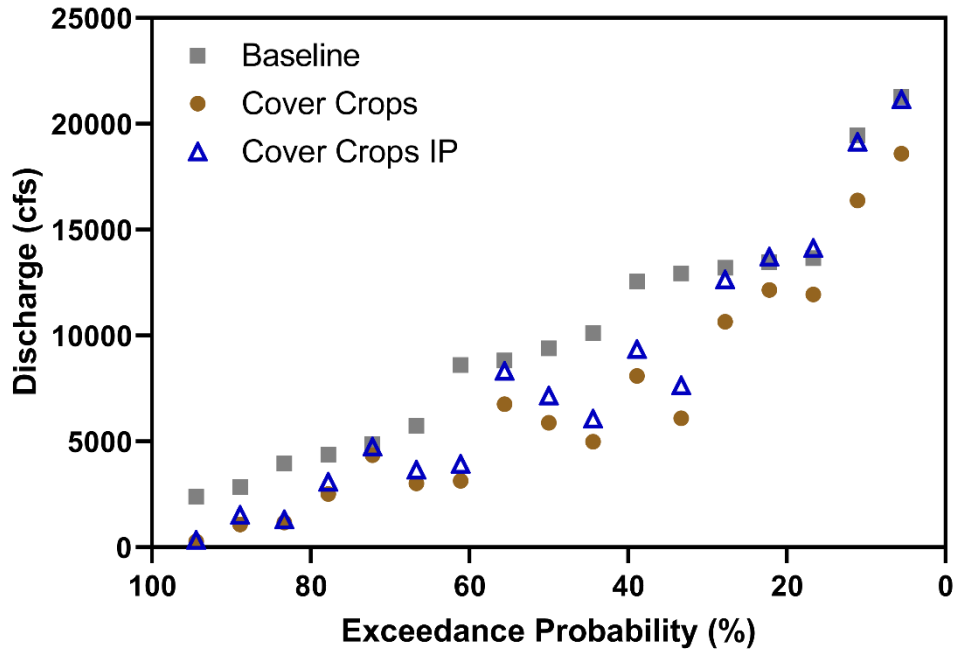Figure 6-31: Discharge versus exceedance probability for the baseline and wetlands scenario.
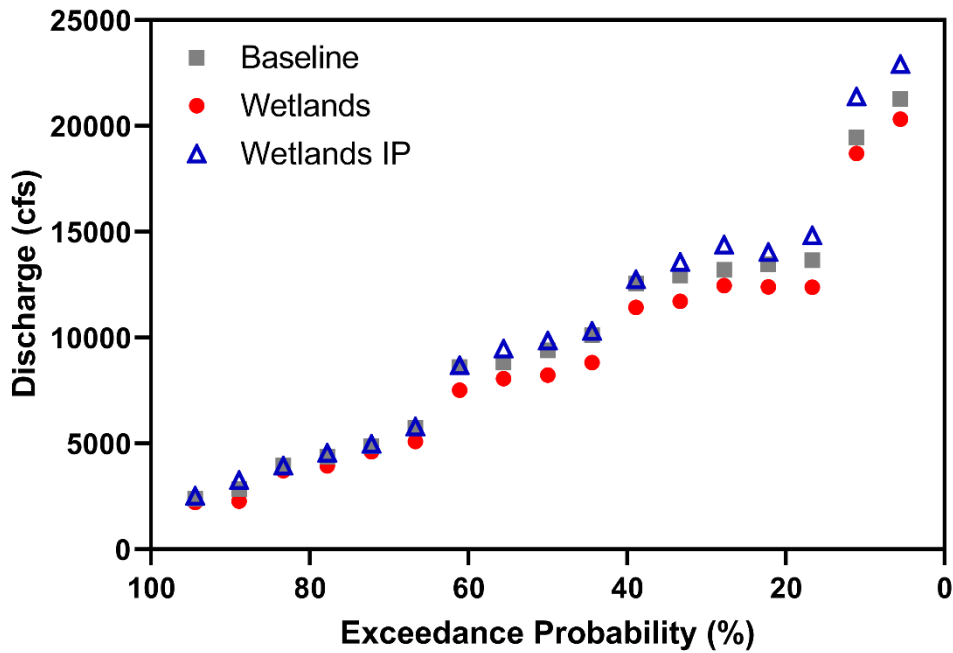
Figure 6-32: Annual maximum discharge versus exceedance probability of discharge for the baseline model, the wetlands scenario, and the wetlands with increased precipitation.
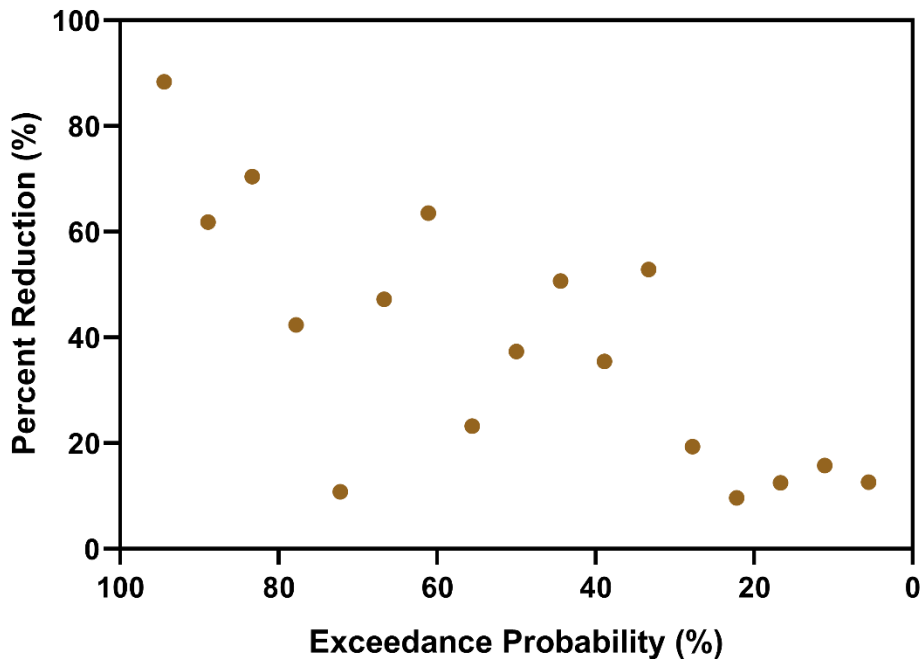
115
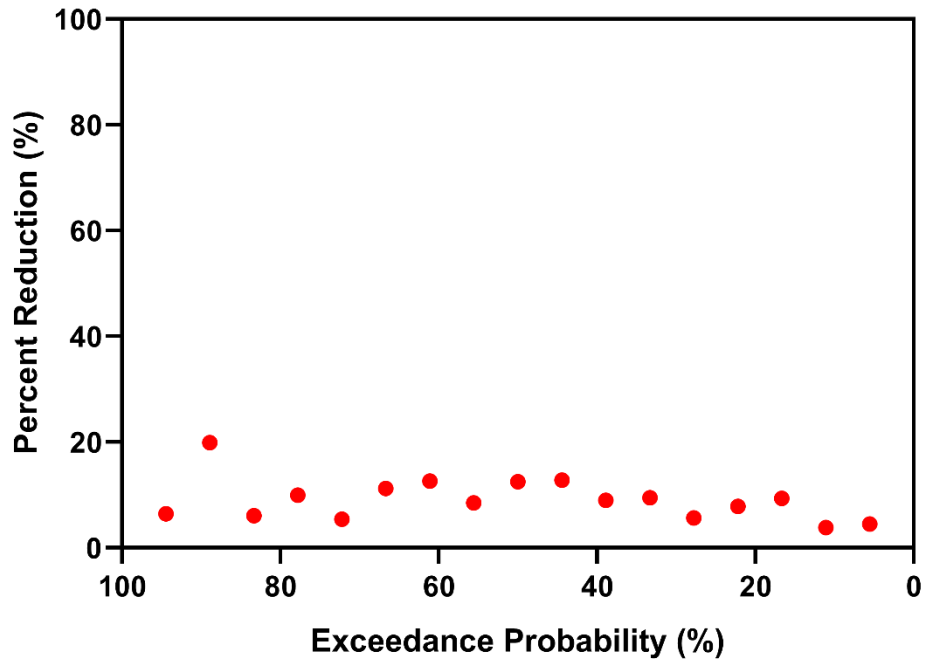
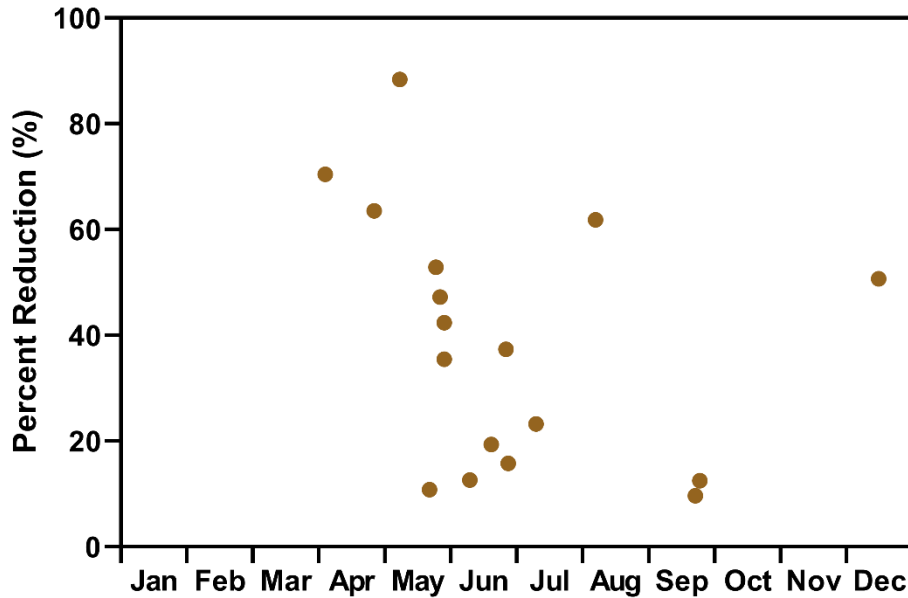Figure 6-33: Annual maximum discharge percent reduction versus exceedance probability for the wetlands scenario.
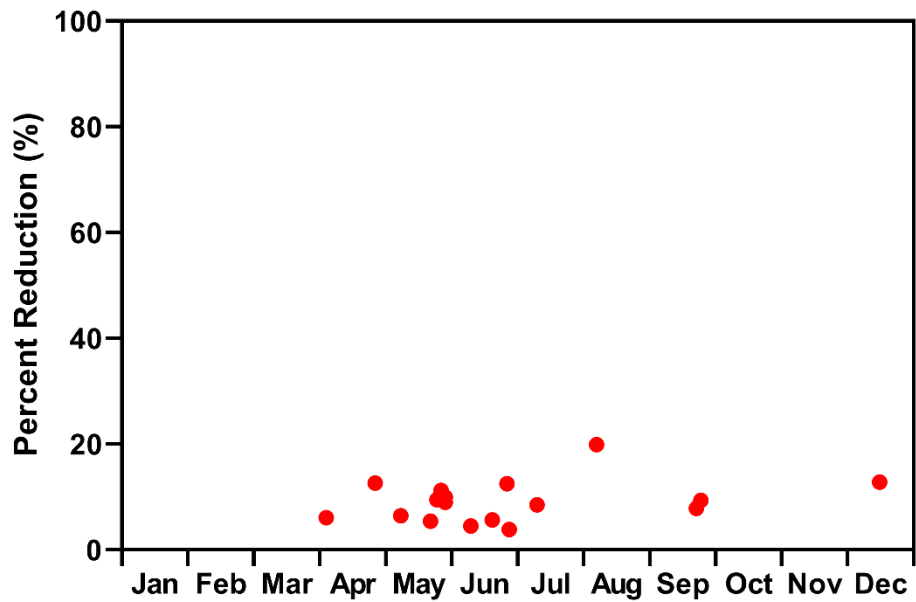
Figure 6-34: Percent reduction of the annual maximum discharge versus month of occurrence for the wetlands scenario.

116

Reductions of peaks identified by POT range from 440 to 1300 cfs with an average reduction of 920 cfs (Figure 6-35). Peaks identified by POT for the wetlands scenario have percent reductions ranging from 3.8 to 14.9 percent and average 9.5 percent (Figure 6-36Figure 6-33). Using the POT method, wetlands are found to not fully offset the effects of the increased precipitation scenario resulting in an average increase of 440 cfs (3.6 percent) over the baseline condition of the model. Analysis of peaks identified by the POT method by their month of occurrence shows no notable trend indicating wetlands have no seasonal variability in their potential to reduce peaks (Figure 6-37).
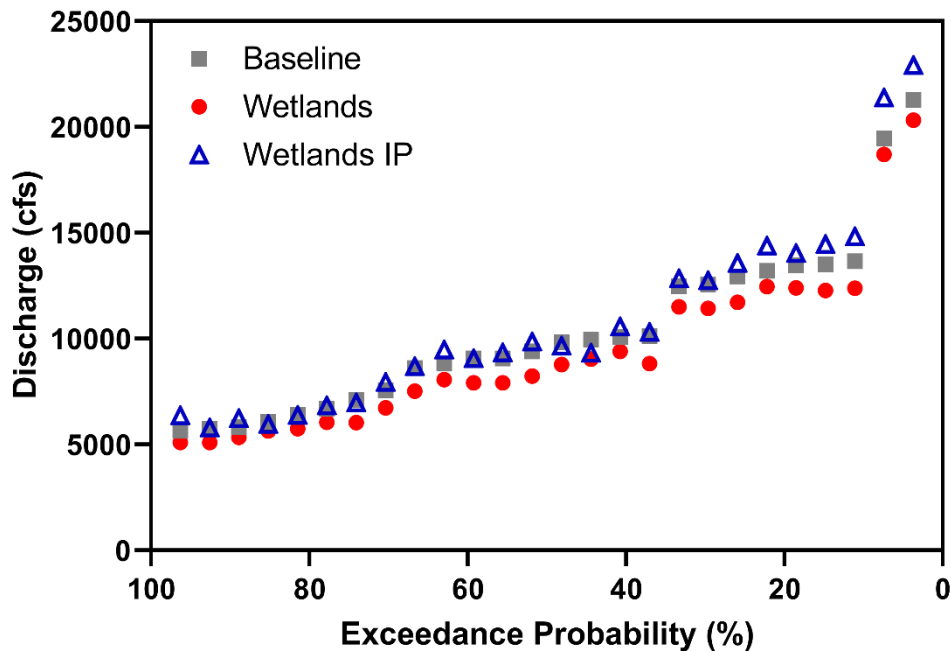
Figure 6-35: Peak discharges identified by POT versus exceedance probability for the baseline model, wetlands scenario, and wetlands with increased precipitation.
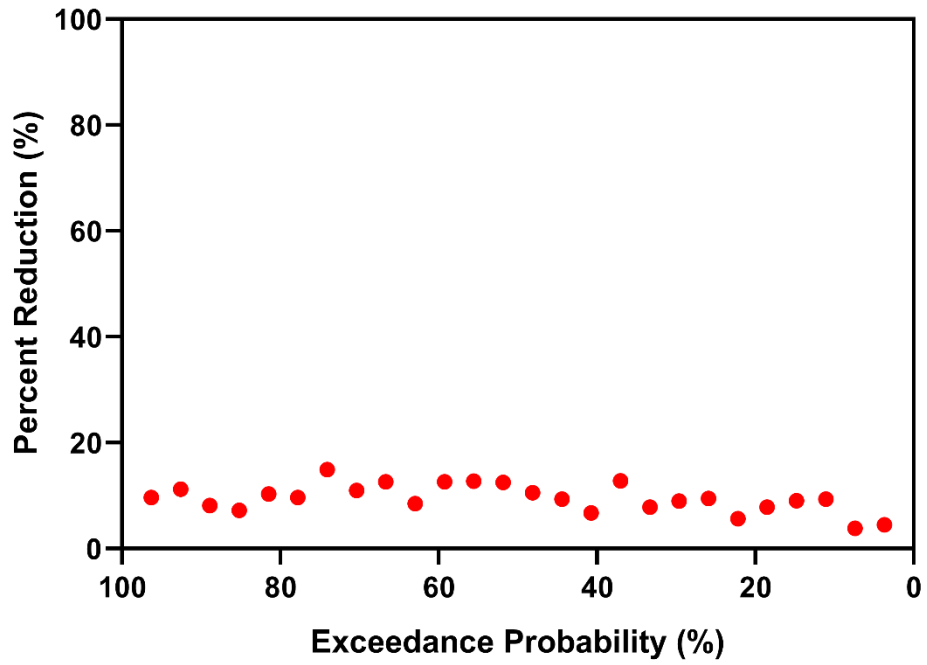
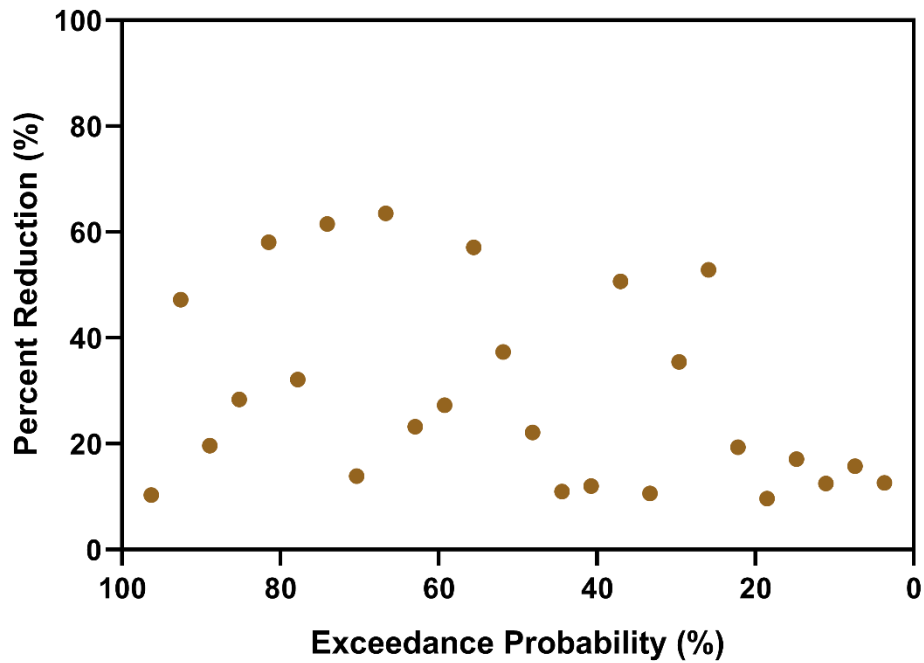Figure 6-36: Percent reduction of peak discharges by POT versus exceedance probability for the wetlands scenario.
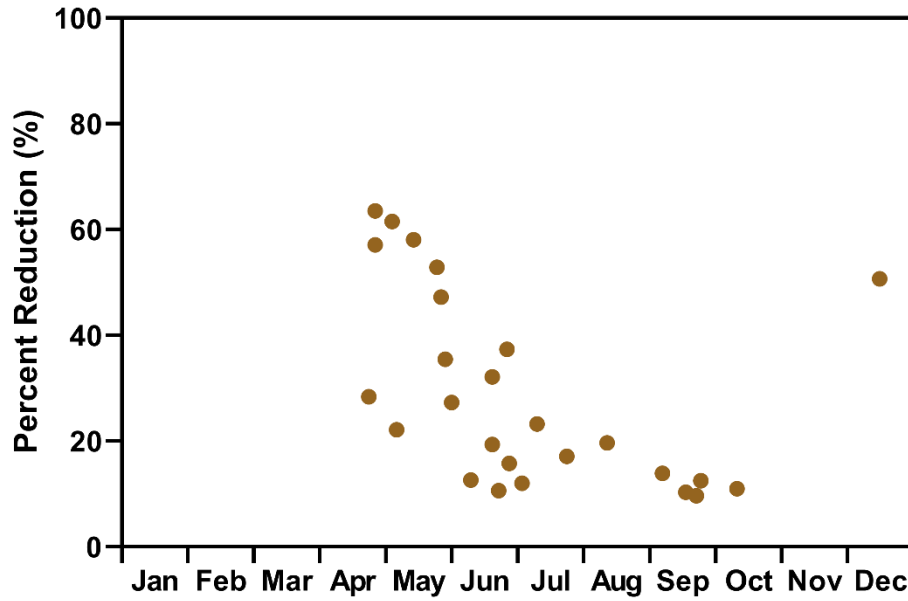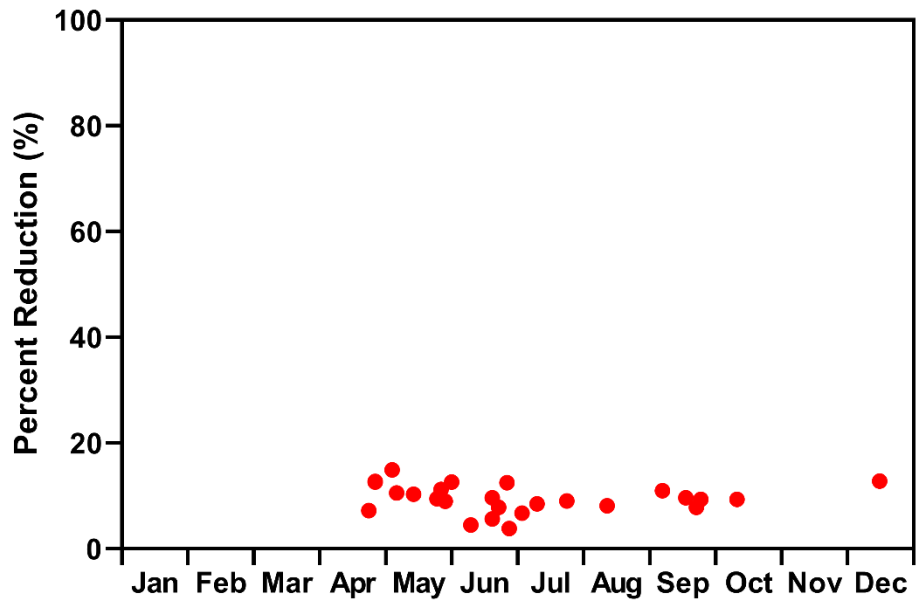

Figure 6-37: Percent reduction of peak discharges by POT versus month of occurrence for the wetlands scenario.

118

6.4 Riparian Corridor

Two scenarios were evaluated to determine if the riparian corridor plays a disproportionately large role in the reductions seen in the native vegetation scenario. The first riparian scenario reassigns all of the river-adjacent row crop elements of the mesh (Figure 6-38) while the second reassigns stream order one river adjacent elements only (Figure 6-39). It is important to note here, the formulation of GHOST used for the work in this thesis does not explicitly model the effects of subsurface tile drainage. In reality, flow from subsurface tile drainage at the field scale would likely bypass riparian practices.

6.4.1 Changes to the Model

For both riparian scenarios, the only change to the model was the reassigning of land cover from row crop to native vegetation for the relevant riparian elements. For the full riparian scenario, the total area of the elements reassigned was 102,400 acres (18.7 percent of all row crop acres) while the conversion of only stream order one adjacent elements meant 56,700 acres (10.4 percent of all row crop acres) were reassigned to native vegetation.
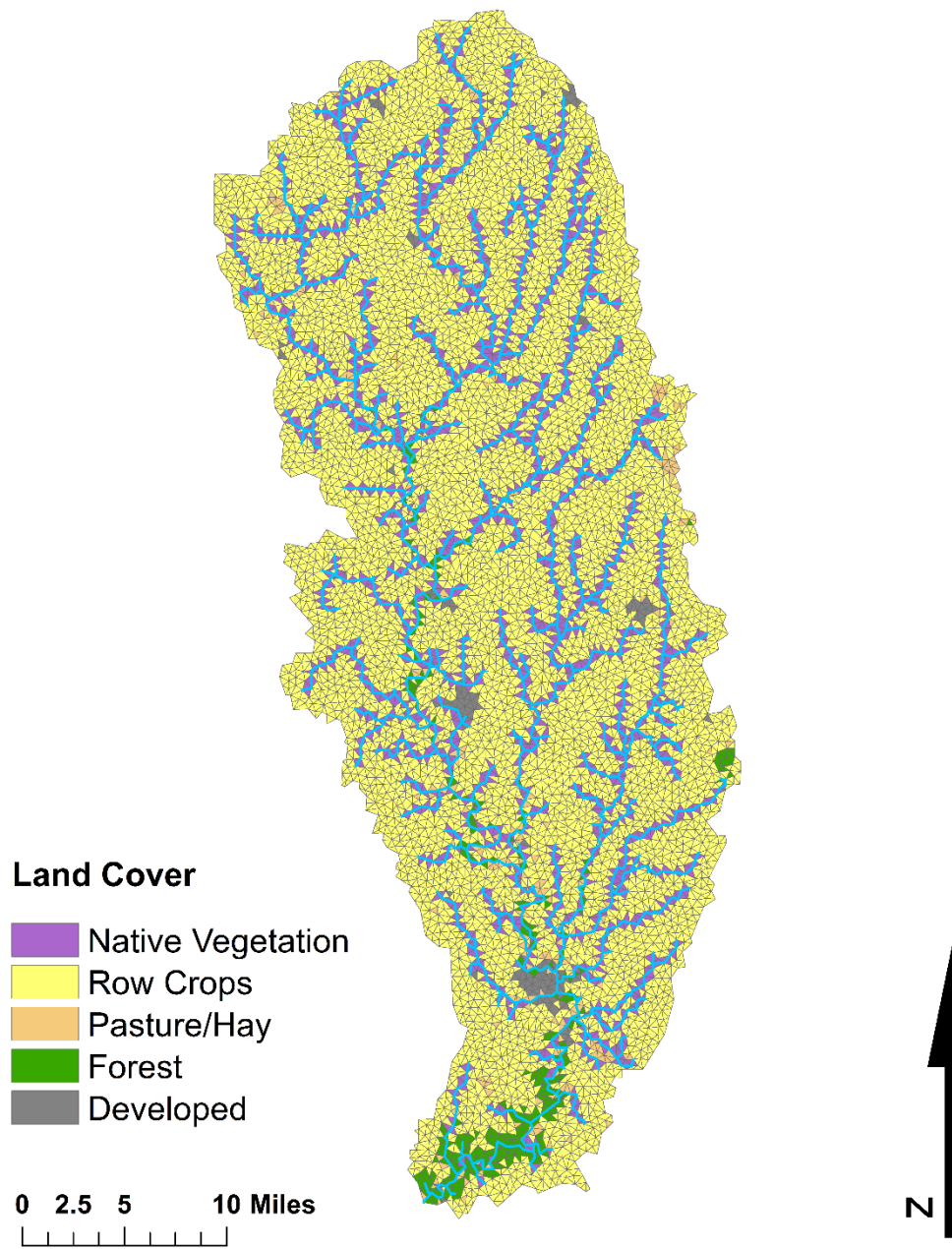
Figure 6-38: Conversion of all river-adjacent row crop elements to native vegetation.
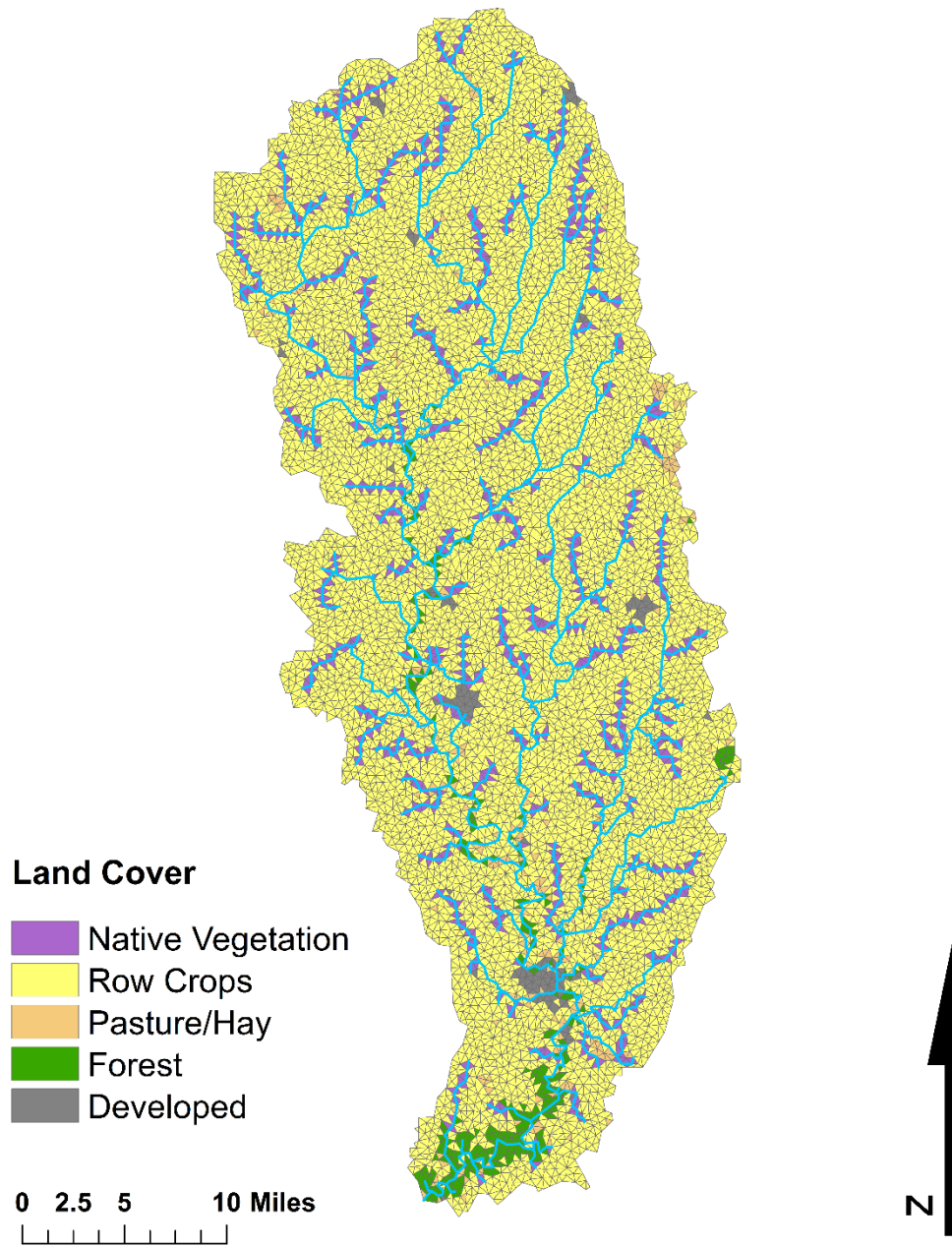
Figure 6-39: Conversion of all stream order one river-adjacent row crop elements to native vegetation.

6.4.2 Riparian Corridor Results

The flow duration curves for the full riparian scenario and the baseline show lower flows at most discharges except for high exceedance probability flows (Figure 6-40). For the riparian scenario with the full conversion of river adjacent row crop to native vegetation, the reductions in the annual maximum discharge range from 300 to 2,380 cfs and average 1,150 cfs (Figure 6-41). In terms of percent reduction of the annual maximum discharges, the full riparian corridor conversion to native vegetation ranges from 3.2 to 19.2 percent with an average of 13.2 percent (Figure 6-42). The full riparian scenario is not able to completely offset the effects of the increase precipitation scenario averaging an increase of 210 cfs (1.0 percent) over the baseline. Monthly percent reductions show no clear trends or patterns (Figure 6-43).
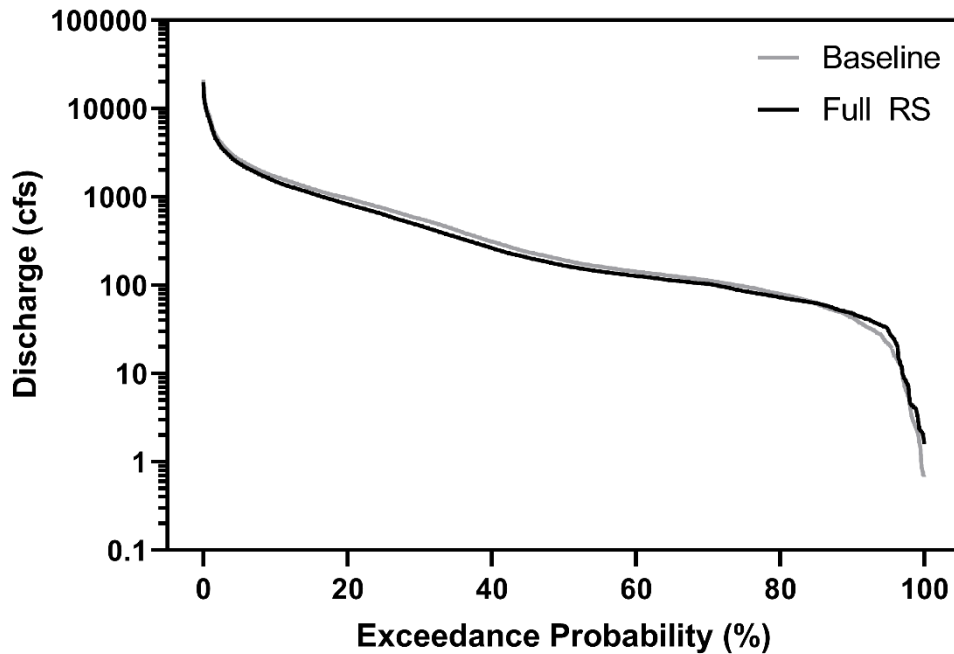
Figure 6-40: Discharge versus exceedance probability for the baseline and full riparian scenario (Full RS).
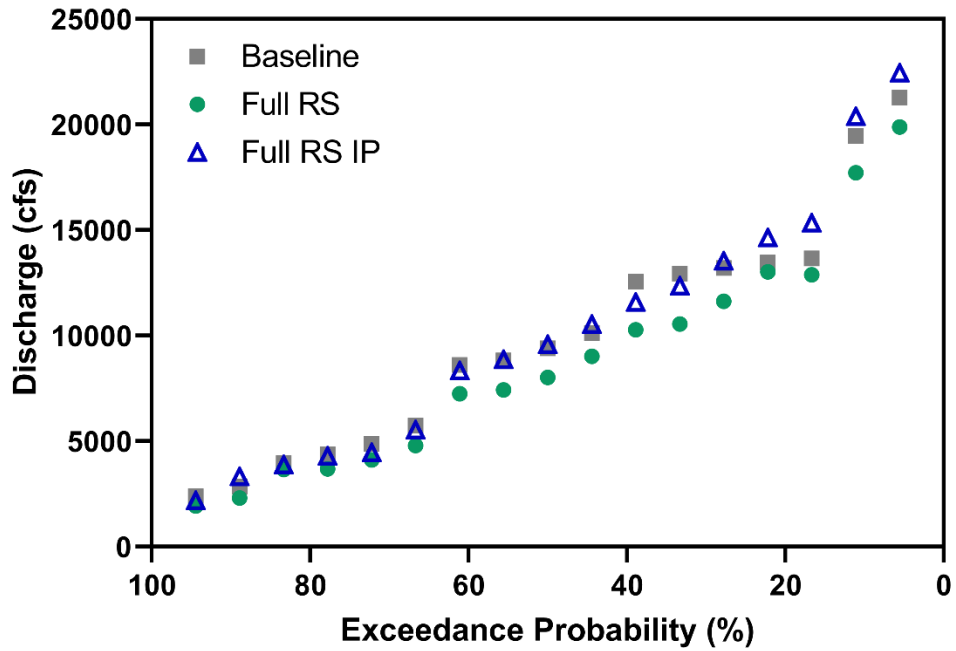
Figure 6-41: Annual maximum discharge versus exceedance probability for the baseline, full riparian scenario (Full RS), and Full RS with increased precipitation.
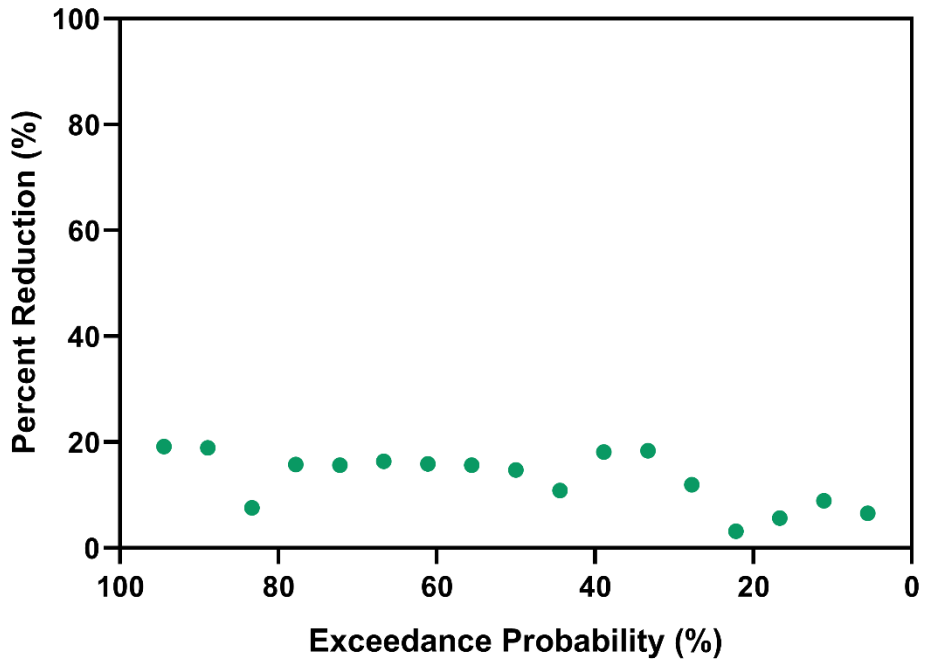
Figure 6-42: Percent reduction of the annual maximum discharge versus exceedance probability for the full riparian scenario.

123
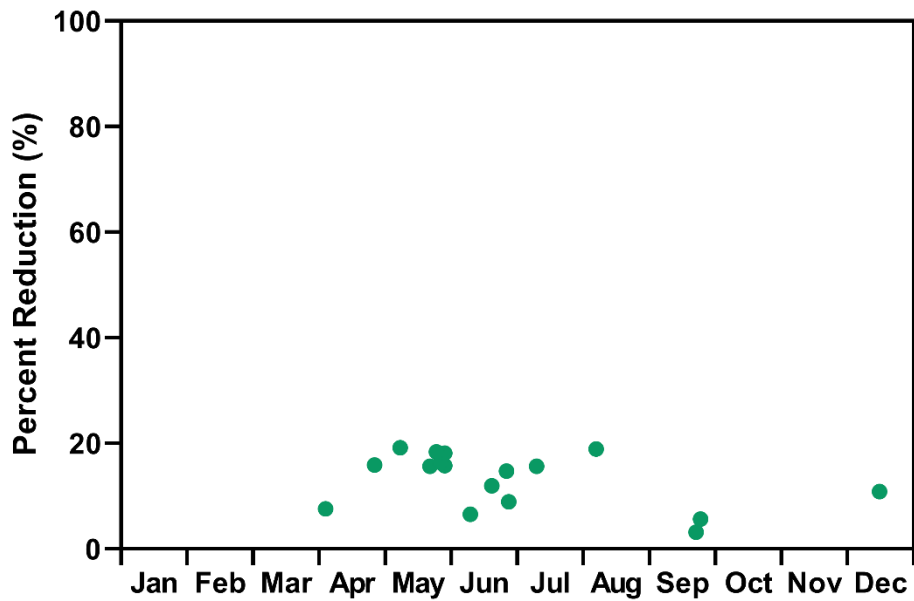
Figure 6-43: Percent reduction of the annual maximum discharge versus month of occurrence for the full riparian scenario.

Using the POT method, peaks are reduced by a range of 170 to 1,390 cfs and 980 cfs on average (Figure 6-44). By percent, the peaks identified are reduced by a range of 3.0 to 19.1 percent and 11.3 percent on average with the highest percent reductions coming from high exceedance probability peaks and falling moving towards low exceedance probability peaks (Figure 6-45). The full riparian scenario analyzed with the POT method does not fully counteract the effects of the increased precipitation scenario producing an average increase over the baseline condition of 250 cfs (2.0 percent). By month, percent reductions reach their highest in April, and May and decrease through September (Figure 6-46).

124
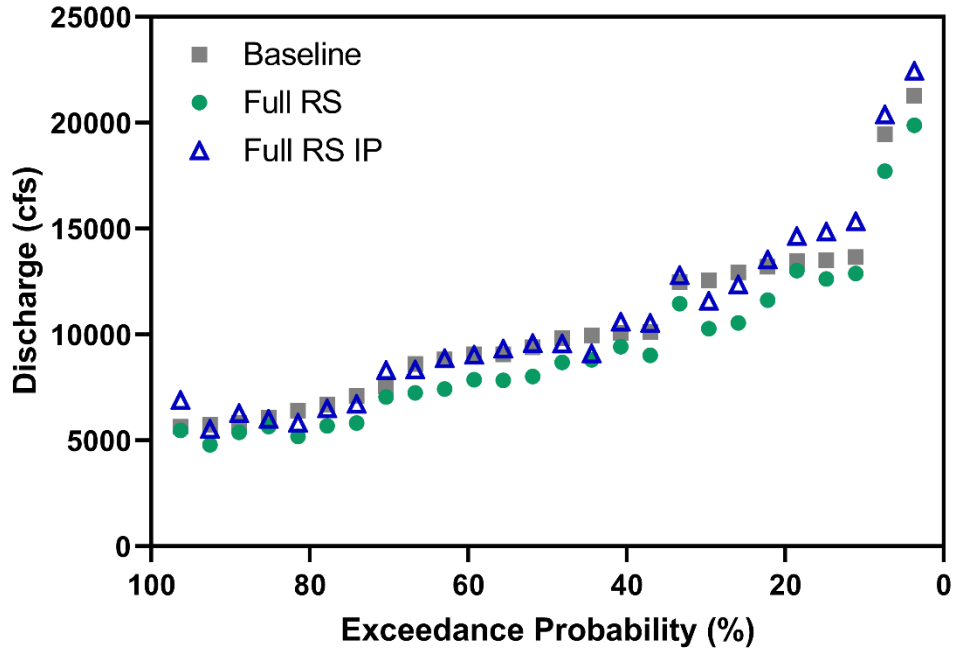
Figure 6-44: Peak discharges identified by POT versus exceedance probability for the baseline model, the full riparian scenario (Full RS), and Full RS with increased precipitation.
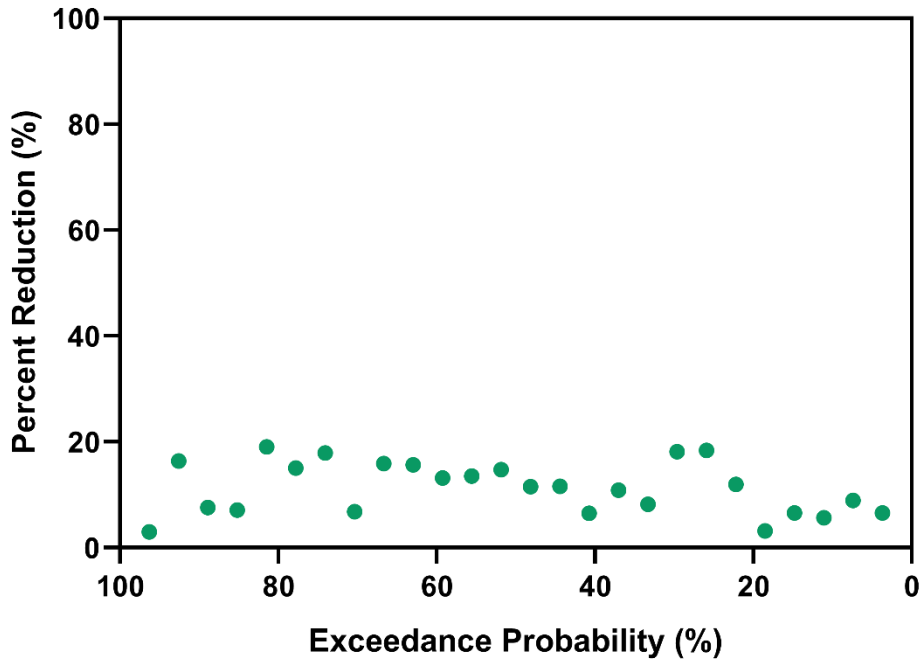
Figure 6-45: Percent reduction of peak discharges identified by POT versus exceedance probability for the full riparian scenario.
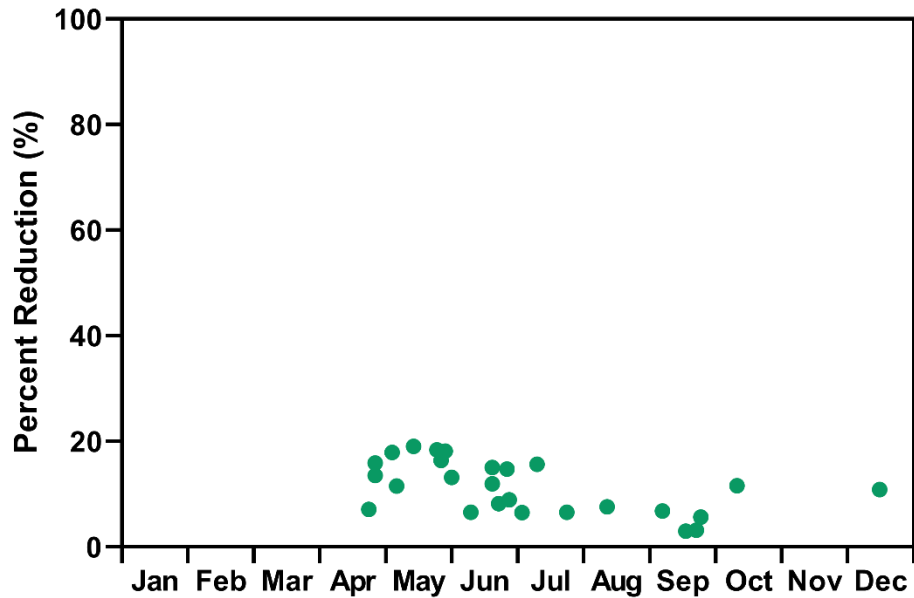
Figure 6-46: Percent reduction of the POT discharge versus month of occurrence for the full riparian scenario.

Similar to the full riparian scenario, the flow duration curve for the stream order one scenario shows reductions at all exceedance probabilities except for the highest (Figure 6-47). Reductions for the stream order one riparian scenario range from 220 to 1,450 cfs and average 760 cfs for the annual maximums (Figure 6-48). Percent reductions for the annual maximums range from 1.7 to 14.2 percent and average 8.9 percent (Figure 6-49). The stream order one scenario does not mitigate the effects of the increased precipitation scenario with an average increase of 640 cfs (5.8 percent). The monthly reductions for the stream order one scenario show no clear trends or patterns (Figure 6-50).
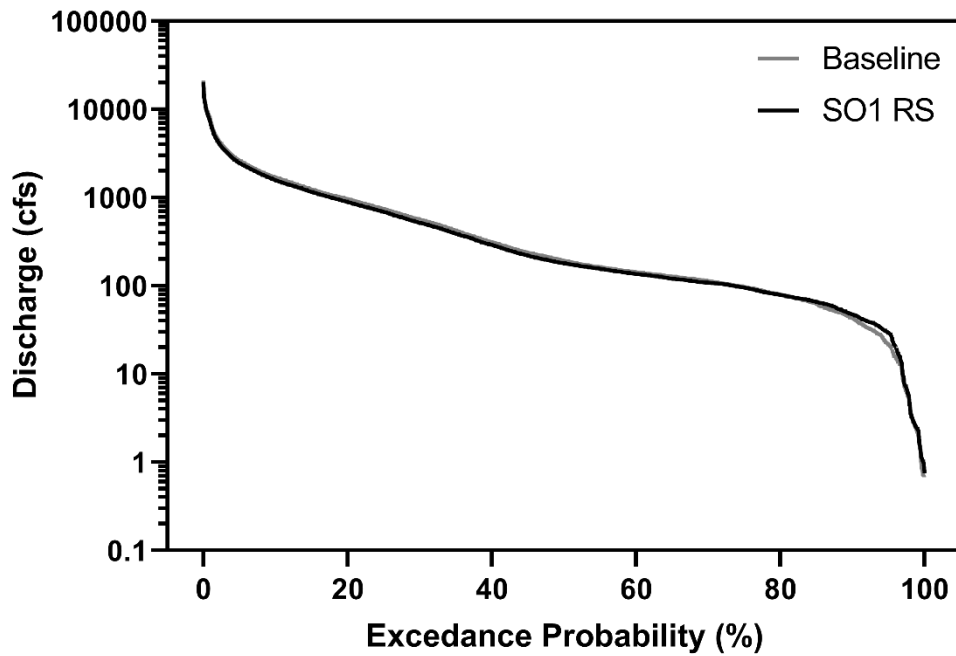
Figure 6-47: Discharge versus exceedance probability for the baseline and stream order one riparian scenario (SO1 RS).
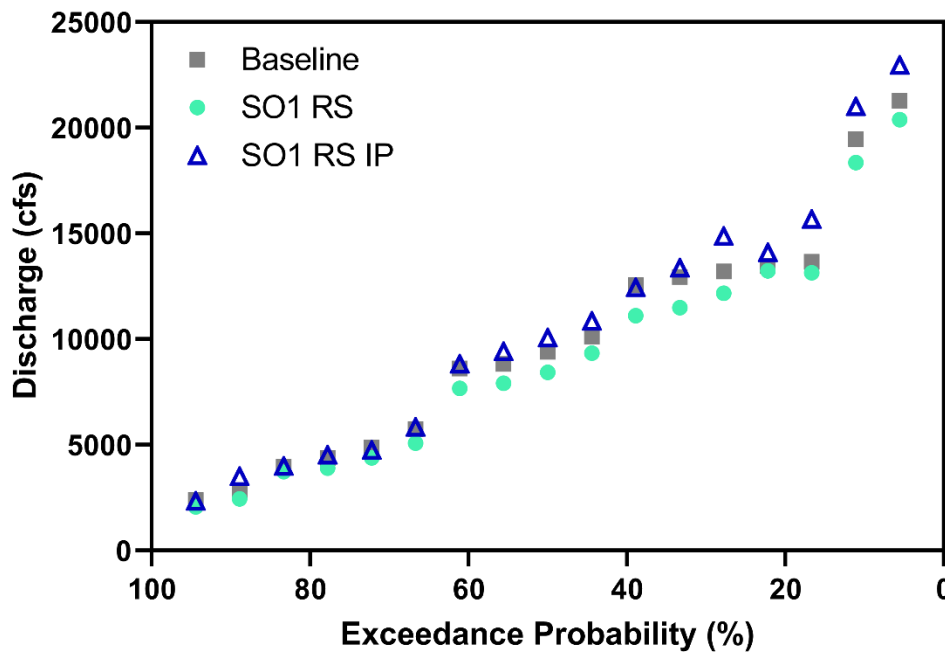
Figure 6-48: Annual maximum discharge versus exceedance probability for the baseline, stream order one riparian scenario (SO1 RS), and SO1 RS with increased precipitation.
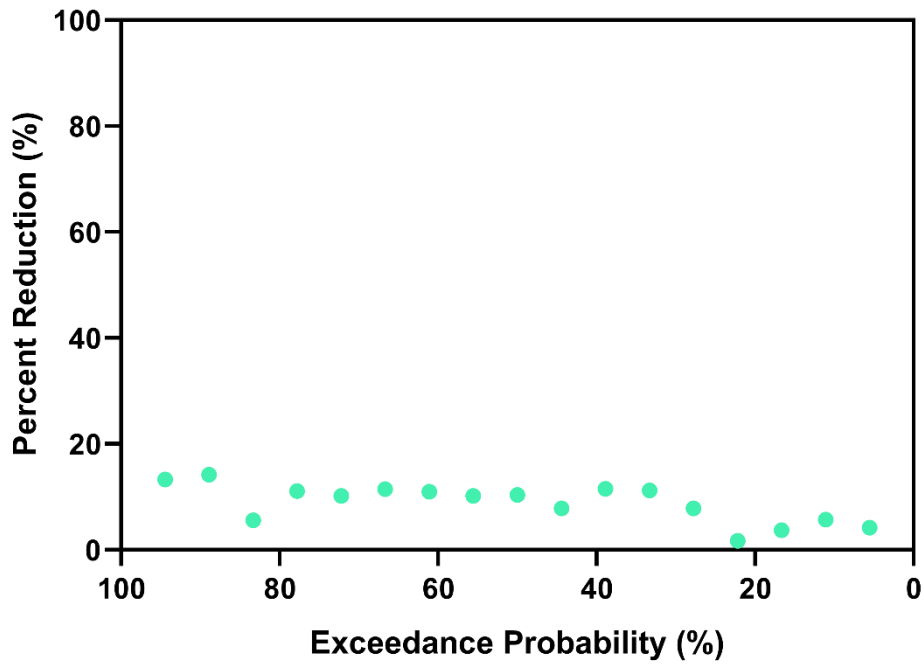
Figure 6-49: Percent reduction of the annual maximum discharge versus exceedance probability of discharge for the stream order one riparian scenario.
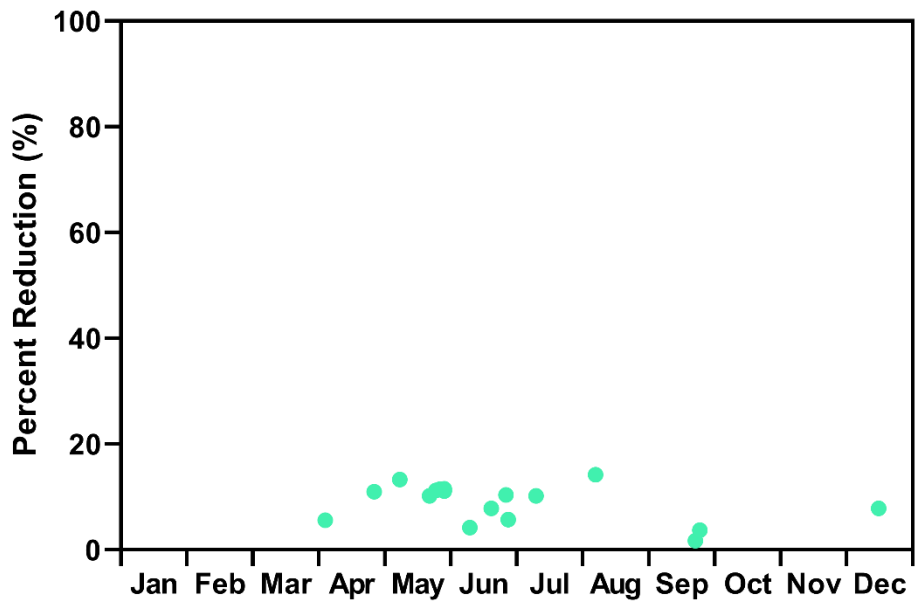
Figure 6-50: Percent reduction of the annual maximum discharge versus month of occurrence for the stream order one riparian scenario

128

Reductions in peaks identified by POT range from 120 to 1,450 cfs and average 740 cfs (Figure 6-51) and in terms of percent reduction, range from 1.7 to 12.4 percent, averaging 7.5 percent (Figure 6-52). The stream order one riparian scenario does not fully offset the effects of the increased precipitation scenario resulting in an increase in POT peaks of 660 cfs (6.1 percent). By month, the stream order one scenario percent reductions peak in April and May and fall off throughout the rest of the year (Figure 6-53).
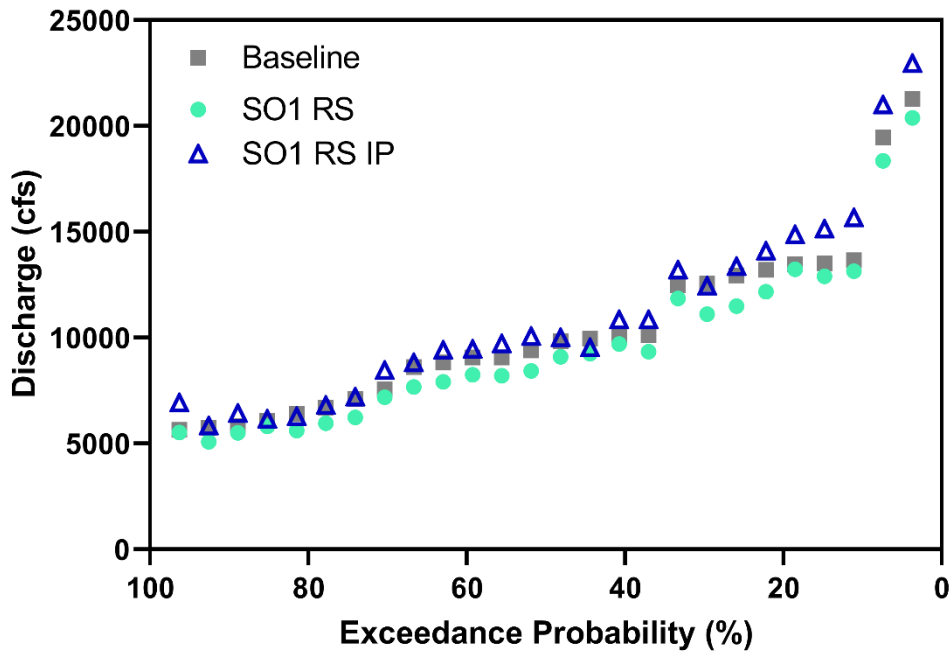
Figure 6-51: Discharge of POT peaks versus exceedance probability for the baseline and stream order one riparian scenario (SO1 RS), and SO1 RS with increased precipitation.

129
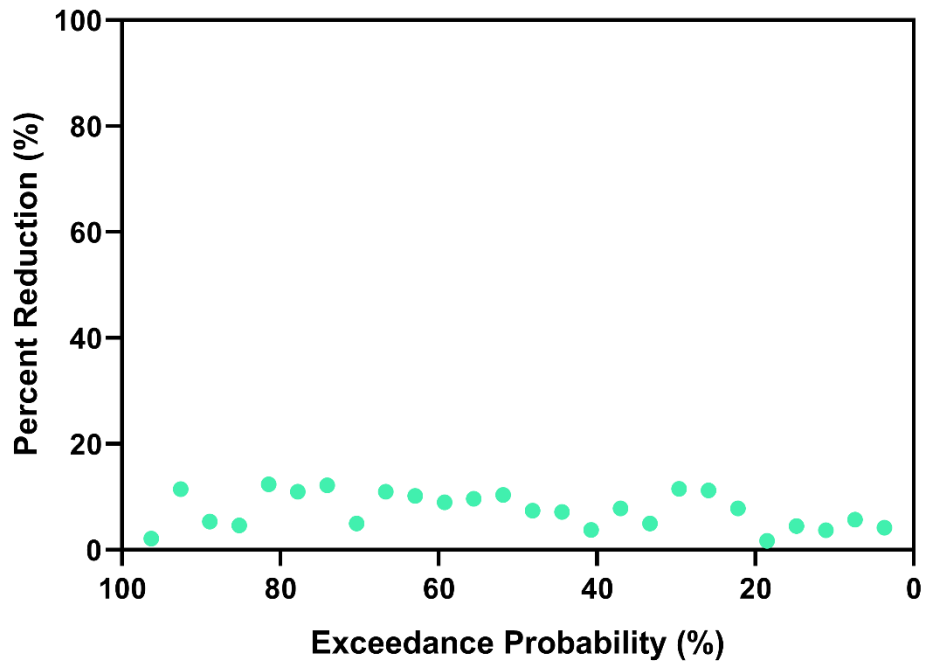
Figure 6-52: Percent reduction of POT peaks versus exceedance probability for the stream order one riparian scenario.
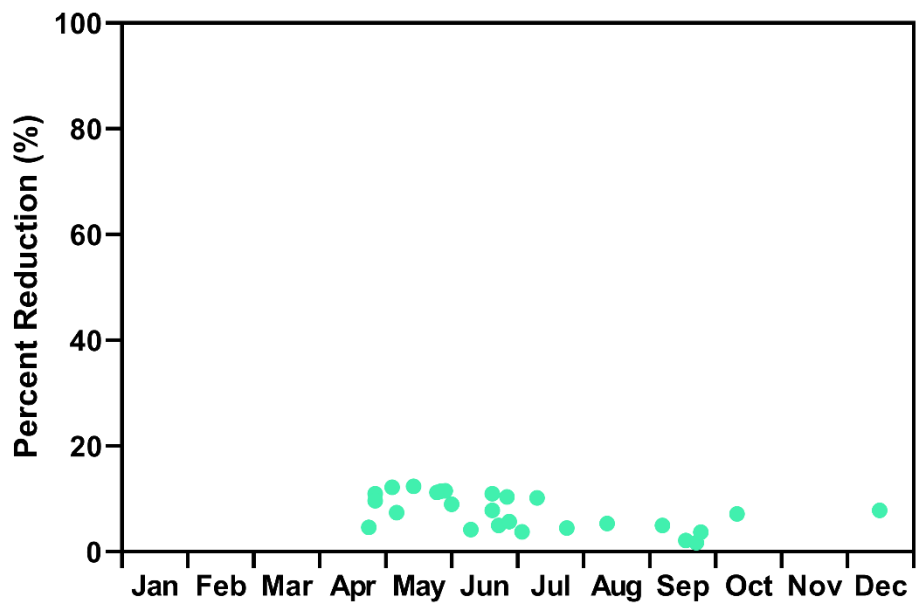
Figure 6-53: Percent reduction of the POT discharge versus month of occurrence for the stream order one riparian scenario.

130

To assess whether or not the full riparian or stream order one scenarios produced disproportionately large reductions, the reductions of both riparian scenarios re compared to the native vegetation scenario reductions. Since the area of the mesh elements reassigned to native vegetation for the full riparian scenario represents 18.7 percent of the row crop area in the baseline model, this is the threshold for determining whether or not the riparian corridor plays an outsized role in discharge reductions. Points above this threshold show disproportionately large reductions for the amount of area changed while points below show disproportionately small reductions. For the full riparian scenario, only five of the 17 annual maximums showed disproportionately large reductions with the scenario having an average reduction of 16.1 percent (Figure 6-54). For the peaks identified by POT, six of the 26 peaks showed disproportionately large reductions with an average reduction of 15.3 percent (Figure 6-55). These results do not indicate the full riparian zone plays a disproportionately large role in flood reductions.
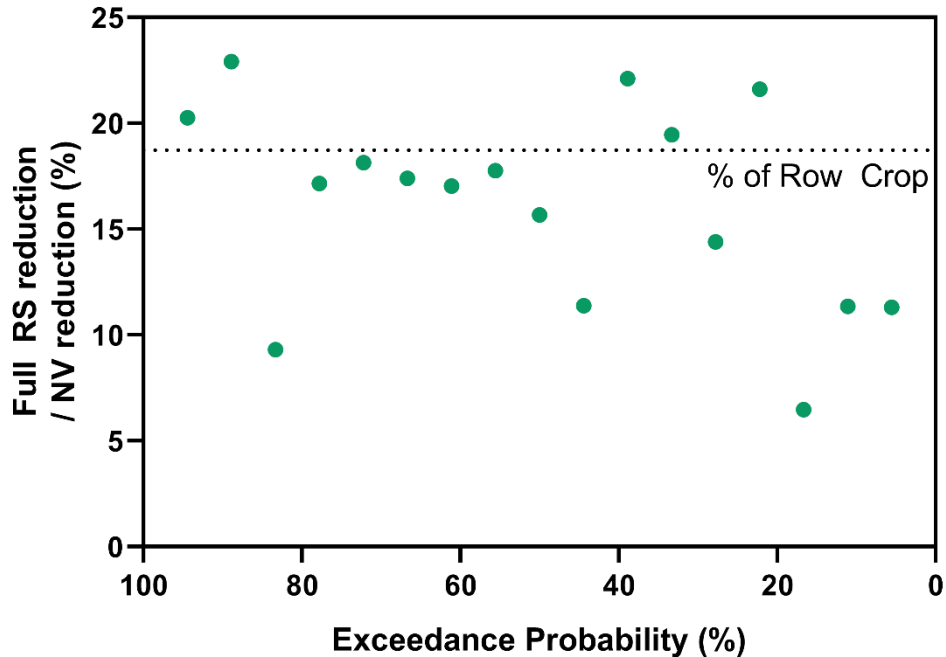
Figure 6-54: Reduction of the annual maximum discharge for the full riparian scenario as a fraction of the reduction by the native vegetation scenario versus exceedance probability of the baseline model. The dotted line marks the percent of row crop by area changed to native vegetation for the full riparian scenario.

131
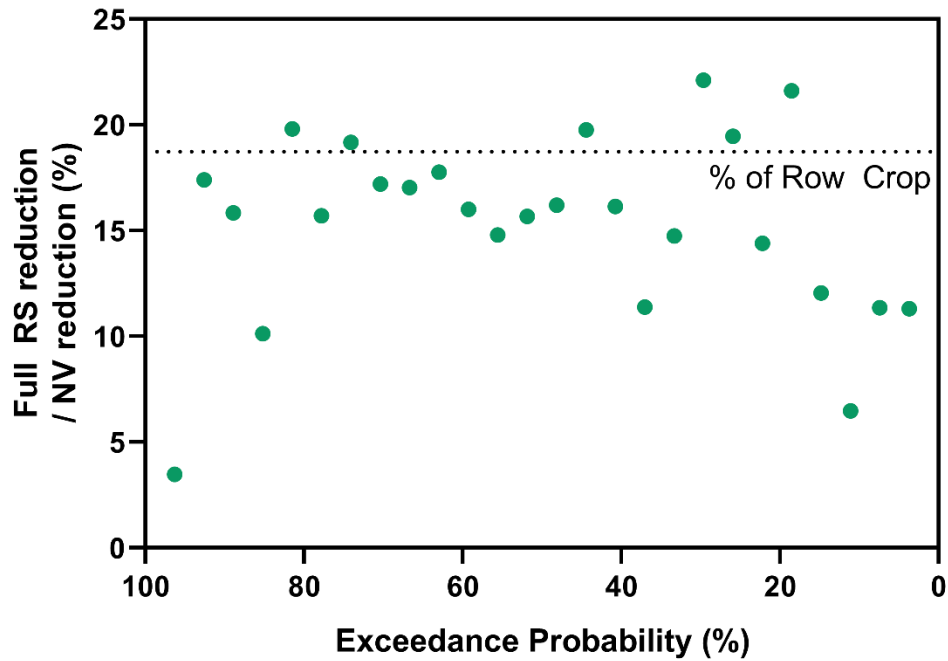
Figure 6-55: Reduction of the POT peaks for the full riparian scenario as a fraction of the reduction by the native vegetation scenario versus exceedance probability of the baseline model. The dotted line marks the percent of row crop by area changed to native vegetation for the full riparian scenario (18.7%).

For the SO1 scenario, the threshold for determining whether or not stream order one riparian practices play a disproportionate role in reducing floods falls to 10.4 percent. For the annual maximum discharge, 11 of the 17 showed disproportionately large reductions with an average reduction of 10.7 percent (Figure 6-56). For the peaks identified by POT, 16 of the 26 peaks showed disproportionately large reductions with an average reduction of 10.1 percent (Figure 6-57). Based on these findings, there is potential for stream order one riparian practices to play a disproportionately large role in flood reductions particularly for discharges up to approximately 13,500 cfs which would be an event with a return period of 10-25 years (Table 3-3).

132
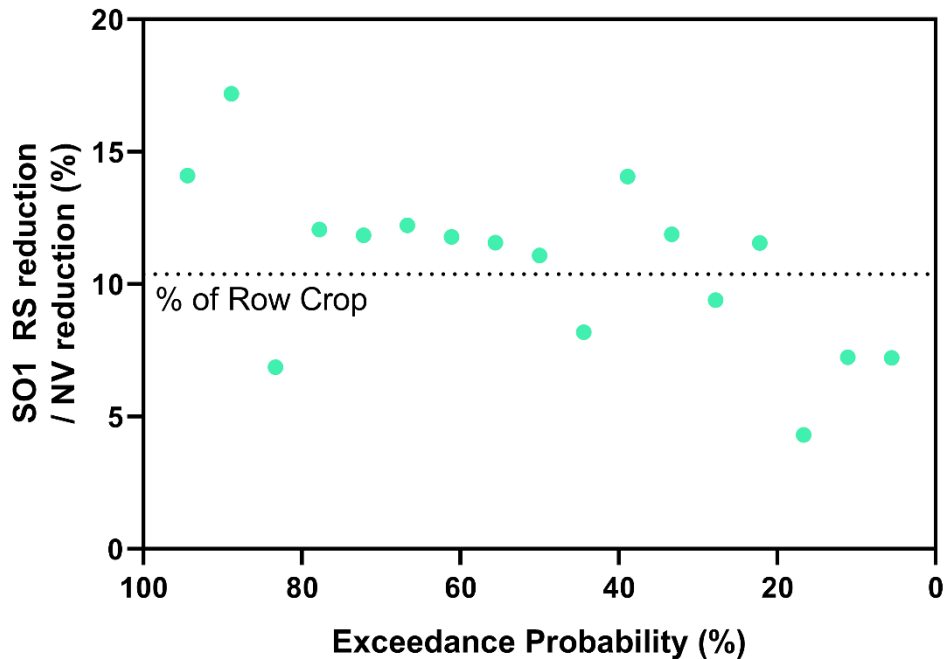
Figure 6-56: Reduction of annual maximum discharges for the stream order one riparian scenario as a fraction of the reduction of the native vegetation scenario versus exceedance probability of the baseline model. The dotted line marks the percent of row crop by area changed to native vegetation for the stream order one scenario (10.4%)
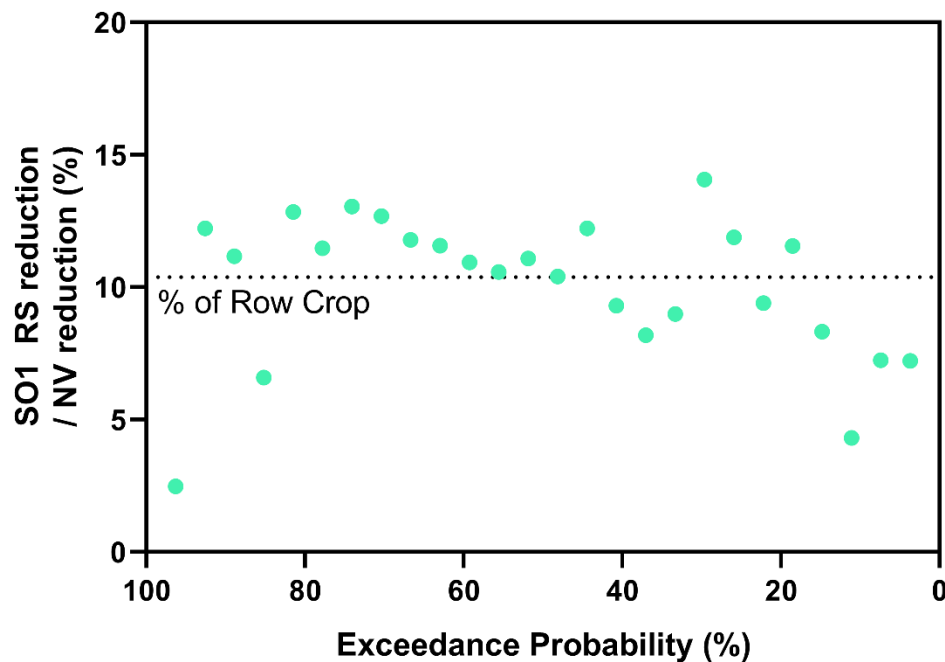
Figure 6-57: Reduction of POT peaks for the stream order one riparian scenario as a fraction of the reduction of the native vegetation scenario versus exceedance probability of the baseline model. The dotted line marks the percent of row crop by area changed to native vegetation for the stream order one scenario (10.4%)

133

6.8 Summary

Using observed precipitation, the conversion of 100 percent of all row crop acres in the Boone River model to native vegetation produced the largest annual maximum and POT reductions of any of the five scenarios discussed here. The average annual maximum reduction for the native vegetation scenario is 82.4 percent and the average reduction for POT is 74.9 percent. The native vegetation scenario was able to fully offset the impacts of the increased precipitation scenario maintaining a 76.3 percent reduction for the annual maximums and a 66.5 percent reduction for the peaks over threshold from the baseline model.

The cover crops scenario, which simulates the full adoption of both cover crops and no-till practices on all row crop acres, produced the second largest reductions. For the annual maximums, cover crops average a reduction of 38.5 percent and for the peaks over threshold average a reduction of 29.3 percent. The effects of increased precipitation are fully mitigated by the cover crop scenario with annual maximums still being reduced by 27.0 percent and POT being reduced by 17.5 percent below the baseline.

The only structural practice evaluated here, the wetlands scenario, with 411 wetlands simulated, produced lackluster reductions. Wetlands produced an average reduction of 9.1 percent for the annual maximums and 9.5 percent for POT. Wetlands were not able to compensate for the increased precipitation scenario, with an average increase over the baseline observed of 5.2 percent for the annual maximums and 3.6 percent for the POT.

For the full riparian scenario, every river-adjacent row crop element was converted to native vegetation. This scenario produced an average reduction in the annual maximums of 13.2 percent and an average reduction of 11.3 percent for POT. This scenario was not able to counter the effects of the increased precipitation and hence produced an increase in the annual maximum discharge of 1.0 percent and an increase of 2.0 percent for peaks over threshold. For the full riparian scenario, 18.7 percent of the row crop land area was converted to native vegetation. For the reductions of the full riparian scenario to have been disproportionate in comparison to the amount of land converted to native vegetation, reductions would have to surpass 18.7 percent of

the reductions from the native vegetation scenario. Only 5 of the annual maximum discharges did so and only 6 of the peak over threshold with average percent reductions of 16.1 and 15.3 percent respectively for each method.

For the stream order one riparian scenario, only the stream order one-adjacent row crop elements were converted to native vegetation. The average reductions produced by this scenario for annual maximum discharge and POT were 8.9 and 7.5 percent. The stream order one riparian scenario did not offset the increased precipitation scenario and instead produced increases in the average annual maximum discharge of 5.8 percent and POT of 6.1 percent. Whereas the threshold for disproportionate reductions for the full riparian scenario was 18.7 percent, the threshold for the stream order one scenario is 10.4. 11 of the 17 annual peaks showed percent reductions that surpassed the 10.4 percent threshold as did 16 of the 26 peaks over threshold with averages of 10.7 and 10.4 respectively.

For both the native vegetation and cover crop scenarios, the changes made to represent the conservation scenarios in terms of vegetation were seasonal. For the growing period, changes to represent native vegetation were small and for the cover crop scenario no changes were made. Because of this, the model tends towards operating as it had for the baseline conditions during these times. Where these changes become apparent however, is in the effects of the non-growing season changes on flooding that occurs early in the growing period. These seasonal effects are not seen with the wetlands scenario and are seen to a much smaller degree with the riparian scenarios.

The findings from the riparian scenarios in this watershed scale modeling effort bolster the field scale findings of Hernandez-Santana et al. (2013). This thesis found the stream order one riparian scenario, which only changed 10.4 percent of the row crop landscape, accounted for proportionally higher reductions than the full riparian scenario. This echoes the findings of Hernandez-Santana et al. (2013) who found small additions (between 20 and 10 percent) of strategically placed native vegetation could have an outsized impact at the in-field, stream order zero scale.

135

For the evaluation of the ability of the conservation scenarios modeled here to reduce peak flows, two methods were used: reductions by annual maximum and reductions by peaks over threshold where the threshold is set at 5,572, the 2-year flood. These two methods capture and characterize the reductions differently. Included in the annual maximums are five discharges that fall below the 2-year flood and therefore are less important when it comes to characterizing the reduction of flooding. Despite this, including the annual maximum method gives insight into what is happening with lower flows and, as it is the more common approach, lends to easier comparison between studies.

It is important to note none of the reduction potentials of the scenarios presented here scale perfectly with increasing discharge in terms of percent reductions. Additionally—with the exception of the native vegetation scenario—the reductions from these scenarios still leave the lowest exceedance probability, highest discharge events within the same order of magnitude as the baseline. This indicates the highest flows, though they will certainly be lessened by increasing the adoption of conservation practices, will persist. Bolstering this is the comparison of the watershed soil moisture conditions leading up to the September annual maximums of 2016 and 2018 (which saw drastically different reductions due to the native vegetation scenario). This comparison highlights an important fact: sometimes watersheds are primed for flooding and even the most ambitious conservation practices cannot prevent it. As evidence of this, the Des Moines River saw flooding in 1851—the year of its founding and well before the Des Moines Lobe was drained and converted from prairie and wetland to row crops. In that year, the annual rainfall reported (the location is unclear, but implied to be the City of Des Moines) of 74.5 inches (Hussey, 1902). For comparison, in 1993 and 2008 Des Moines reported rainfall of 53 and 45 inches respectively.

CHAPTER 7: FUTURE WORK AND SUMMARY

8.1 Future Work

With limited time, limited resources, and endless areas of investigation, there are inevitably potential areas of work left unapproached in the scope of this thesis. The following is a brief assessment of a four of those areas of work, with rationale and methods outlined where possible.

8.1.1 Sinuosity and Re-Meandering

One of the features of future versions of GHOST will be the ability to rectify the simplifications to the river network through a sinuosity factor in the .riv input file. These values represent the factor between a river segment's length as it exists in the model and its length as it exists in the real world. With the sinuosity factors set for each segment of the river network, in agricultural watersheds, segments representing channelized streams will have a sinuosity very near one. Changing the sinuosity of these river segments to values consistent with meandering streams would reflect river re-meandering via restoration and help to quantify the watershed scale hydrologic consequences. One resource for establishing the historic sinuosity of channelized streams could be historical aerial photography.

8.1.2 Mixed Scenarios

With the ability to change the land cover type by element, it is possible to conceive of more land cover scenarios than those presented here. Alongside the replacement of row crops with 100 percent native vegetation and 100 percent adoption of cover crops, it would be informative to develop systems to simulate different conversion and adoption rates. Additionally, the riparian scenarios could, in the model and in application, be practiced alongside in the cover crops scenario perhaps illustrating a more feasible scenario than high rates of conversion to native vegetation.

137

8.1.3 Historic Wetlands

Rather than being limited by the design constraints of the ACPF NRW siting standards, the historic wetlands scenario would compare current wetland extents to historical values reported in the literature to determine how many wetlands to add. The National Wetlands Inventory datasets made available through the Iowa DNR could be used to identify the existing wetlands on the Des Moines Lobe to establish current wetland extents and the work of Miller et al. (2009) and Miller et al. (2012) could be used to establish the historical wetland extents. An historic wetlands scenario could serve as an informative end member for the implementation of wetlands in the model and further inform on the historical hydrology of the watershed.

8.1.4 Drainage Water Management

With future versions of GHOST it will be possible to model the effects of tile drainage within a watershed. With this ability comes the potential to model the hydrologic effects of drainage water management. Simple soil wetness or water table depth thresholds could be established to reflect the levels at which producers would likely intercede in the normal functioning of drainage tile to maintain preferred or optimal soil moisture levels for crop growth. Archontoulis et al. (2017) and others have established relationships between water table depth and crop yield which could be used to guide this effort.

8.2 Summary

The work presented in this thesis focuses on the Boone River watershed as a first step toward understanding the hydrologic processes that operate in the Des Moines River watershed of the City of Des Moines. The goal of this thesis is to quantifying the potential benefits of conservation practices being applied across the Des Moines River watershed. To accomplish this goal, first, background information is supplied to put the work in context including the history of the Des Moines Lobe, conservation in Iowa, the benefits of conservation practices, the history of hydrologic modeling, modern uses of hydrologic modeling, a comparison of modeling approaches, and conservation siting tools.

138

Second, the watershed is described in terms of land use and land cover, topography, geology, soils, hydrologic alterations, the monitoring network, and hydrology. By area, 84.2 percent of the Boone River watershed is in use for the production of either corn or soybeans with the next most common uses being developed at 6.6 percent, pasture/hay at 5.2 percent, forest at 2.9 percent, and other at 1.1 percent. Geologically, at over 90% of the watershed by area, the Boone River watershed is dominated by the glacial tills left after the retreat of the Altamont Advance. The soils of the Boone River watershed are dominated by clay loams that are classified as poorly drained and moderately high runoff potential with low saturated hydraulic conductivity. Hydrologic alterations are extensive with over 75% of the watershed included in a drainage district and over 1,180 miles of drainage infrastructure estimated to exist.

The hydrology of the watershed is assessed on both annual and monthly timescales as well as for the flood climatology and floods of record. Annually, both precipitation and discharge were found to be increasing during the period of record from 1991 to 2017. Baseflow and baseflow as a fraction of discharge were both found to be increasing over the same period. Through the analysis of the long term water balances of the Boone River watershed, the only element of the annual water cycle found to be decreasing was estimated evapotranspiration. The thirty year normal monthly precipitation (1981-2010) follows the prototypical distribution of the U.S. Midwest with the lowest precipitation months being January, February, and December and the highest precipitation months being May, June, and July. Monthly runoff for the same 30 year period sees January, September, and December being the lowest discharge months and April, May and June being the highest discharge months. According to Bulletin 17B guidelines, the 2-year, 10-year, 50-year, and 100-year floods occur at 5,572, 12,610, 19,640, 22,760 cfs respectively. For the period 1991 to 2018, peaks over the 2-year flood occur most often in the month of June (28 percent of peaks) with May and April being the second and third most common months (18 and 14 percent of peaks respectively). The all-time historic crest identified by the NWS for the USGS gage at Webster City came in 1918. Recent years have seen the

139

setting of the third, fourth, sixth, eighth and ninth in 2010, 2008, 2010, 1991, 2004 and 1993 respectively.

Third, the GHOST hydrologic model is described along with the model construction process. The major processes represented within the model include climatological forcing, evapotranspiration, surface processes, fluxes between zones, the subsurface zone, boundary conditions and retention basins. Model construction is a complicated process with many steps for preparing the mesh and assigning the attributes that describes the steps for making the mesh and establishing the model element attributes and model inputs. The Boone River watershed model is composed of 12,728 individual elements which average 46 acres to comprise the 908 square mile watershed and 1,579 river elements which average 2,036 feet to comprise the 608 miles of rivers in the watershed.

Fourth, the model is calibrated against the observations from the USGS gaging station at Webster City for the entire 17 year study period and achieves very good performance for both Nash-Sutcliffe efficiency and R^2 (0.78 and 0.80 respectively) and good performance for percent bias (-6.0 percent) (according to thresholds set by Moriasi et al. (2015)). Annual model performance for NSE, PBIAS and R^2 range from 0.31 to 0.94. -48 to 31 percent, and 0.46 to 0.94 respectively. Monthly calibration performance ranges from -0.25 to 0.91, -44.7 to 35.5 percent, and 0.35 to 0.92 for NSE, PBIAS, and R^2 respectively. For the annual maximum discharges, the model achieved an R^2 of 0.88 and for the peaks-over threshold of the 2-year flood (5,572cfs), the model achieved an R^2 of 0.54.

Fifth, the model was run with changes made to represent different conservation scenarios and the increased precipitation scenario to compare the results to the baseline, calibrated model. Scenarios include two each—one with normal precipitation and one with increased precipitation—of native vegetation, cover crops/no-till/soil health (cover crops), wetlands, the full riparian scenario, and the stream order one riparian scenario. The average reduction from the native vegetation scenario for the annual maximums and POT methods are 82.4 and 74.9 percent respectively. For the increased precipitation scenario, the reductions fall to 76.3 and 66.5 percent

140

for the annual maximum and POT methods respectively. For the cover crops scenario, the average reductions for the annual maximums and POT methods are 38.5 and 29.3 percent respectively. For the increased precipitation scenario, these reductions fall to 27.0 and 17.5 percent respectively. The wetlands scenario saw a reductions of 9.1 and 9.5 percent for annual maximums and POT respectively while the increased precipitation scenario was not offset by the wetlands scenario and produced increase of 5.2 and 3.6 percent for each of the methods. For the full riparian scenario, reductions of 13.2 and 11.3 percent occur for the two evaluation methods. The full riparian scenario was not able to fully offset the increased precipitation producing 1.0 and 2.0 percent increases for each of the evaluation methods. This scenario was not found to disproportionately affect discharge reductions relative to the native vegetation scenario. For the stream order one riparian scenario, reductions produced for annual maximum discharge and POT were 8.9 and 7.5 percent respectively. This scenario was not able to fully mitigate the effects of the increased precipitation scenario producing an increases in average annual maximum discharge of 5.8 percent while the POT method saw an increase of 6.1 percent. The stream order one riparian scenario did produce disproportionately large reductions compared to the native vegetation scenario for the amount of land area changed for 11 of the 17 annual maximums and 16 of the 26 POT.

8.3 Final Remarks

This thesis is the result of an effort to better understand and confront the challenges watersheds across the Midwest face as they try to find balance between their agricultural prowess and the natural systems with which they interact. The work presented here is at once both part of the collective efforts of the field of watershed modeling as a whole and part of the specific efforts of those at IIHR Hydrosciences and Engineering to advance the field of watershed modeling so that we may better understand the natural systems with which we coexist.

Watershed scale hydrologic modeling is a valuable tool for gaining insights into the workings of one of the most basic natural divisions of the Earth's surface—the watershed. The

welfare of communities and ecosystems around the world depends on our ability to understand the effects of both natural and anthropogenic change. Informing decision making at a watershed scale has the potential to move us closer to developing sustainable, resilient systems which can provide for those who depend on them even in times of adversity. Hydrologic models move us closer to making fully informed decisions and understanding the consequences of our actions.

REFERENCES

Ahiablame, L., & Shakya, R. (2016). Modeling flood reduction effects of low impact development at a watershed scale. *Journal of Environmental Management*, *171*, 81–91. https://doi.org/10.1016/j.jenvman.2016.01.036

Alam, M. J., & Dutta, D. (2016). A Sub-Catchment Based Approach for Modelling Nutrient Dynamics and Transport at a River Basin Scale. *Water Resources Management*, *30*(14), 5455–5478. https://doi.org/10.1007/s11269-016-1500-x

Allen, R. G., Pereira, L. S., Raes, D., & Smith, M. (1998). *FAO Irrigation and Drainage Paper No. 56. Crop Evapotranspiration (guidelines for computing crop water requirements).* https://doi.org/10.1016/j.eja.2010.12.001

Andersen, K. L. (2000). *Historical alterations of surface hydrology in Iowa's small agricultural watersheds*. Iowa State University.

Archontoulis, S., Licht, M., Castellano, M., Ordonez, R., & Iqbal, J. (2017). Water availability, root depths and 2017 crop yields. *Proceedings of the 29th Annual Integrated Crop Management Conference*, *4*, 25–33.

Arenas Amado, A., Schilling, K. E., Jones, C. S., Thomas, N., & Weber, L. J. (2017). Estimation of tile drainage contribution to streamflow and nutrient loads at the watershed scale based on continuously monitored data. *Environmental Monitoring and Assessment*, *189*(9). https://doi.org/10.1007/s10661-017-6139-4

Asbjornsen, H., Hernandez-Santana, V., Liebman, M., Bayala, J., Chen, J., Helmers, M., … Schulte, L. A. (2014). Targeting perennial vegetation in agricultural landscapes for enhancing ecosystem services. *Renewable Agriculture and Food Systems*, *29*(2), 101–125. https://doi.org/10.1017/S1742170512000385

143

Babbar-Sebens, M., Barr, R. C., Tedesco, L. P., & Anderson, M. (2013). Spatial identification and optimization of upland wetlands in agricultural watersheds. *Ecological Engineering*, *52*, 130–142. https://doi.org/10.1016/j.ecoleng.2012.12.085

Baron, V. S., Najda, H. G., Salmon, D. F., & Dick, A. C. (1993). Cropping systems for spring and winter cereals under simulated pasture: Yield and yield distribution. *Canadian Journal of Plant Science*, *73*, 703–712.

Basche, A. (2017). Turning Soils into Sponges. Retrieved from http://www.ucsusa.org/sites/default/files/attach/2017/08/turning-soils-into-sponges-full-report-august-2017.pdf

Bates, P. D., Marks, K. J., & Horritt, M. S. (2003). Optimal use of high-resolution topographic data in flood inundation models. *Hydrological Processes*, *17*(3), 537–557. https://doi.org/10.1002/hyp.1113

Beck, W. J., Moore, P. L., Schilling, K. E., Wolter, C. F., Isenhart, T. M., Cole, K. J., & Tomer, M. D. (2019). Changes in lateral floodplain connectivity accompanying stream channel evolution: Implications for sediment and nutrient budgets. *Science of the Total Environment*, *660*, 1015–1028. https://doi.org/10.1016/j.scitotenv.2019.01.038

Beven, K. J., & O'Connell, P. E. (1982). *On the Role of Physically-Based Distributed Modelling in Hydrology*.

Bharati, L., Lee, K. H., Isenhart, T. M., & Schultz, R. C. (2002). Soil-water infiltration under crops, pasture, and established riparian buffer in Midwestern USA. *Agroforestry Systems*, *56*(3), 249–257. https://doi.org/10.1023/A:1021344807285

144

Blaser, B. C., Singer, J. W., & Gibson, L. R. (2011). Winter cereal canopy effect on cereal and interseeded legume productivity. *Agronomy Journal*, *103*(4), 1180–1185. https://doi.org/10.2134/agronj2010.0506

Bradley, A. A. (2018). Watershed Hydrology and Ecosystem Processes - Spring 2018. Iowa City, Iowa.

Cain, Z., & Lovejoy, S. (2004). History and outlook for Farm Bill conservation programs. *Choices*, 37–42. Retrieved from http://www.researchgate.net/publication/227364617_History_and_Outlook_for_Farm_Bill_Conservation_Programs/file/5046352376f054c060.pdf

Carlson, A. E. (2010). The Other Kind of Reclamation: Wetlands Drainage and National Water Policy, 1902-1912. *Agricultural History*, *84*(4), 451–478. https://doi.org/10.3098/ah.2010.84.4.451

Casas, A., Benito, G., Thorndycraft, V. R., & Rico, M. (2006). The topographic data source of digital terrain models as a key element in the accuracy of hydraulic flood modelling. *Earth Surface Processes and Landforms*, *31*(4), 444–456. https://doi.org/10.1002/esp.1278

Cedfeldt, P. T., Watzin, M. C., & Richardson, B. D. (2000). Using GIS to identify functionally significant wetlands in the Northeastern United States. *Environmental Management*, *26*(1), 13–24. https://doi.org/10.1007/s002670010067

Chiang, L. C., Chaubey, I., Hong, N. M., Lin, Y. P., & Huang, T. (2012). Implementation of BMP strategies for adaptation to climate change and land use change in a pasture-dominated watershed. *International Journal of Environmental Research and Public Health*, *9*(10), 3654–3684. https://doi.org/10.3390/ijerph9103654

145

City of Des Moines. (2015). City of Des Moines and Des Moines Metropolitan Wastewater Reclamation Authority Application for Sales Tax Increment Funding. Des Moines.

Daniel, E. B., Camp, J. V., LeBoeuf, E. J., Penrod, J. R., Dobbins, J. P., & Abkowitz, M. D. (2011). Watershed Modeling and its Applications: A State-of-the-Art Review. *The Open Hydrology Journal*, 26–50. https://doi.org/10.2174/1874378101105010026

De Laney, T. A. (1995). Benefits to downstream flood attenuation and water quality as a result of constructed wetlands in agricultural landscapes. *Jounrnal of Soil and Water Conservation*, *50.6*(Nov), 620+.

Deletic, A. (2001). Modelling of water and sediment transport over grassed areas. *Journal of Hydrology*, *248*(1–4), 168–182. https://doi.org/10.1016/S0022-1694(01)00403-6

Devia, G. K., Ganasri, B. P., & Dwarakish, G. S. (2015). A Review on Hydrological Models. *Aquatic Procedia*, *4*(Icwrcoe), 1001–1007. https://doi.org/10.1016/j.aqpro.2015.02.126

Dierauer, J., Pinter, N., & Remo, J. W. F. (2012). Evaluation of levee setbacks for flood-loss reduction, Middle Mississippi River, USA. *Journal of Hydrology*, *450–451*, 1–8. https://doi.org/10.1016/j.jhydrol.2012.05.044

Dietz, A. C., & Schnoor, J. L. (2001). Advances in phytoremediation. Environ Health Perspect. *Environ Health Perspect*, *109*(March), 163–68. https://doi.org/10.2307/3434854

Dosskey, M. G., Neelakantan, S., Mueller, T. G., Kellerman, T., Helmers, M. J., & Rienzi, E. (2015). AgBufferBuilder: A geographic information system (GIS) tool for precision design and performance assessment of filter strips. *Journal of Soil and Water Conservation*, *70*(4), 209–217. https://doi.org/10.2489/jswc.70.4.209

Dosskey, M. G., Vidon, P., Gurwick, N. P., Allan, C. J., Duval, T. P., & Lowrance, R. (2010). The role of riparian vegetation in protecting and improving chemical water quality in streams. *Journal of the American Water Resources Association*, *46*(2), 261–277. https://doi.org/10.1111/j.1752-1688.2010.00419.x

Dudula, J., & Randhir, T. O. (2016). Modeling the influence of climate change on watershed systems: Adaptation through targeted practices. *Journal of Hydrology*, *541*, 703–713. https://doi.org/10.1016/j.jhydrol.2016.07.020

Edwards, W. M., Norton, L. D., & Redmond, C. E. (1988). Characterizing Macropores that Affect Infiltration into Nontilled Soil. *Soil Science Society of America Journal*, *52*(2), 483–487. https://doi.org/10.2136/sssaj1988.03615995005200020033x

El Alfy, M. (2016). Assessing the impact of arid area urbanization on flash floods using GIS, remote sensing, and HEC-HMS rainfall–runoff modeling. *Hydrology Research*, *47*(6), 1142–1160. https://doi.org/10.2166/nh.2016.133

England, J. F., Cohn, T. A., Faber, B. A., Stedinger, J. R., Thomas, W. O., Veilleux, A. G., … Mason, R. R. J. (2018). Guidelines for determining flood flow frequency--Bulletin 17C. In *U.S. Geological Survey Techniques and Methods: Book 4: Hydrologic Analysis and Interpretation*.

Enloe, S. K., Schulte, L. A., & Tyndall, J. C. (2014). Toward a collaborative approach to watershed management: Lessons learned from the Boone River Watershed, Iowa. *Journal of Soil and Water Conservation*, *69*(5), 149A–153A. https://doi.org/10.2489/jswc.69.5.149a

147

Fang, H., Liang, S., Townshend, J. R., & Dickinson, R. E. (2008). Spatially and temporally continuous LAI data sets based on an integrated filtering method: Examples from North America. *Remote Sensing of Environment*, *112*(1), 75–93. https://doi.org/10.1016/j.rse.2006.07.026

Fiener, P., & Auerswald, K. (2005). Measurement and modeling of concentrated runoff in grassed waterways. *Journal of Hydrology*, *301*(1–4), 198–215. https://doi.org/10.1016/j.jhydrol.2004.06.030

Guida, R. J., Remo, J. W. F., & Secchi, S. (2016). Tradeoffs of strategically reconnecting rivers to their floodplains: The case of the Lower Illinois River (USA). *Science of the Total Environment*, *572*, 43–55. https://doi.org/10.1016/j.scitotenv.2016.07.190

Hansen, A. T., Dolph, C. L., Foufoula-Georgiou, E., & Finlay, J. C. (2018). Contribution of wetlands to nitrate removal at the watershed scale. *Nature Geoscience*, *11*(2), 127–132. https://doi.org/10.1038/s41561-017-0056-6

Hartmann, H. C. (2002). Wetlands Drainage, River Modification, and Sectoral Conflict in the Lower Illinois Valley, 1890-1930. *Eos*, *83*(40). Retrieved from https://bayes.wustl.edu/etj/articles/disturbing.memory.pdf

Heaton, E. A., Dohleman, F. G., & Long, S. P. (2008). Meeting US biofuel goals with less land: The potential of Miscanthus. *Global Change Biology*, *14*(9), 2000–2014. https://doi.org/10.1111/j.1365-2486.2008.01662.x

Helmers, M., Christianson, R., Brenneman, G., Lockett, D., & Pederson, C. (2012). Water table, drainage, and yield response to drainage water management in southeast Iowa. *Journal of Soil and Water Conservation*, *67*(6), 495–501. https://doi.org/10.1081/TXR-120026921

Her, Y., Chaubey, I., Frankenberger, J., & Jeong, J. (2017). Implications of spatial and temporal variations in effects of conservation practices on water management strategies. *Agricultural Water Management*, *180*, 252–266. https://doi.org/10.1016/j.agwat.2016.07.004

Hernandez-Santana, V., Zhou, X., Helmers, M. J., Asbjornsen, H., Kolka, R., & Tomer, M. (2013). Native prairie filter strips reduce runoff from hillslopes under annual row-crop systems in Iowa, USA. *Journal of Hydrology*, *477*, 94–103. https://doi.org/10.1016/j.jhydrol.2012.11.013

Hladik, M. L., Bradbury, S., Schulte, L. A., Helmers, M., Witte, C., Kolpin, D. W., … Harris, M. (2017). Neonicotinoid insecticide removal by prairie strips in row-cropped watersheds with historical seed coating use. *Agriculture, Ecosystems and Environment*, *241*, 160–167. https://doi.org/10.1016/j.agee.2017.03.015

Hoegh-Guldberg, O., Jacob, D., Taylor, M., Bindi, M., Brown, S., Camilloni, I., … Zhou, G. (2018). *Impacts of 1.5ºC Global Warming on Natural and Human Systems. Global Warming of 1.5 °C. An IPCC Special Report on the Impacts of Global Warming of 1.5 °C above Pre-Industrial Levels and Related Global Greenhouse Gas Emission Pathways, in the Context of Strengthening the Global Response to the Threat of Climate Chang*. https://doi.org/10.1093/aje/kwp410

Hsu, C.-B., Hsieh, H.-L., Yang, L., Wu, S.-H., Chang, J.-S., Hsiao, S.-C., … Lin, H.-J. (2011). Biodiversity of constructed wetlands for wastewater treatment. *Ecological Engineering*, *37*(10), 1533–1545. https://doi.org/10.1016/j.ecoleng.2011.06.002

Hussey, T. (1902). *The Flood of 1851*. *The Annals of Iowa* (Vol. 5). https://doi.org/10.17077/0003-4827.2797

Hutchinson, S. L., Koelliker, J. K., & Knapp, A. K. (2007). Development of Water Usage
Coefficients for a Fully Watered Tallgrass Prairie. *American Society of Agricultural and Biological Engineers*, *51*(1), 153–159.

Interagency Advisory Committee on Water Data. (1982). *Guidelines For Determining Flood Flow Frequency: Bulletin #17B of the Hydrology Subcommittee*.

Iowa Association of Naturalists. (1995). Important Iowa Conservationsists. Guthrie Center, Iowa: Iowa Association of Naturalists.

Iowa Geodata. (n.d.). Iowa Geodata. Retrieved March 31, 2019, from https://geodata.iowa.gov/

Iowa State University: Geographic Information Systems Facility. (n.d.). ACPF DEM Download. Retrieved March 31, 2019, from https://www.gis.iastate.edu/gisf/projects/acpf

Islam, Z. (2011). *Literature review on physically based hydrological modeling*. https://doi.org/10.13140/2.1.4544.5924

Jackson, R. B., Canadell, J., Ehleringer, J. R., Mooney, H. A., & Sala, O. E. (1996). A Global Analysis of Root Distributions for Terrestrial Biomes. *Oecologia*, *108*(3), 389–411.

Jae Lim, K., Engel, B. A., Tang, Z., Choi, J., Kim, K.-S., Muthukrishnan, S., & Tripathy, D. (2005). Automated Web GIS Based Hydrograph Analysis Tool, What. *Journal of the American Water Resources Association*, *41*(6), 1407–1416. https://doi.org/10.1111/j.1752-1688.2005.tb03808.x

Jajarmizadeh, M., Harun, S., & Salarpour, M. (2012). A Review on the Theoretical Considerations and Types of Models in Hydrology. *Journal of Environmental Science and Technology*, *5*(5), 249–261.

150

Javaheri, A., & Babbar-Sebens, M. (2014). On comparison of peak flow reductions, flood

inundation maps, and velocity maps in evaluating effects of restored wetlands on channel

flooding. *Ecological Engineering*, *73*, 132–145.

https://doi.org/10.1016/j.ecoleng.2014.09.021

Jaynes, D. B. (2012). Changes in yield and nitrate losses from using drainage water management

in central Iowa, United States. *Journal of Soil and Water Conservation*, *67*(6), 485–494.

https://doi.org/10.2489/jswc.67.6.485

Jobe, A., Kalra, A., & Ibendahl, E. (2018). Conservation Reserve Program effects on floodplain

land cover management. *Journal of Environmental Management*, *214*, 305–314.

https://doi.org/10.1016/j.jenvman.2018.03.016

Johnston, C. A., Detenbeck, N. E., & Niemi, G. J. (1990). The Cumulative Effect of Wetland

Degradation on Water Quality at a Landscape Scale. *Biogeochemistry*, *10*, 105–141.

Kadlec, R. H., & Wallace, S. D. (2009). *Treatment Wetlands*.

https://doi.org/10.1201/9781420012514

Kang, S., Gu, B., Du, T., & Zhang, J. (2003). Crop coefficient and ratio of transpiration to

evapotranspiration of winter wheat and maize in a semi-humid region. *Agricultural Water

Management*, *59*(3), 239–254.

Karamouz, M., Fallahi, M., & Nazif, S. (2012). Evaluation of climate change impact on regional

flood characteristics. *Iranian Journal of Science and Technology - Transactions of Civil

Engineering*, *36*(C2), 225–238.

Karim, F., Petheram, C., Marvanek, S., Ticehurst, C., Wallace, J., & Hasan, M. (2016). Impact of climate change on floodplain inundation and hydrological connectivity between wetlands and rivers in a tropical river catchment. *Hydrological Processes*, *30*(10), 1574–1593. https://doi.org/10.1002/hyp.10714

Kelly, S. A., Takbiri, Z., Belmont, P., & Foufoula-Georgiou, E. (2017). Human amplified changes in precipitation-runoff patterns in large river basins of the Midwestern United States. *Hydrology and Earth System Sciences*, *21*(10), 5065–5088. https://doi.org/10.5194/hess-21-5065-2017

Kjaersgaard, J. H., Plauborg, F., Mollerup, M., Petersen, C. T., & Hansen, S. (2008). Crop coefficients for winter wheat in a sub-humid climate regime. *Agricultural Water Management*, *95*(8), 918–924. https://doi.org/10.1016/j.agwat.2008.03.004

Knight, R. L. (1997). Wildlife habitat and public use benefits of treatment wetlands. *Water Science and Technology*, *35*(5), 35–43. https://doi.org/10.1016/S0273-1223(97)00050-4

Kolbert, E. (2015). *The Sixth Extinction: An Unnatural History* (1st ed.). New York: Picador.

Kristensen, K. J., & Jensen, S. E. (1975). A Model for Estimating Actual Evapotranspiration from Potential Evapotranspiration. *Nordic Hydrology*, *6*(3), 170–188. Retrieved from http://www.iwaponline.com/nh/006/0170/0060170.pdf

Kumar, M., Duffy, C. J., & Salvage, K. M. (2009). A Second-Order Accurate, Finite Volume–Based, Integrated Hydrologic Modeling (FIHM) Framework for Simulation of Surface and Subsurface Flow. *Vadose Zone Journal*, *8*(4), 873. https://doi.org/10.2136/vzj2009.0014

Larson, D. L., Bright, J. B., Drobney, P., Larson, J. L., Palaia, N., Rabie, P. A., … Wells, D. (2011). Effects of planting method and seed mix richness on the early stages of tallgrass prairie restoration. *Biological Conservation*, *144*(12), 3127–3139. https://doi.org/10.1016/j.biocon.2011.10.018

Lavaire, T., Gentry, L. E., David, M. B., & Cooke, R. A. (2017). Fate of water and nitrate using drainage water management on tile systems in east-central Illinois. *Agricultural Water Management*, *191*, 218–228. https://doi.org/10.1016/j.agwat.2017.06.004

Lee, K. E. (1985). *Earthworms: their ecology and relationships with soils and land use*. New York: Academic Press.

Leopold, L. B. (1994). *A View of the River*. Harvard University Press.

Lin, Y. (2011). GCIP/EOP Surface: Precipitation NCEP/ECM 4km Gridded Data (GRIB) Stage IV Data. https://doi.org/https://doi.org/10.5065/D6PG1QDD

Lister, B. C., & Garcia, A. (2018). Climate-driven declines in arthropod abundance restructure a rainforest food web. *Proceedings of the National Academy of Sciences*, *115*(44), E10397–E10406. https://doi.org/10.1073/pnas.1722477115

Lu, Q., Futter, M. N., Nizzetto, L., Bussi, G., Jürgens, M. D., & Whitehead, P. G. (2016). Fate and transport of polychlorinated biphenyls (PCBs) in the River Thames catchment – Insights from a coupled multimedia fate and hydrobiogeochemical transport model. *Science of the Total Environment*, *572*, 1461–1470. https://doi.org/10.1016/j.scitotenv.2016.03.029

Mallakpour, I., & Villarini, G. (2015). The changing nature of flooding across the central United States. *Nature Climate Change*, *5*(3), 250–254. https://doi.org/10.1038/nclimate2516

153

Mansoor, S. Z., Louie, S., Lima, A. T., Van Cappellen, P., & MacVicar, B. (2018). The spatial and temporal distribution of metals in an urban stream: A case study of the Don River in Toronto, Canada. *Journal of Great Lakes Research*, *44*(6), 1314–1326. https://doi.org/10.1016/j.jglr.2018.08.010

McCorvie, M. M., & Lant, C. L. (1993). Drainage District Formation and the Loss of Midwestern Wetlands , 1850-1930. *Agricultural History*, *67*(4), 13–39.

Miller, B. A., Crumpton, W. G., & Valk, A. G. (2009). Spatial distribution of historical wetland classes on the Des Moines Lobe, Iowa. *Wetlands*, *29*(4), 1146–1152. https://doi.org/10.1672/08-158.1

Miller, B. A., Crumpton, W. G., & van der Valk, A. G. (2012). Wetland hydrologic class change from prior to European settlement to present on the Des Moines Lobe, Iowa. *Wetlands Ecology and Management*, *20*(1), 1–8. https://doi.org/10.1007/s11273-011-9237-z

Milly, P. C. D., Betancourt, J., Falkenmark, M., Hirsch, R. M., Kundzewicz, Z. W., Lettenmaier, D. P., & Stouffer, R. J. (2008). Stationarity Is Dead: Whither Water Management? *Science*, *319*(5863), 573–574. https://doi.org/10.1126/science.1151915

Mishra, P. K., Neelkanth, J. K., Babu, B. M., & Kumathe, S. S. (2006). Effectiveness of Bermuda grass as vegetative cover in grassed waterway: A simulated study. *Journal of Irrigation and Drainage Engineering-Asce*, *132*(3), 288–292. https://doi.org/10.1061/(ASCE)0733-9437(2006)132:3(288)

Mitchell, K. E. (2004). The multi-institution North American Land Data Assimilation System (NLDAS): Utilizing multiple GCIP products and partners in a continental distributed hydrological modeling system. *Journal of Geophysical Research*, *109*(D7), 1–32. https://doi.org/10.1029/2003jd003823

Mohamoud, Y. M. (1992). Evaluating Manning's roughness coefficients for tilled soils. *Journal of Hydrology*, *135*(1–4), 143–156. https://doi.org/10.1016/0022-1694(92)90086-B

Moriasi, D. N., Arnold, J. G., Liew, M. W. Van, Bingner, R. L., Harmel, R. D., & Veith, T. L. (2007). Model Evaluation Guidelines for Systematic Quantification of Accuracy in Watershed Simulations, *50*(3), 885–900.

Moriasi, D. N., Gitau, M. W., Pai, N., & Daggupati, P. (2015). Hydrologic and Water Quality Models: Performance Measures and Evaluation Criteria. *Transactions of the ASABE*, *58*(6), 1763–1785. https://doi.org/10.13031/trans.58.10715

Moriasi, D. N., Wilson, B. N., Arnold, J. G., & Gowda, P. H. (2012). Hydrologic and Water Quality Models: Use, Calibration, and Validation, *55*(4), 1241–1247.

National Agricultural Statistics Service. (2016). Cropscape - Crop Data Layer. Retrieved March 31, 2019, from https://nassgeodata.gmu.edu/CropScape/

National Weather Service. (2018). Historic Crests. Retrieved from https://water.weather.gov/ahps2/crests.php?wfo=dmx&gage=desi4&crest_type=historic

National Weather Service. (2019). Historic Crests. Retrieved March 2, 2019, from https://water.weather.gov/ahps2/crests.php?wfo=dmx&gage=wbci4&crest_type=historic

Natural Resources Conservation Service. (2007). *Chapter 7 Hydrologic Soil Groups*. *Part 630 Hydrology National Engineering Handbook*.

Otis, D. L., Crumpton, Wi. G., Green, D., Loan-Wilsey, A. K., McNeely, R. L., Kane, K. L., …
Vandever, M. (2010). *Assessment of Environmental Services of CREP Wetlands in Iowa and the Midwestern Corn Belt*. Ames, Iowa. Retrieved from
http://www.researchgate.net/profile/Kevin_Kane/publication/270892607_Assessment_of_Environmental_Services_of_CREP_Wetlands_in_Iowa_and_the_Midwestern_Corn_Belt/links/54b828f70cf2c27adc48ab8c.pdf

Panday, S., & Huyakorn, P. S. (2004). A fully coupled physically-based spatially-distributed model for evaluating surface/subsurface flow. *Advances in Water Resources*, *27*(4), 361–382. https://doi.org/10.1016/j.advwatres.2004.02.016

Pidwirny, M. (2006). The Drainage Basin Concept. In *Fundamentals of Physical Geography* (2nd ed.). Retrieved from http://www.physicalgeography.net/fundamentals/10aa.html

Politano, M. (2018). *GHOST - Generic Hydrologic Overland-Subsurface Toolkit Theory Guide*. Iowa City, Iowa.

Porter, S. A., Tomer, M. D., James, D. E., & Boomer, K. M. B. (2016). Agricultural Conservation Planning Framework ArcGIS® Toolbox User's Manual. Retrieved from http://northcentralwater.org/acpf/

Prior, J. C. (1991). *Landforms of Iowa* (1st ed.). Iowa City: University of Iowa Press.

PRISM Climate Group. (n.d.). PRISM Climate Data. Retrieved March 3, 2019, from http://www.prism.oregonstate.edu/

Qi, Z., & Helmers, M. J. (2010). Soil Water Dynamics under Winter Rye Cover Crop in Central Iowa. *Vadose Zone Journal*, *9*(1), 53. https://doi.org/10.2136/vzj2008.0163

Qu, Y., & Duffy, C. J. (2007). A semidiscrete finite volume formulation for multiprocess watershed simulation. *Water Resources Research*, *43*(8), 1–18. https://doi.org/10.1029/2006WR005752

Radke, J. K., & Berry, E. C. (1993). Infiltration as a tool for detecting soil changes due to cropping, tillage, and grazing livestock. *American Journal of Alternative Agriculture*, *8*(4), 164–174. https://doi.org/10.1017/S0889189300005385

Rasmussen, I. S., & Thorup-Kristensen, K. (2016). Does earlier sowing of winter wheat improve root growth and N uptake? *Field Crops Research*, *196*, 10–21. https://doi.org/10.1016/j.fcr.2016.05.009

Sánchez-Bayo, F., & Wyckhuys, K. A. G. (2019). Worldwide decline of the entomofauna: A review of its drivers. *Biological Conservation*, *232*(September 2018), 8–27. https://doi.org/10.1016/j.biocon.2019.01.020

Scasta, J. D., Engle, D. M., Harr, R. N., & Debinski, D. M. (2014). Fire induced reproductive mechanisms of a Symphoricarpos (Caprifoliaceae) shrub after dormant season burning. *Botanical Studies*, *55*(1). https://doi.org/10.1186/s40529-014-0080-4

Schilling, K. E., Chan, K. S., Liu, H., & Zhang, Y. K. (2010). Quantifying the effect of land use land cover change on increasing discharge in the Upper Mississippi River. *Journal of Hydrology*, *387*(3–4), 343–345. https://doi.org/10.1016/j.jhydrol.2010.04.019

Schilling, K. E., Gassman, P. W., Kling, C. L., Campbell, T., Jha, M. K., Wolter, C. F., & Arnold, J. G. (2014). The potential for agricultural land use change to reduce flood risk in a large watershed. *Hydrological Processes*, *28*(8), 3314–3325. https://doi.org/10.1002/hyp.9865

Schilling, K. E., & Helmers, M. (2008). Tile drainage as karst: Conduit flow and diffuse flow in a tile-drained watershed. *Journal of Hydrology*, *349*(3–4), 291–301. https://doi.org/10.1016/j.jhydrol.2007.11.014

Schilling, K. E., Jindal, P., Basu, N. B., & Helmers, M. J. (2012). Impact of artificial subsurface drainage on groundwater travel times and baseflow discharge in an agricultural watershed, Iowa (USA). *Hydrological Processes*, *26*(20), 3092–3100. https://doi.org/10.1002/hyp.8337

Schnoor, J. L., Licht, L. A., McCUTCHEON, S. C., Wolfe, N. L., & Carreira, L. H. (1995). Phytoremediation of Organic and Nutrient Contaminants. *Environmental Science and Technology*, *29*(7), 318–323. https://doi.org/10.1021/es00007a002

Schott, L., Lagzdins, A., Daigh, A. L. M., Craft, K., Pederson, C., Brenneman, G., & Helmers, M. J. (2017). Drainage water management effects over five years on water tables, drainage, and yields in southeast Iowa. *Journal of Soil and Water Conservation*, *72*(3), 251–259. https://doi.org/10.2489/jswc.72.3.251

Schulte, L. A., Niemi, J., Helmers, M. J., Liebman, M., Arbuckle, J. G., James, D. E., … Witte, C. (2017). Prairie strips improve biodiversity and the delivery of multiple ecosystem services from corn–soybean croplands. *Proceedings of the National Academy of Sciences*, *114*(42), 11247–11252. https://doi.org/10.1073/pnas.1620229114

Sharma, V., & Irmak, S. (2017). Soil-Water Dynamics, Evapotranspiration, and Crop Coefficients of Cover-Crop Mixtures in Seed Maize Cover-Crop Rotation Fields. II: Grass-Reference and Alfalfa-Reference Single (Normal) and Basal Crop Coefficients. *Journal of Irrigation and Drainage Engineering*, *143*(9), 4017033. https://doi.org/10.1061/(asce)ir.1943-4774.0001215

Sharma, V., Irmak, S., Sharma, V., Djaman, K., & Odhiambo, L. (2017). Soil-Water Dynamics, Evapotranspiration, and Crop Coefficients of Cover-Crop Mixtures in Seed Maize Cover-Crop Rotation Fields. I: Soil-Water Dynamics and Evapotranspiration. *Journal of Irrigation and Drainage Engineering*, *143*(9), 4017032. https://doi.org/10.1061/(asce)ir.1943-4774.0001214

Sloan, B. P., Mantilla, R., Fonley, M., & Basu, N. B. (2017). Hydrologic impacts of subsurface drainage from the field to watershed scale. *Hydrological Processes*, *31*(17), 3017–3028. https://doi.org/10.1002/hyp.11218

Snapp, S., Labarta, S., Mutch, R., Black, D., Leep, R., Nyiraneza, J., & O'Neil, K. (2005). Evaluating cover crops for benefits, costs and performance within cropping system niches. *Agronomy Journal*, *97*, 322–332. https://doi.org/10.2134/agronj2005.0322

Soil Science Division Staff. (2017). Chapter 3: Examination and Description of Soil Profiles. In C. Ditzler, K. Scheffe, & H. C. Monger (Eds.), *Soil Survey Manual: Handbook 18*. Washington, D.C.: Government Printing Office.

Soil Survey Staff. (2015). The Gridded Soil Survey Geographic (gSSURGO) Database for Iowa. Department of Agriculture, Natural Resources Conservation Service. Retrieved from https://gdg.sc.egov.usda.gov/

Sustainable Agriculture Research and Education. (2012). *Managing Cover Crops Profitably*. (A. Clark, Ed.).

Thomas, N. W., Arenas, A. A., Schilling, K. E., & Weber, L. J. (2016). Numerical investigation of the spatial scale and time dependency of tile drainage contribution to stream flow. *Journal of Hydrology*, *538*, 651–666. https://doi.org/10.1016/j.jhydrol.2016.04.055

Thompson, J. (2002). *Wetlands Drainage, River Modification, and Sectoral Conflict in the Lower Illinois Valley, 1890-1930*. Carbondale, Ill: Southern Illinois University Press.

Thorup-Kristensen, K., Cortasa, M. S., & Loges, R. (2009). Winter wheat roots grow twice as deep as spring wheat roots, is this important for N uptake and N leaching losses? *Plant and Soil*, *322*(1), 101–114. https://doi.org/10.1007/s11104-009-9898-z

Thorup-Kristensen, K., & Rasmussen, C. R. (2015). Identifying new deep-rooted plant species suitable as undersown nitrogen catch crops. *Journal of Soil and Water Conservation*, *70*(6), 399–409.

Tomer, M. D., Crumpton, W. G., Bingner, R. L., Kostel, J. A., & James, D. E. (2013). Estimating nitrate load reductions from placing constructed wetlands in a HUC-12 watershed using LiDAR data. *Ecological Engineering*, *56*, 69–78. https://doi.org/10.1016/j.ecoleng.2012.04.040

Tomer, M. D., Porter, S. A., James, D. E., Boomer, K. M. B., Kostel, J. A., & McLellan, E. (2013). Combining precision conservation technologies into a flexible framework to facilitate agricultural watershed planning. *Journal of Soil and Water Conservation*, *68*(5), 113A–120A. https://doi.org/10.2489/jswc.68.5.113A

Tufekcioglu, A., Raich, J. W., Isenhart, T. M., & Schultz, R. C. (1999). Fine root dynamics, coarse root biomass, root distribution, and soil respiration in a multispecies riparian buffer in Central Iowa, USA. *Agroforestry Systems*, *44*(2–3), 163–174. https://doi.org/10.1023/A:1006221921806

U.S. Geological Survey. (1996). *National Water Summary on Wetland Resources*.

United States Department of Agriculture. (2015). *Cool Season Cover Crop Species and Planting Dates and Techniques: Plant Materials Technical Note*.

160

van Genuchten, M. T. (1980). A Closed-form Equation for Predicting the Hydraulic Conductivity of Unsaturated Soils1. *Soil Science Society of America Journal*, *44*(5), 892. https://doi.org/10.2136/sssaj1980.03615995004400050002x

Vanderhoof, M. K., Christensen, J. R., & Alexander, L. C. (2017). Patterns and drivers for wetland connections in the Prairie Pothole Region, United States. *Wetlands Ecology and Management*, *25*(3), 275–297. https://doi.org/10.1007/s11273-016-9516-9

VanLoocke, A., Twine, T. E., Zeri, M., & Bernacchi, C. J. (2012). A regional comparison of water use efficiency for miscanthus, switchgrass and maize. *Agricultural and Forest Meteorology*, *164*, 82–95. https://doi.org/10.1016/j.agrformet.2012.05.016

Villarini, G., Smith, J. A., Baeck, M. L., Vitolo, R., Stephenson, D. B., & Krajewski, W. F. (2011). On the frequency of heavy rainfall for the Midwest of the United States. *Journal of Hydrology*, *400*(1–2), 103–120. https://doi.org/10.1016/j.jhydrol.2011.01.027

Villarini, G., Smith, J. A., & Vecchi, G. A. (2013). Changing frequency of heavy rainfall over the central United States. *Journal of Climate*, *26*(1), 351–357. https://doi.org/10.1175/JCLI-D-12-00043.1

Villarini, G., & Strong, A. (2014). Roles of climate and agricultural practices in discharge changes in an agricultural watershed in Iowa. *Agriculture, Ecosystems and Environment*, *188*, 204–211. https://doi.org/10.1016/j.agee.2014.02.036

Wang, X., Shang, S., Qu, Z., Liu, T., Melesse, A. M., & Yang, W. (2010). Simulated wetland conservation-restoration effects on water quantity and quality at watershed scale. *Journal of Environmental Management*, *91*(7), 1511–1525. https://doi.org/10.1016/j.jenvman.2010.02.023

Weber, L. J., Muste, M., Bradley, A. A., Amado, A. A., Demir, I., Drake, C. W., … Thomas, N. W. (2018). The Iowa Watersheds Project: Iowa's prototype for engaging communities and professionals in watershed hazard mitigation. *International Journal of River Basin Management*, *16*(3), 315–328. https://doi.org/10.1080/15715124.2017.1387127

Xu, C. (2002). Hydrologic Models. *University of Uppsala*, *72*, 1–168. https://doi.org/10.1002/2015WR017910.Received

Yang, W., Liu, Y., Simmons, J., Oginskyy, A., & McKague, K. (2013). *SWAT Modelling of Agricultural BMPs and Analysis of BMP Cost Effectiveness in the Gully Creek Watershed*.

Yang, W., Wang, X., Liu, Y., Gabor, S., Boychuk, L., & Badiou, P. (2009). Simulated environmental effects of wetland restoration scenarios in a typical Canadian prairie watershed. *Wetlands Ecology and Management*, *18*(3), 269–279. https://doi.org/10.1007/s11273-009-9168-0

Yu, X., Bhatt, G., Duffy, C., & Shi, Y. (2013). Parameterization for distributed watershed modeling using national data and evolutionary algorithm. *Computers and Geosciences*, *58*, 80–90. https://doi.org/10.1016/j.cageo.2013.04.025

Zedler, J. B. (2003). Wetlands at Your Service: Reducing Impacts of Agriculture at the Watershed Scale. *Frontiers in Ecology and the Environment*, *1*(2), 65. https://doi.org/10.2307/3868032

Zedler, J. B., & Kercher, S. (2005). WETLAND RESOURCES: Status, Trends, Ecosystem Services, and Restorability. *Annual Review of Environment and Resources*, *30*(1), 39–74. https://doi.org/10.1146/annurev.energy.30.050504.144248

Zeri, M., Anderson-Teixeira, K., Hickman, G., Masters, M., DeLucia, E., & Bernacchi, C. J.

(2011). Carbon exchange by establishing biofuel crops in Central Illinois. *Agriculture,*

Ecosystems and Environment, *144*(1), 319–329. https://doi.org/10.1016/j.agee.2011.09.006